

# An Integrated System Model For Variation Reduction In Manufacturing Systems

by

Rajiv Suri

B.S., Mechanical Engineering, Massachusetts Institute of Technology, 1993  
B.S., Literature, Massachusetts Institute of Technology, 1993  
M.S., Mechanical Engineering, University of Michigan, 1994

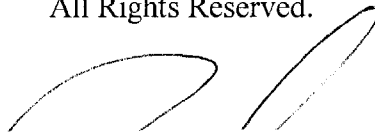
Submitted to the Department of Mechanical Engineering in  
Partial Fulfillment of the Requirements for the Degree of

Doctor of Philosophy

at the

Massachusetts Institute of Technology  
February 1999

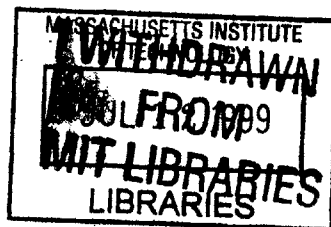
© 1999 Massachusetts Institute of Technology  
All Rights Reserved.



Signature of Author: \_\_\_\_\_  
Department of Mechanical Engineering  
January 15, 1999

Certified By: \_\_\_\_\_  
Kevin N. Otto  
Robert Noyce Career Development Associate Professor of Mechanical Engineering  
Committee Chairman

Accepted By: \_\_\_\_\_  
Ain A. Sonin  
Professor of Mechanical Engineering  
Chairman, Departmental Graduate Committee



ENG

# An Integrated System Model For Variation Reduction In Manufacturing Systems

by

Rajiv Suri

Submitted to the Department of Mechanical Engineering on January 15, 1999  
in partial fulfillment of the Requirements for the Degree of  
Doctor of Philosophy In Mechanical Engineering

## Abstract

This thesis presents a new method for mathematically modeling and reducing variation in manufacturing systems. While this domain has traditionally been the focus of statistical analysis methods, this work outlines the development of a physics-based *Integrated System Model (ISM)*, which predicts the nominal values and variation of each output quality characteristic in a manufacturing system. Analytical expressions for the evaluation of variation propagation through systems are developed and used to construct the ISM. Techniques are presented that use the ISM to identify the major sources of variation in a system, and to evaluate the need for process control. One such method is a system-level parameter design formulation, to select input parameter settings that render the system insensitive to input variation. This approach is shown to be more effective than traditional methods in reducing end-of-line variation. A second technique involves back-propagating end-of-line tolerances through a system, in order to determine process limits on each operation. The output variation of an operation must fall within these limits to ensure that the workpiece is capable of meeting final specifications. A third method is presented for using process limits to evaluate the need for measurement or process control in a system. The effects of both feedback and feed-forward process control on variation are discussed, and analytical expressions are developed to predict variation from an operation utilizing feed-forward control. Finally, these variation modeling and reduction techniques are demonstrated on a sheet stretch-forming system used to manufacture aircraft skin components. An ISM of this system is developed, incorporating two operations: heat treatment and stretch-forming. This ISM is validated against production data, and is used to identify major sources of variation in the system. Various process control strategies are then compared in simulation. A feed-forward strategy is chosen for demonstration, and is implemented on the shop floor. Data are presented showing that the feed-forward approach leads to a 30% reduction in end-of-line strain variation, and an 18% reduction in thickness variation on production parts. The methods presented in this work can be applied to other manufacturing systems as well.

Thesis Committee: Prof. Kevin N. Otto, Chairman  
Prof. David Gossard  
Prof. David Hardt  
Prof. Warren Seering

## ***Dedication***

*To my parents, for all of their love and support*

## Acknowledgements

First and foremost, I would like to thank my parents, without whose support and encouragement this thesis would not exist.

My advisor, Kevin Otto, made many contributions to both my thesis and my academic development. Kevin gave me the freedom to explore my interests, and has taught me a great deal about research and academia.

My committee members, Warren Seering, David Hardt, and David Gossard, were extremely generous with their time and advice. Their assistance has been invaluable.

This project would not have been possible without the support of Northrop-Grumman Corporation. In particular, I would like to thank Wes Burrowes, for countless hours of time and energy, as well as many early morning breakfasts at the plant. I would also like to thank Joe Boivan for seeing potential in this project, and both Doug Wolfe and Gary Kuhn for providing resources and making it possible.

My officemates have been a constant source of feedback and friendship. In particular, I would like to thank Dan Frey, who motivated me through the qualifiers and interested me in variation reduction; Bill Singhose, who provided many hours of discussion; and Javier Gonzalez-Zugasti, who let me bother him on a frequent basis. Thanks go as well to Brian Welker and Kan Ota for making the lab a fun place (well, as much as possible).

I also owe a great deal to Marko Valjavec, my local expert on stretch forming. Simona Socrates provided me with her Abaqus drape forming code, and cheerfully gave me much advice on how to adapt it to my needs. Andrew Parris was kind enough to provide me with his data for leading edges; his thesis was my most useful single source of information.

Finally, I want to thank my wife-to-be, Bindu Nair, and my friends, Jeffrey Stovall, Lucksman Parameswaran, and Jill Jowers for helping to make my non-thesis time pleasurable and relaxing.

Financial support for this research was provided by the United States Department of Energy, through an Integrated Manufacturing Pre-Doctoral Fellowship, and by the Leaders for Manufacturing Program, a collaboration between MIT and U.S. Industry.

# Table of Contents

<b>Chapter 1: Introduction</b>	<b>8</b>
<b>1.1 Systems Approach</b>	<b>8</b>
<b>1.2 Manufacturing Process Variation</b>	<b>9</b>
<b>1.3 Thesis Goal</b>	<b>10</b>
<b>1.4 Variation Reduction Method</b>	<b>11</b>
<b>1.5 Example System</b>	<b>11</b>
<b>1.6 Thesis Overview</b>	<b>13</b>
<b>Chapter 2: Traditional Approaches To Variation</b>	<b>14</b>
<b>2.1 Diagnostic Techniques</b>	<b>14</b>
2.1.1 Process Capability Indices	14
2.1.2 Statistical Process Control (SPC)	16
<b>2.2 Parameter Design</b>	<b>17</b>
2.2.1 Evolutionary Operation	17
2.2.2 Quality Loss and Taguchi	17
2.2.3 Response Surface Methodology (RSM)	19
2.2.3 Other Work	20
<b>2.3 Engineering Design Research Laboratory</b>	<b>21</b>
<b>2.4 Variation Modeling</b>	<b>21</b>
<b>2.5 Robust Design Approaches</b>	<b>22</b>
<b>2.6 Controls</b>	<b>22</b>
<b>Chapter 3: Variation in Systems</b>	<b>23</b>
<b>3.1 Variation in a Single Operation</b>	<b>23</b>
<b>3.2 Linearization</b>	<b>25</b>
<b>3.3 Root-Sum Squares Approach</b>	<b>26</b>
<b>3.4 Modeling Error</b>	<b>26</b>
<b>3.5 Manufacturing Process Tolerance Threshold</b>	<b>29</b>
3.5.1 Worst Case Tolerance Threshold Determination	30
3.5.2 RSS Tolerance Threshold Determination	30
<b>3.6 Serial Systems</b>	<b>31</b>
<b>3.7 Parallel Operations</b>	<b>32</b>
<b>3.8 Integrated System Model</b>	<b>33</b>
3.8.1 Predictive Models	34
3.8.2 Variational Models	35
3.8.3. Linking the ISM	37

<b>3.9 System-Level Parameter Design</b>	<b>37</b>
3.9.1 Variation in the Presence of Adjustments	38
3.9.2 System-Level Variation Reduction	40
3.9.3 Approximating Sensitivities	42
3.9.4 Discussion of Related Work	42
<b>3.10 Selective Biasing</b>	<b>43</b>
<b>3.11 Chapter Summary</b>	<b>45</b>
<b><i>Chapter 4: Process Limits and Control</i></b>	<b>47</b>
<b>4.1. Process Limits</b>	<b>47</b>
4.1.1 Bounding the Process Limits	49
4.1.2. Parallel Operations	52
4.1.3 Application of Process Limits	52
<b>4.2 Process Control</b>	<b>54</b>
4.2.1 Feed-Forward Control	54
4.2.2 Feedback Control	59
4.2.3 Controllability	60
<b>4.3 Chapter Summary</b>	<b>61</b>
<b><i>Chapter 5: Sheet Stretch-Forming Example</i></b>	<b>62</b>
<b>5.1 Target Part</b>	<b>62</b>
<b>5.2 System Overview</b>	<b>63</b>
5.2.1 Process Description	63
5.2.2 Modeling Considerations	65
<b>5.3 Integrated System Model</b>	<b>65</b>
5.3.1 Heat Treatment	65
5.3.2 Stretch-Forming	72
5.3.3 Assembling the ISM	82
<b>5.4 Modeling Validation</b>	<b>83</b>
5.4.1 Measured Parameters	83
5.4.2 Measured Values	85
5.4.3 System Model Predictions	89
<b>5.5 Major Sources of Variation</b>	<b>93</b>
<b>5.6 System-Level Robustness</b>	<b>94</b>
<b>5.7 Tolerance Threshold</b>	<b>98</b>
<b>5.8 Process Limits</b>	<b>100</b>
5.8.1 Stretch-Forming Process Limits	100
5.8.2 Heat Treatment Process Limits	104
<b>5.9 Process Control Strategies</b>	<b>106</b>
5.9.1 Analytic Approach to Feed-Forward	108
5.9.2 Numerical Simulation of Variation Propagation	116
<b>5.10 Feed-Forward Control Experiment</b>	<b>123</b>
5.10.1 Experiment Overview	124
5.10.2 Experimental Procedure	124
5.10.3 Experimental Results	128
5.10.4 Discussion	128

<b>5.11 Chapter Summary</b>	<b>129</b>
<b><i>Chapter 6: Summary and Conclusions</i></b>	<b><i>130</i></b>
<b>6.1 Major Contributions</b>	<b>130</b>
6.1.1 Variation Reduction Method	130
6.1.2 Integrated System Model	131
6.1.3 Tolerance Threshold	131
6.1.4 System-Level Parameter Design	131
6.1.5 Process Limits	131
6.1.6 Analytical Treatment of Feed-Forward Control	131
6.1.7 Stretch-Forming ISM	132
6.1.8 Feed-Forward Control Validation	132
<b>6.2 Generalizing These Methods</b>	<b>132</b>
<b>6.3 Opportunities for Further Research</b>	<b>132</b>
<b>6.4 Conclusions</b>	<b>133</b>
<b><i>References</i></b>	<b><i>134</i></b>
<b><i>Appendix A: Abaqus Input Deck for Drape Forming</i></b>	<b><i>138</i></b>
<b><i>Appendix B: Stretch Forming Sensitivity Matrices</i></b>	<b><i>157</i></b>

# Chapter 1: Introduction

Over the past twenty years, American industry has steadily increased its focus on manufacturing quality. Following the second World War, American manufacturers were the world leaders in production. Their comfortable reliance on a captive world market was shattered in the 1970's by the Japanese, who had learned how to produce higher quality products at lower costs from the likes of Demming, Juran, and Taguchi. Japanese products quickly became identified with both quality and value, while American manufacturers found themselves unable to compete.

Today, quality improvement is a major concern at every level of American industry. The concepts of quality and variation reduction are marketed through programs such as "6 Sigma Production" and "ISO 9000 certification," while numerous consultants and researchers seek to understand and implement Japanese production practices.

The main tools for variation analysis and reduction in a production environment are based on process measurement and experiment. Diagnostic methods, such as Statistical Process Control (SPC) and process capability indices, rely on the measurement and statistical analysis of process output quality characteristics (DeVor, Chang et al. 1992). Parameter design techniques, such as Evolutionary Operation (Box and Draper 1969) or Taguchi's robust design philosophies (Phadke 1989), rely on designed experiments conducted on the process.

This thesis presents a new method for variation reduction, based on the mathematical modeling of manufacturing systems. While this domain has traditionally been limited to statistical analysis methods, this work outlines the development of a physics-based Integrated System Model (ISM), which maps the nominal value and variation of each input parameter to each output parameter in a manufacturing system. This model can be used to determine the major sources of variation in a system, and to evaluate different variation reduction strategies. The approach is demonstrated through the development of an ISM of an actual sheet stretch-forming system from the aerospace industry.

## 1.1 Systems Approach

A *manufacturing operation* can be defined as a transformation of material from one state to another, through directed interaction with a machine (Hardt 1998). The material being acted upon is often called the *workpiece*, and descriptions of its geometry and material properties are considered *inputs* to the operation. Additional inputs are settings of the *process parameters*, which are variables determining the energy flow between the workpiece and the machine. The operation also has a set of *outputs*, containing information about the geometry and material properties of the workpiece after the operation. The dimensions and properties that are most important to the performance of the workpiece are also called *quality characteristics*.



A *manufacturing system* is a network of manufacturing operations with shared inputs and outputs. A system can have *serial* operations, in which the output of a single operation becomes the input to a single successive operation, or *parallel* operations, where multiple operations feed into a single operation. A transfer line is an example of a serial system, while a parallel system might consist of piece part processes feeding an assembly operation where multiple parts and subassemblies are joined.

Most quality control philosophies focus on a single operation in isolation. This implies that by minimizing the output variation of each operation within a system, the output variation of the entire system is also minimized. This is not always true. The sensitivity of an operation to input variation is a function of its nominal operating point. As most manufacturing operations are part of a larger manufacturing system, the operating point of an operation cannot be changed without simultaneously making changes to other operations as well. As this thesis will show, it is often possible to find a more robust operating point for the entire system by making a coordinated change in the operating points of several operations. This cannot be done without considering the system as a whole. It is also sometimes cost-effective to have an operation with non-minimized output variation. This situation can occur when a downstream operation reduces variation (perhaps through in-process control), thereby allowing a more expensive upstream operation to have larger variation.

It is also possible to reduce variation through inter-operation process control strategies. An understanding of the relationship between process variables in different operations can lead to feed-forward and feedback control strategies, in which variables in one operation are measured and used to determine variable settings in another operation. This systems approach can be used to determine the most efficient or lowest cost adjustments to compensate for input or process variation.

For both of these reasons, it is important to consider the effect of each operation on work-in-process (WIP), understand the impact of each operation on end-of-line product variation, and to then set target outputs for each operation in the system to ensure that the final product will meet specifications. This approach requires an understanding of variation propagation through multiple operations and a method for determining in-process tolerances on work-in-process moving through a system.

## **1.2 Manufacturing Process Variation**

Process variation can be described qualitatively as a measure of the amount that each produced part differs from some “ideal” part. Variation is usually expressed as a statistical quantity such standard deviation, which measures the amount that a quality characteristic of a set of parts varies from some “target” specification. Mathematical definitions of variation will be presented in Chapter 3.

The concept of variation is often confused with the idea of tolerance. The tolerance on a part dimension is the allowable deviation from some target value. Tolerance is determined by a designer, based on some set of product performance specifications.

Process variation, on the other hand, is a statistical measure of the deviation of a group of parts from some target values, caused by natural events occurring during the manufacturing process. These effects could be purely random, or may be the result of identifiable special events. In short, process variation is a natural phenomenon, inherent in a manufacturing system, while tolerances are performance-based specifications imposed by a designer.

Manufacturing variation is costly for two main reasons: low yield, and quality loss. Yield is a measure of the number of parts that meet tolerance specifications. The schematic in Figure 1.1 shows that for each toleranced output quality characteristic, the number of parts which meet specification is a function of both the bias (deviation of the process mean from the target value) and the variation. In general, larger variation leads to a smaller percentage of parts that meet the tolerance specifications. Those parts that do not meet tolerances are subject to either rework or scrap. Process yield is thus directly related to production cost.

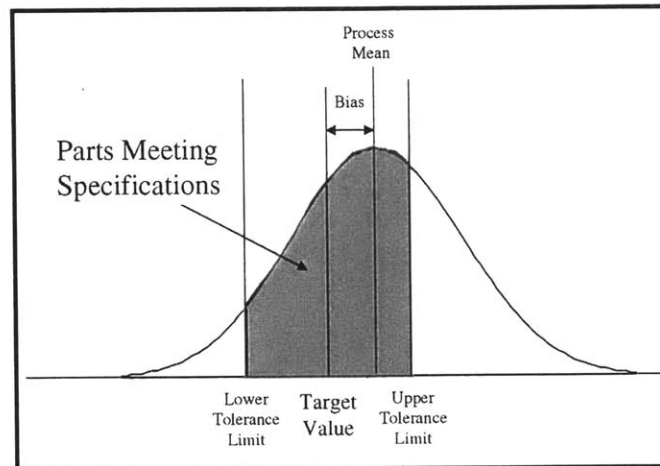


**Figure 1.1 Process Variation and Tolerance Limits**

Quality loss is a concept introduced by Taguchi (Phadke 1989). He suggested that while a product might meet its design tolerances, deviation from target values is a measure of product quality, and in turn, of customer satisfaction. Taguchi argued mathematically that a product's value increases as its variation from target values decreases. According to Taguchi's philosophy, all process variation is associated with a cost to the manufacturer.

### **1.3 Thesis Goal**

The goal of this thesis is to develop and demonstrate a new method for mathematically modeling and reducing variation in manufacturing systems. This approach is based on the development of physics-based process models, which are used to predict both the nominal values and variation of product quality characteristics. Techniques are developed to find the most robust operating point for the system, and to set limits on the

output variation from each operation, based on end-of-line tolerances. The method is demonstrated through the development of a model of a sheet stretch-forming system from the aerospace industry. This example model is used to explore several variation reduction strategies, and is validated through comparison with production data. The methods presented in this thesis can be generalized to apply to other manufacturing systems as well.

## **1.4 Variation Reduction Method**

The techniques outlined in this thesis can be combined into a comprehensive variation-reduction method for manufacturing systems. The method can be outlined as follows:

- 1) Develop an Integrated System Model of the manufacturing system
- 2) Identify major sources of variation in the system
- 3) Conduct system-level parameter design
- 4) Evaluate the need for measurement or control in a system
- 5) Formulate several variation reduction strategies
- 6) Evaluate strategies in simulation using the ISM
- 7) Implement the most promising strategy

The mathematical tools for implementing each of these steps are developed throughout this thesis. The method is then demonstrated, step by step, on a manufacturing system used to produce aircraft skin components. Data is presented from a shop-floor experiment, showing that the process control strategy developed using this approach was successful in reducing end-of-line variation.

## **1.5 Example System**

The variation reduction strategy outlined in the previous section will be demonstrated in detail on a sheet stretch-forming manufacturing system. Stretch-forming is a widely used process for forming aircraft skins, in which a flat sheet of metal is stretched over a die in order to produce some desired curvature (Figure 1.2). The sheet metal is often heat treated before or after forming in order to alter its material properties, specifically yield strength.

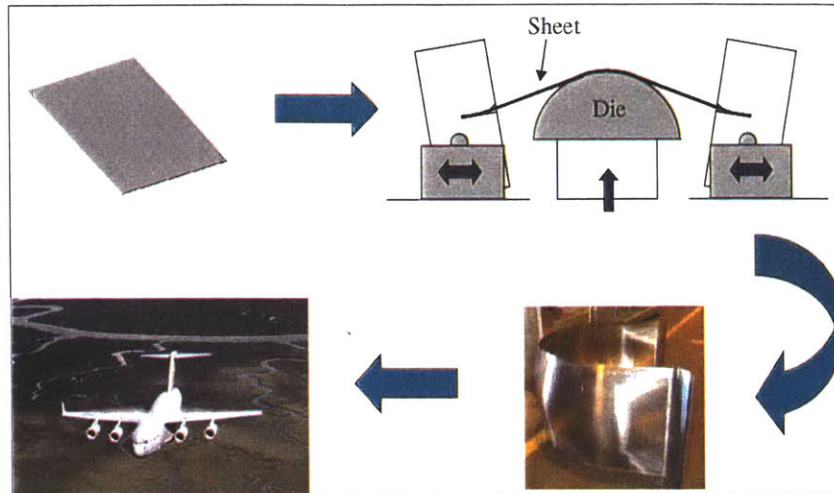


**Figure 1.2: Stretch Forming of Aircraft Skins**

The system model developed in this thesis consists of two operations: heat treatment and stretch-forming. Photographs of each of these operations are shown in Figure 1.3. The specific part manufactured by this system is a nacelle doubler, shown before and after trimming in Figure 1.4. A detailed description of the manufacturing process used to make this part is presented in Chapter 5, along with system model development and validation. Chapter 5 also contains a discussion of the use of the system model to formulate a process control strategy which has been shown to reduce both strain and thickness variation on production parts.

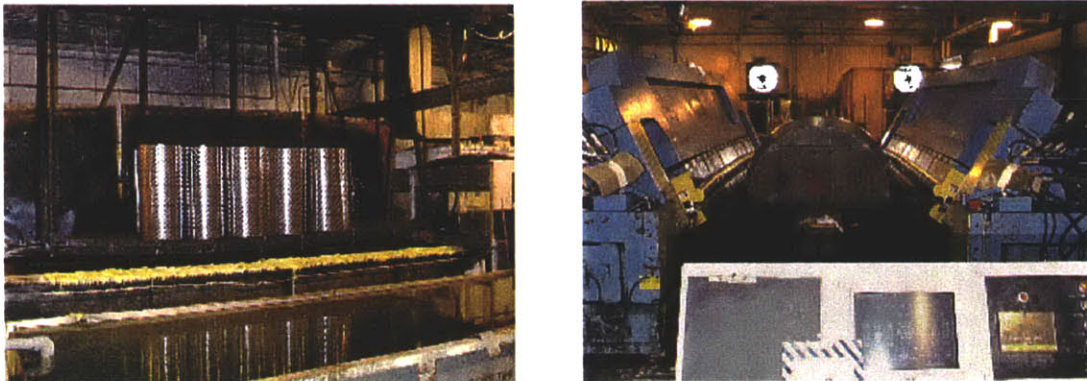


**Figure 1.3: Heat Treatment and Stretch Forming Operations.**

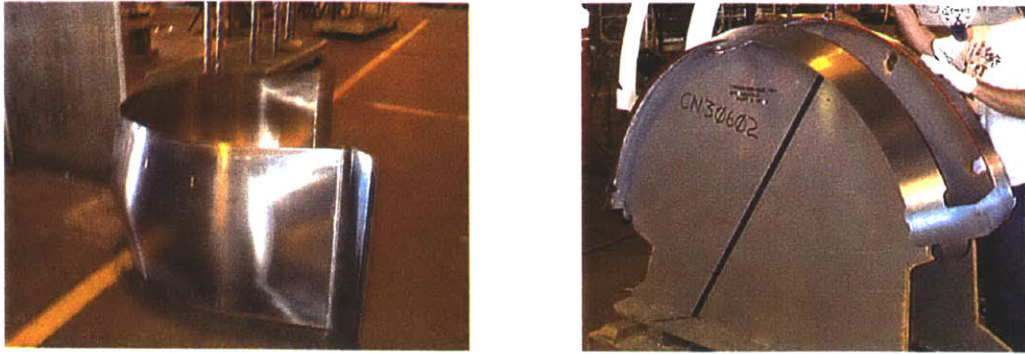


**Figure 1.4: Modeled Part Before and After Trim.**

## 1.6 Thesis Overview

The second chapter of this thesis contains a discussion of quality improvement methods and philosophies. Diagnostic techniques are considered first, including Statistical Process Control (SPC) and Process Capability Indices. This is followed by an overview of parameter design, ranging from Evolutionary Operation (EVOP) to Taguchi's methods. We then focus on the direct precursors to this thesis, most notably the work of Frey and Otto. Finally we touch upon the work of a number of other researchers in the fields of variational modeling and process control.

Chapter 3 outlines the theoretical underpinnings of this work. We derive analytical expressions for variation propagation through operations and through systems. These expressions become the basis for the Integrated System Model (ISM): a mapping between the nominal values and variations of system inputs and outputs. We discuss using the ISM to identify the major sources of variation within a manufacturing system, and to implement system-level parameter design.

Some further applications of the ISM are presented in Chapter 4. We develop a method for setting process limits on each operation within a system, to ensure that the final product meets specifications. This method is then extended to determine where process control is needed in a system. We discuss both feed-forward and feedback process control, in regard to their effects on variation. Analytical expressions are derived to predict variation reduction in the presence of feed-forward control.

The fifth chapter is a demonstration of the methods developed in Chapters 3 and 4. We first generate an ISM of a sheet stretch-forming manufacturing system, and validate it against production data. We then use this model to analyze the sources of variation in the system, and develop a process control strategy. We present the results of an implementation of this strategy, showing that it is successful in reducing variation in a production environment.

In Chapter 6 we summarize the contents of this thesis. The major contributions are highlighted, and we draw conclusions about the methods that we have developed.

## Chapter 2: Traditional Approaches To Variation

A number of tools and methods exist in both the design and manufacturing communities to identify and reduce sources of variation in systems. Diagnostic techniques, such as SPC and Process Capability Indices, have long been popular in the manufacturing community as methods for detecting problematic systems. These techniques are capable of identifying a problem, but do not aid the engineer in determining its root cause. Parameter design originated as a class of techniques to actually identify problems and to reduce their impact in practice. Box and Draper's Evolutionary Operation (Box and Draper 1969) and Montgomery's Response Surface Methods (Montgomery 1984) are means of identifying process parameter settings which reduce the sensitivity of an operation to input variation. Lead by Taguchi (Phadke 1989), the design community has followed these methods with a number of robust design strategies. More recently, advances in computational process modeling have supported the development of mathematical models of process variation, for use in the identification and reduction of quality problems.

The techniques outlined in this thesis are related to all of the areas discussed in this section. The diagnostic techniques serve as a basis for a statistical approach to manufacturing variation. We extend the parameter design techniques of Taguchi and Box and Draper by implementing a system-level parameter design through the use of mathematical models. We also extend the previous work done in variational modeling by applying it to systems rather than single operations. The rest of this chapter discusses each of these methods in more detail.

### 2.1 Diagnostic Techniques

There are several methods commonly used for detecting the presence of excessive variation within a manufacturing operation. These *diagnostic techniques* can identify the existence of a problem, but are incapable of identifying the cause. The two most popular diagnostic methods are Process Capability Indices and Statistical Process Control (SPC). Process Capability Indices are dimensionless ratios reflecting the amount of variation and/or bias (deviation from a target nominal value) in a system. They provide the engineer with a single number reflecting the performance of the system relative to required tolerances, indicating any need for improvement. SPC is a method of continuously monitoring the output of a process to detect changes in the process mean or range. SPC can be used to detect problems on-line and to determine whether a process is "in control." Each of these methods is discussed in more detail below.

#### 2.1.1 Process Capability Indices

The variation in a manufacturing system is often gauged by a measure of process capability. Kalpakjian (1995) defines process capability as "the limits within which individual measurement values resulting from a particular manufacturing process would normally be expected to fall when only random variation is present." Process capability

is commonly combined with tolerances to produce a dimensionless number representing the operation's ability to meet the desired specifications for a single output quality characteristic. One such index is the Process Capability Index ( $C_p$ ), a dimensionless ratio of the amount of acceptable variation to the amount of variation in the operation.  $C_p$  is defined as:

$$C_p \equiv \frac{(U - L)/2}{3\sigma} \quad (2.1)$$

where  $U$  and  $L$  are the upper and lower specification limits (tolerances) on the quality characteristic and  $\sigma$  is the standard deviation. While  $C_p$  provides an adequate evaluation of process variation, it does not take into account any deviation of the mean value of the quality characteristic from its target value. This deficiency was discussed by Kane (1986), who added bias effects to create a new index,  $C_{pk}$ :

$$C_{pk} = C_p \cdot (1 - k) \quad (2.2)$$

where  $k$  is a dimensionless ratio of the absolute value of bias to tolerance width:

$$k \equiv \frac{\left| \mu - \frac{U + L}{2} \right|}{(U - L)/2} \quad (2.3)$$

and  $\mu$  is the mean value of the quality characteristic. These indices are commonly used in industry to evaluate the variational state of an operation. Processes with  $C_{pk} > 1$  are generally considered "capable," while processes for which  $C_{pk} < 1$  are candidates for improvement. The process capability index can be applied to determine the process "first time yield" ( $Y_{FT}$ ). This quantity is the probability that a single quality characteristic meets its tolerances. Six sigma analysis suggests multiplying all of the first time yields together to determine yield for a product with multiple quality characteristics (Harry and Lawson 1992). As Frey (1997) points out, this assumes statistical independence among quality characteristics, something that is rarely true. As such, the yield estimate formed in this way can be off by several orders of magnitude. This problem has been addressed by Frey and Otto (1998), who propose use of the "Process Capability Matrix,"  $C$ :

$$C_{ij} \equiv \frac{3\sigma_j \cdot \left( \frac{\partial q}{\partial n} \right)_{ij}}{(U_i - L_i)/2} \quad (2.4)$$

where  $\sigma_j$  is the standard deviation of the  $j^{th}$  noise variable, and  $U_i$  and  $L_i$  are upper and lower bounds on the  $i^{th}$  quality characteristic (Frey 1997). This matrix, which accounts for multiple quality characteristics, can be used in conjunction with "Rolled Throughput

Yield” to accurately assess the yield of a product with multiple, correlated quality characteristics. Rolled Throughput Yield refers to the probability that every quality characteristic of an individual process is simultaneously met (Frey 1997). Frey and Otto also present methods for determining rolled-throughput yield based on a vector of specifications and process capabilities.

### 2.1.2 Statistical Process Control (SPC)

Statistical Process Control was developed in the 1950's by Shewhart, working at Bell Labs. Shewhart identified two main causes of variation in manufacturing processes: *chance causes*, and *assignable causes*. Assignable causes are unpredictable incidents which alter the mean or variation of the operation. They can usually be fixed through some change in the machine or process. DeVor and his colleagues list some examples of assignable causes as broken tools, a jammed machine, and machine-setting drift (DeVor, Chang et al. 1992). Chance causes, on the other hand, describe the baseline causes of variation in the system. These are due to poor methods, operator inconsistency or error, and variation in the material or machine. Shewhart states that processes under *statistical control* are driven solely by common causes of variation. A system showing instability or a lack of control is afflicted with assignable causes. He goes on to say that any process which is not operating under statistical control is not economic; it costs more to run than a process under control, even if the product meets design specifications (DeVor, Chang et al. 1992). This is similar to Taguchi's concept of quality loss, which suggests that the economics of a process is not tied to the percentage of acceptable product, but to the quality of the product produced (Phadke 1989).

It should be noted that Shewhart places total emphasis on the process, with no mention of the product. The state of being in statistical control is a function of the process, without consideration of the design specifications. A process could, therefore, produce 100% acceptable parts while out of statistical control. Conversely, a process completely in statistical control could produce very few acceptable parts, suggesting that the process capability does not meet the desired specifications.

The Statistical Process Control method involves creating time-varying control charts which plot the process mean and range over time (DeVor, Chang et al. 1992). Each of these charts has an upper and lower control limit, representing the expected  $3\sigma$  variation of the mean and range. The chart is observed during production, and can be used to quickly detect mean shifts and the presence of assignable causes of variation. An operator can use the charts to determine whether a process is in statistical control, or whether corrective action is necessary. The SPC charts allow easy on-line detection of mean shifts and the presence of assignable causes.

The control chart method is a diagnostic technique, as it identifies the presence of a problem, but does not aid in determining the cause. Shewhart suggests using statistical data to detect correlations between input and output variables to help trace the sources of problems (DeVor, Chang et al. 1992). The variation reduction methods we outline in this thesis are complementary to control chart methods. While Shewhart primarily addresses



the identification and elimination of assignable causes, our modeling approach seeks to identify the sources and contributions of all of the chance causes. Once our methods have been used to reduce the base level of variation in a system, SPC can be used to ensure that the process remains in statistical control during operation.

## **2.2 Parameter Design**

Parameter design is the process of selecting input variable settings that minimize an operation's sensitivity to input variation. The technique is based around a designed experiment or perturbation study, which assesses the sensitivity of each process output to each process input. This information is then used to identify the combination of parameter settings which result in the lowest output to input sensitivities. One of the first parameter design methods was the Evolutionary Operation (EVOP) technique, introduced by Box and Draper in the 1960's (Box and Draper 1969). EVOP involves performing a continuous designed experiment on a factory, in which process parameter settings are evaluated and adjusted on a daily basis to optimize some output quantity. Taguchi presented a more sophisticated parameter design scheme in the 1980's, involving the use of orthogonal designed experiments to determine sensitivities in conjunction with an objective function (the Signal-To-Noise ratio) that accounts for variation (Phadke 1989). In this section, we discuss both of these methods, as well as some relevant extensions.

### **2.2.1 Evolutionary Operation**

Evolutionary Operation is a plant-scale process for parameter selection. The premise is to introduce "controlled variation" into a manufacturing plant, observe the effects on output, and use this information to guide a gradient search towards a "preferred" operating point (Box and Draper 1969). A  $2^2$  or  $2^3$  factorial design is used to determine which parameter settings to test, and several "variants" of the nominal operating point are determined. The EVOP process involves cycling through these variant several times, and then using the accumulated data to determine a new base operating point and new set of variants. The process is then repeated.

Box and Draper intend that EVOP should be considered "a basic operating method" to be used continuously through the life of the plant and product (Box and Draper 1969). While EVOP does not directly address the issue of variation, it can be easily modified into a variation reduction technique.

### **2.2.2 Quality Loss and Taguchi**

A number of important ideas in the field of manufacturing quality have been advanced by Genichi Taguchi. His work, which has been advocated in America by Phadke, Kackar, and Clausing, has been instrumental in shifting industry's focus from meeting tolerances to improving quality (Kackar 1985; Clausing 1988; Phadke 1989). Taguchi's contributions center around two fundamental concepts: quality loss and robust design. Quality loss is a measure of the cost to society of a product's deviation from target specifications. Robust design is a methodology developed to minimize quality loss in

manufacturing systems. We will briefly describe these concepts in this section; an excellent presentation of the subject matter is given in (Phadke 1989).

#### 2.2.2.1 Quality Loss

Taguchi's work has prompted a re-evaluation of the significance of product tolerances. Traditional bilateral tolerances imply that a product is acceptable if its quality characteristic values fall within the tolerated limits. Thus for a product with a quality characteristic target value  $m$  and acceptable tolerance  $\Delta_0$ , the bilateral tolerance would be:

$$m \pm \Delta_0 \quad (2.5)$$

The traditional acceptability standards imply that a product with a quality characteristic value exactly corresponding to the target value  $m$  is no better than a product with quality characteristic value  $m + \Delta_0$ ; both meet the specification, and thus both are acceptable. Taguchi postulates that, in fact, there is a cost associated with *any* deviation from the target specification. If the deviation causes the product quality characteristic to fall outside the acceptable tolerance band, the associated cost will come from scrap or rework. Even if the quality characteristic value is within the tolerated limits, however, Taguchi suggests that any deviation from the target value will result in costs related to customer satisfaction, repair, and miscellaneous costs to society (Phadke 1989). These costs are the "quality loss" of a product. Taguchi formally defines quality loss using a quadratic function:

$$Q(y) = c \cdot (y - m)^2 \quad (2.6)$$

in which  $Q$  is the quality loss associated with a product with quality characteristic value  $y$  and target value  $m$  (Phadke 1989). The variable  $c$  is a quality loss coefficient, related to the dollar cost of the product. For a series of manufactured parts, Taguchi defines the average quality loss  $\bar{Q}$  as:

$$\bar{Q} = c[(\mu - m)^2 + \sigma^2] \quad (2.7)$$

where  $\mu$  and  $\sigma$  are the mean and standard deviation of the quality characteristics, respectively (Phadke 1989).

#### 2.2.2.2 Robust Design

By relating the deviation of a product's quality characteristic value to cost, Taguchi implicitly associated product variation with cost. Taguchi defines causes of variation as *noise factors* (Phadke 1989). These can be external (due to environmental conditions and loading), process non-uniformity (due to manufacturing variations), and deterioration (aging and wear). The manufacturing variations can be further subdivided into external causes (environmental variables, raw material, operator effects), process non-uniformity, and process drift. Taguchi presents a methodology called "Robust Design" to reduce the effects of process variation. Robust Design involves the use of a designed experiment to determine the optimum settings of process parameters to minimize sensitivity to input

noise. Process insensitivity is commonly termed “robustness.” Phadke outlines the major steps in robust design as:

- 1) Planning the experiment – identifying noise factors and levels, and designing an experiment to test them
- 2) Performing the experiment
- 3) Analyzing the experiment – determine optimum levels for the control factors

The control factors are optimized to maximize what Taguchi calls the “Signal to Noise Ratio (S/N ratio),” defined as:

$$\eta = 10 \cdot \log_{10} \left( \frac{\mu^2}{\sigma^2} \right) \quad (2.8)$$

where  $\eta$  is the signal-to-noise ratio in decibels,  $\mu$  is the mean value of the system response, and  $\sigma$  is the standard deviation of the system response. Several case studies are presented in (Phadke 1989) illustrating successful industrial implementations of the Robust Design philosophies. A number of authors have extended Taguchi’s work, including (Chang, Ward et al. 1994), (Chen, Allen et al. 1996), and (Kackar 1985).

### 2.2.3 Response Surface Methodology (RSM)

Response Surface Methodology (RSM) is described by Montgomery (1984) as a collection of mathematical and statistical techniques for optimizing a response controlled by several independent variables. RSM involves the use of a polynomial surface to approximate the relationship between multiple input variables and a single output variable. The parameters of this polynomial are determined through least-squares fitting of input and output data, obtained through a designed experiment over the parameter space. The output response is then optimized by first using a linear approximation and “hill-climbing” technique to reach the optimal region, and then using a localized higher-order surface in combination with “canonical analysis” to find the optimum (Montgomery 1984).

Guo and Sachs (1993) present an interesting modification of the RSM. Their method involves using “Multiple Response Surfaces (MRS),” each modeling the response characteristics at a different location within a product or batch of products. These multiple surfaces, which can often be of lower-order than a single response surface, are then combined into a single output variable. As Guo and Sachs demonstrate, the use of MRS requires less data, can be more accurate, and is less computationally intensive than using single response surfaces.

Sachs, Prueger, and Guerrieri (1992) have developed a “semi-empirical model” of the Polysilicon Low Pressure Chemical Vapor Deposition (LPCVD) process used in the semiconductor manufacturing industry. Their modeling approach involved the generation of a “smart response surface,” consisting of a physics-based finite-element

model with 4 adjustable coefficients, determined through designed experiments on the actual system. The designed experiments were used both to fit the response surface and to aid in parameter selection for process optimization. Sachs and his colleagues present data showing that the model correctly predicts actual system response and can be used to aid in parameter design as well.

### **2.2.3 Other Work**

A number of other researchers have approached the problem of parameter design. For the most part, this work is an extension of either the work of Box and Draper, or the work of Taguchi. In this section we highlight several of these extensions.

#### 2.2.3.1. Chinnam and Kolarik

Chinnam and Kolarik (1997) have developed a method for parameter design involving the use of neural net models of the manufacturing process. They suggest that optimizing the controllable variables in a process requires:

- 1) A detailed parametric model of the plant
- 2) An empirical model accounting for errors in the parametric model
- 3) An optimization routine
- 4) The ability to adjust controllable variables on-line

They address the second of these points, by introducing the “Intelligent Quality Controller,” which can track changes in process response characteristics over time, monitor uncontrollable variables, and conduct real-time process parameter design. To do this, they first develop a neural net of the system response, possibly from the actual system, or possibly from the parametric model. They then take a vector of target output characteristic values, and back-propagate through the neural net using a gradient search technique, for the set of input values which best produces the desired output values. These input values are then the optimized parameters. Finally, they present a software tool they have developed to implement these steps (Chinnam and Kolarik 1997).

#### 2.2.3.2 Chen and Mistree

Chen and Mistree have combined Taguchi’s approach with Response-Surface Methodology in formulating their Robust Concept Exploration Method (RCEM) (Chen, Allen et al. 1996; Chen, Allen et al. 1997). There are four steps in applying the RCEM to a design problem. First the problem is analyzed from a robust design standpoint, in order to classify design variables into control factors and noise factors. Next, screening experiments are conducted, to fit a low-order response surface to the problem. This response surface is used to identify which variables are important to the problem. Additional experiments are then conducted to fit a higher-order response surface to the reduced problem. RSM methods are used to express output parameter values and variances as a function of the inputs. These functions are then used within the non-linear Decision Support Problem (DSP) solver, to optimize the output by selecting desired values or ranges of the inputs. Another application of the RCEM approach is discussed in (Peplinski, Allen et al. 1996).

## 2.3 Engineering Design Research Laboratory

The research presented in this thesis follows directly upon work in variational modeling conducted by Professor Kevin Otto and Professor Daniel Frey in the Engineering Research Design Laboratory (EDRL) at MIT. A brief outline of this work is presented here.

Otto and Antonsson (1994) first discussed the use of manufacturing adjustment selection for variation reduction during the development process. The idea of representing manufacturing operations as matrix transforms for the purpose of variational modeling was developed by Frey and Otto, who defined the Process Capability Matrix,  $C$  (Frey, Otto et al. 1998). The capability matrix is effectively a sensitivity matrix, which has been normalized with the product tolerances. Frey and Otto also developed a set of block-diagram reduction rules, allowing the capability matrices for multiple operations to be combined into a matrix representation of a manufacturing system (Frey, Otto et al. 1997). This representation allowed for numerical simulation of variation propagation through a system with feed-forward control. There are two fundamental differences between Frey's work and the research presented in this thesis. The ISM is intended as a tool for designers; we do not presuppose the existence of tolerances. As such, we use non-normalized sensitivity matrices rather than process capability matrices. In addition, we seek to present analytical expressions for the propagation of variation. Frey's work relied on numerical simulation.

Soyucayli and Otto (1998) developed a simple variational model of a manufacturing system. Suri and Otto (1999) then presented the concept of an Integrated System Model, and developed a sheet-stretch forming system model. Process limits, one application of the ISM methodology, were demonstrated on an automotive frame welding system in (Suri and Otto 1998).

## 2.4 Variation Modeling

The use of physics-based models of manufacturing processes to reduce variation is an active area of research. Kazmer and his colleagues use finite-element based process models to analyze the variation within a single operation (Kazmer, Barkan et al. 1996). Their technique involves the use of Monte Carlo simulation to predict yield for several different designs of a net-shape part. Design robustness is then evaluated based on the theoretical yield.

S.J. Hu (1997) has developed a "Stream of Variation" theory to examine variation propagation in the assembly of flexible components. He uses finite-element models to evaluate deflection (but not deformation) due to spot welding, and then uses Monte Carlo simulation to predict final variation. Hu focuses only on variation in product geometry, and does not consider the effects of in process adjustment or control.

Mantripragada and Whitney (1997) have explored the idea of using assembly sequencing and datum logic to make in-process adjustments to reduce final variation. As they only consider geometric stack-up in each assembly operation, there is no need for actual process models, which are effectively replaced with transformation matrices. Mantipragada and Whitney use a classical controls state-space representation for their assembly system, allowing the use of block-diagram formulations and the application of traditional controls techniques.

## **2.5 Robust Design Approaches**

Taguchi's concept of robust design has received much attention within the design community, where it has been applied to the selection of design variables. Ford and Barkan (1995) have proposed a methodology for incorporating robust design concepts into the early concept stage of design. Chang and his colleagues (1994) have adapted Taguchi's methods to product design by introducing the idea of "virtual noise," which accounts for uncertainty due to the presence of multiple decision-making agents during simultaneous design. Garcia and Sriram (1997) have investigated a framework for evaluating trade-offs between competing designs which evolve with additional information. Chen and colleagues (1997) have extended Taguchi's methods in developing their *Robust Concept Exploration Method* (RCEM) which assists designers in identifying robust and flexible designs. While modifying design variable values can aid in making the product quality characteristics insensitive to the manufacturing process variation, there are limits to independently optimizing the design without also considering optimizing the manufacturing system. Process variation may still be too high or the cost of the modified design may be too expensive

## **2.6 Controls**

The final area of related work is within the controls community. Boning's work in Run-by-Run control is an example of a related approach (Boning, Moyne et al. 1996). They use designed experiments to determine a response surface, which is then linearized around an operating point and used to determine control for the system. Gershwin and his colleagues have also considered the implementation of new controls strategies on systems (Gershwin, Hildebrant et al. 1984; Bonvik 1996). They focus primarily on time and information, considering the effects of variation on throughput, rather than quality.

## Chapter 3: Variation in Systems

As discussed in Chapter 1, variation is inherent in any manufacturing operation or system. In order to reduce end-of-line variation and improve product quality, we must first identify the major sources of variation and then understand how it propagates through a system. In this chapter we will develop analytical expressions that predict the output variation of operations and systems. These expressions are based in statistics; we consider the inputs and outputs of a manufacturing operation to be random variables, with some nominal values and associated probability distribution functions. We then predict output means and variances based on the inputs and process sensitivities. Variance will be used as a quantitative measure of product variation throughout this thesis.

In this chapter, we first derive analytical expressions for the output variation of a single operation, and then extend the analysis to systems composed of multiple operations. We present the concept of the Integrated System Model (ISM), a framework for modeling variation propagation in manufacturing systems. Finally we develop a method for system-level parameter selection to reduce end-of-line variation.

### 3.1 Variation in a Single Operation

A manufacturing operation can be abstracted as a mapping between vectors. The schematic in Figure 3.1 depicts a generalized operation, where  $F$  is the functional mapping between input vectors  $\bar{x}$  and  $\bar{q}_1$ , and output vector  $\bar{q}_2$ . In this representation, the inputs are separated into two categories. Vector  $\bar{q}_1$  represents either raw material or the output of a previous operation (work-in-process). This vector will generally contain information about geometry and material properties. The vector  $\bar{x}$  contains values of process parameters unique to this operation. These might be settings on a machine or characteristic times or temperatures. The vector of output quality characteristics,  $\bar{q}_2$ , contains information describing important geometric characteristics or material properties of the processed part. This vector may then act as the input to a successive operation. For the purposes of this derivation, the nominal values of the process parameters are considered fixed. In a later section we will consider making changes to nominal operating conditions for increased robustness.

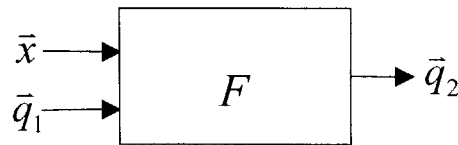


Figure 3.1: Schematic Representation of Operation.

We can represent the generalized operation of Figure 3.1 analytically as:

$$\bar{q}_2 = F(\bar{x}, \bar{q}_1) \quad (3.1)$$

This equation describes the output of the operation for any nominal values of the incoming material characteristics and process parameters. In order to use (3.1) to understand how manufacturing variations affect the product, we must consider not just a single trial  $(\bar{x}, \bar{q}_1)$ , but a number of input and output trials over time. We consider the inputs to be random variables, each with a mean and an associated probability density function (pdf). The outputs are then also random variables, whose expected values and probability density functions can be determined from the means and probability density functions of the inputs.

Making these assumptions, we can determine the expected values of the output quality characteristics  $\bar{q}_2$  of a series of  $N$  parts produced by the operation (3.1) as:

$$E(\bar{q}_2) = \int_N F(\bar{x}, \bar{q}_1) pdf(\bar{x}) pdf(\bar{q}_1) d\bar{x} d\bar{q}_1 \quad (3.2)$$

In (3.2),  $pdf(\bar{x})$  is the probability density function of the process parameter vector  $\bar{x}$ , and  $pdf(\bar{q}_1)$  is the probability density function of the input material vector  $\bar{q}_1$ . We can also determine the variance of the output quality characteristics as:

$$\sigma^2(\bar{q}_2) = \int_N (F(\bar{x}, \bar{q}_1) - \bar{y})^2 pdf(\bar{x}) pdf(\bar{q}_1) d\bar{x} d\bar{q}_1 \quad (3.3)$$

where  $\bar{y}$  is the expected value of each output variable as defined by (3.2).

These analytical expressions are difficult to calculate in many real situations. They can be solved numerically using Monte Carlo simulation, a technique in which a series of random numbers following a given input distribution is generated and used as a stream of inputs to equation (3.1). This results in a series of output quality characteristic values, allowing statistical determination of the output mean and distribution.

It is useful in some cases, however, to develop a closed-form analytical expression for output variation. We can derive such an expression by making two assumptions. First, we assume that the inputs to a manufacturing operation are independent random variables, with normal distributions. Second, we assume that the operation is linear in the vicinity of a given operating point. The latter assumption is also useful for Monte Carlo simulation, as it can significantly reduce computational time. The details of linearization are discussed in the following section.



### 3.2 Linearization

Although manufacturing systems are rarely linear over their full operating range, they do generally exhibit linear behavior in a small region around a given operating point. For the purposes of examining small variations, it is common practice to utilize a linear approximation around an operating point (Sachs, Prueger et al. 1992; Soons 1993; Frey and Otto 1996). The generalized operation of (3.1) can be linearized around the operating point  $(\bar{x}^*, \bar{q}_1^*)$  using a Taylor series expansion:

$$\bar{q}_2 = \bar{F}(\bar{x}^*, \bar{q}_1^*) + \left( \frac{\partial \bar{F}}{\partial \bar{x}} \right)_{\bar{x}^*, \bar{q}_1^*} (\bar{x} - \bar{x}^*) + \left( \frac{\partial \bar{F}}{\partial \bar{q}_1} \right)_{\bar{x}^*, \bar{q}_1^*} (\bar{q}_1 - \bar{q}_1^*) + H.O.T. \quad (3.4)$$

This can also be written as:

$$\bar{q}_2 = \bar{q}_2^* + [F_{\bar{x}}]_{\bar{q}^*, \bar{x}^*} \Delta \bar{x} + [F_{\bar{q}_1}]_{\bar{q}^*, \bar{x}^*} \Delta \bar{q}_1 + \bar{b} \quad (3.5)$$

where  $[F_{\bar{q}_1}]_{\bar{q}^*, \bar{x}^*}$  and  $[F_{\bar{x}}]_{\bar{q}^*, \bar{x}^*}$  are sensitivity matrices (Jacobians) composed of partial derivatives of  $F$ , and  $\bar{q}_2^*$  is the output vector containing values of  $\bar{q}_2$  evaluated at the operating point  $(\bar{x}^*, \bar{q}_1^*)$ . The vectors  $\Delta \bar{x}$ , and  $\Delta \bar{q}_1$  are deviations in the values of  $\bar{x}$  and  $\bar{q}_1$  from their values evaluated at the operating point ( $\bar{x}^*$  and  $\bar{q}_1^*$  respectively), and  $\bar{b}$  is bias error caused by neglecting higher-order terms ( $H.O.T.$ ), simplification in modeling, and random events. Error will be discussed in detail in section 3.4. The process sensitivities can be derived from the partial derivatives of the function  $F$  if it is available as a closed-form expression. Otherwise, the sensitivities can be obtained through numerical methods or designed experiments using function evaluation. Note that the sensitivity matrix components are themselves functions of the nominal operating point,  $(\bar{x}^*, \bar{q}_1^*)$ . A more detailed discussion of the sensitivity terms follows in a later section.

Returning to (3.5), we can represent the deviation of the values of  $\bar{q}_2$  from their nominal values as:

$$\Delta \bar{q}_2 = [F_{\bar{x}}]_{\bar{q}^*, \bar{x}^*} \Delta \bar{x} + [F_{\bar{q}_1}]_{\bar{q}^*, \bar{x}^*} \Delta \bar{q}_1 + \bar{b} \quad (3.6)$$

where  $\Delta \bar{q}_2$  is the deviation vector:

$$\Delta \bar{q}_2 = \bar{q}_2 - \bar{q}_2^* \quad (3.7)$$

### 3.3 Root-Sum Squares Approach

Having now linearized the generalized operation of (3.1), we can develop a closed-form analytical expression for output quality characteristic variation. By assuming that the input random variables are independent and normally distributed, we can propagate the variances of the distributions, rather than the distributions themselves. Making these assumptions and using the linearized representation (3.6), it can be shown that (Drake 1967):

$$\sigma_{\bar{q}_2, i}^2 = \sum_j \left( \frac{\partial F_i}{\partial x_j} \right)^2 \sigma_{x_j}^2 + \sum_k \left( \frac{\partial F_i}{\partial q_{1, k}} \right)^2 \sigma_{q_{1, k}}^2 + \varepsilon_v \quad (3.8)$$

where  $\varepsilon_v$  is the variance error, defined below in Section 4.3. Equation (3.8) can be written in matrix form as:

$$\bar{\sigma}_{\bar{q}_2}^2 = \left[ \bar{F}_{\bar{x}} \right]_{\bar{q}_1^*, \bar{x}^*} \bar{\sigma}_{\bar{x}}^2 + \left[ \bar{F}_{\bar{q}_1} \right]_{\bar{q}_1^*, \bar{x}^*} \bar{\sigma}_{\bar{q}_1}^2 + \bar{\varepsilon}_v \quad (3.9)$$

This equation, known as the Root-Sum Squares (RSS) formula, calculates the variance of the output quality characteristics with respect to the input variances and process sensitivities. Output variance is an indicator of process capability, as discussed below. Through the rest of this thesis, the term variation will be synonymous with output standard deviation.

### 3.4 Modeling Error

In this section we will define the bias and variance error terms,  $b$  and  $\varepsilon_v$ , in equations (3.5) and (3.9). We previously represented a generalized manufacturing operation as:

$$\bar{q}_2 = F(\bar{x}, \bar{q}_1) \quad (3.1)$$

Suppose now that  $q_2$  is a measured value of an output quality characteristic, and  $F(\bar{x}, \bar{q}_1)$  is a model prediction. The actual measured value will deviate from the prediction due to the presence of unmodeled effects and random events. This can be represented as:

$$q_2 = F(\bar{x}, \bar{q}_1) + \varepsilon_u + \varepsilon_r \quad (3.10)$$

where  $\varepsilon_u$  is a term representing unmodeled error and  $\varepsilon_r$  is a term accounting for random events. We can linearize this model around a given operating point, giving:

$$q_2 = \bar{F}(\bar{x}^*, \bar{q}_1^*) + \left( \frac{\partial \bar{F}}{\partial \bar{x}} \right)_{\bar{x}^*, \bar{q}_1^*} (\bar{x} - \bar{x}^*) + \left( \frac{\partial \bar{F}}{\partial \bar{q}_1} \right)_{\bar{x}^*, \bar{q}_1^*} (\bar{q}_1 - \bar{q}_1^*) + H.O.T. + \varepsilon_u + \varepsilon_r \quad (3.11)$$

The higher order terms can be represented as an error,  $\varepsilon_H$ , such that:

$$\varepsilon_H = \left( \frac{\partial^2 \bar{F}}{\partial \bar{x}^2} \right)_{\bar{x}^*, \bar{q}_1^*} (\bar{x} - \bar{x}^*)^2 + \left( \frac{\partial^2 \bar{F}}{\partial \bar{q}_1^2} \right)_{\bar{x}^*, \bar{q}_1^*} (\bar{q}_1 - \bar{q}_1^*)^2 + \left( \frac{\partial^3 \bar{F}}{\partial \bar{x}^3} \right)_{\bar{x}^*, \bar{q}_1^*} (\bar{x} - \bar{x}^*)^3 + \left( \frac{\partial^3 \bar{F}}{\partial \bar{q}_1^3} \right)_{\bar{x}^*, \bar{q}_1^*} (\bar{q}_1 - \bar{q}_1^*)^3 + \dots \quad (3.12)$$

Therefore:

$$q_2 = \bar{F}(\bar{x}^*, \bar{q}_1^*) + \left( \frac{\partial \bar{F}}{\partial \bar{x}} \right)_{\bar{x}^*, \bar{q}_1^*} (\bar{x} - \bar{x}^*) + \left( \frac{\partial \bar{F}}{\partial \bar{q}_1} \right)_{\bar{x}^*, \bar{q}_1^*} (\bar{q}_1 - \bar{q}_1^*) + \varepsilon_H + \varepsilon_u + \varepsilon_r \quad (3.13)$$

for a given measurement. If we express the predicted value of the model as  $q_p$ , we can write:

$$q_2 = q_p + \varepsilon_H + \varepsilon_u + \varepsilon_r \quad (3.14)$$

Over a series of measurements, the mean measured quality characteristic value,  $\bar{q}_2$ , can be represented in terms of the predicted quality characteristic value and the mean value of each of the errors. Error due to unmodeled effects and error due to higher-order terms will have mean values  $b_u$  and  $b_H$ , respectively. The error due to random effects will be represented by a standard deviation; the mean value of this error is zero. We can thus calculate the mean value of the measurements as:

$$\bar{q}_2 = q_p + b_H + b_u \quad (3.15)$$

The errors in mean can be grouped into a single mean bias term:  $b$  :

$$\bar{q}_2 = q_p + b \quad (3.16)$$

We can then define mean bias as the difference between the mean measured value of a quality characteristic and its predicted value:

$$b = \bar{q}_2 - q_p \quad (3.17)$$

Having derived the bias term,  $b$ , we now turn to variance error,  $\varepsilon_v$ . To determine this error, we must return to equation (3.13):

$$q_2 = \bar{F}(\bar{x}^*, \bar{q}_1^*) + \left( \frac{\partial \bar{F}}{\partial \bar{x}} \right)_{\bar{x}^*, \bar{q}_1^*} (\bar{x} - \bar{x}^*) + \left( \frac{\partial \bar{F}}{\partial \bar{q}_1} \right)_{\bar{x}^*, \bar{q}_1^*} (\bar{q}_1 - \bar{q}_1^*) + \varepsilon_H + \varepsilon_u + \varepsilon_r \quad (3.13)$$

Using the root-sum square approach, we can represent the measured quality characteristic variance in terms of the variance of the inputs and the variance of the errors:

$$\sigma_{\bar{q}2}^2 = \left[ \bar{F}_{\bar{x}}^2 \right]_{\bar{q}_1^*, \bar{x}^*} \bar{\sigma}_{\bar{x}}^2 + \left[ \bar{F}_{\bar{q}_1}^2 \right]_{\bar{q}_1^*, \bar{x}^*} \bar{\sigma}_{\bar{q}_1}^2 + \sigma_{\bar{\varepsilon}_H}^2 + \sigma_{\bar{\varepsilon}_u}^2 + \sigma_{\bar{\varepsilon}_r}^2 + \varepsilon_s \quad (3.18)$$

Here  $\sigma_{\bar{\varepsilon}_H}$  is the standard deviation of the higher-order term error,  $\sigma_{\bar{\varepsilon}_u}$  is the standard deviation of the error due to unmodeled terms, and  $\sigma_{\bar{\varepsilon}_r}$  is the standard deviation of the error due to random events. A new error term,  $\varepsilon_s$ , is introduced, representing the error in the prediction due to approximation of the sensitivities. If we write the predicted quality characteristic variance as:

$$\sigma_p^2 = \left[ \bar{F}_{\bar{x}}^2 \right]_{\bar{q}_1^*, \bar{x}^*} \bar{\sigma}_{\bar{x}}^2 + \left[ \bar{F}_{\bar{q}_1}^2 \right]_{\bar{q}_1^*, \bar{x}^*} \bar{\sigma}_{\bar{q}_1}^2 \quad (3.19)$$

then the measured value of quality characteristic variance  $\sigma_{\bar{q}2}^2$  will be a function of the predicted variance, the variance of the errors, and the error due to sensitivity approximation:

$$\sigma_{\bar{q}2}^2 = \sigma_p^2 + \sigma_{\bar{\varepsilon}_H}^2 + \sigma_{\bar{\varepsilon}_u}^2 + \sigma_{\bar{\varepsilon}_r}^2 + \varepsilon_s \quad (3.20)$$

We can group the error variance terms into a single term,  $\sigma_\varepsilon^2$  such that:

$$\sigma_\varepsilon^2 = \sigma_{\bar{\varepsilon}_H}^2 + \sigma_{\bar{\varepsilon}_u}^2 + \sigma_{\bar{\varepsilon}_r}^2 \quad (3.21)$$

allowing us to re-write (3.20) as:

$$\sigma_{\bar{q}2}^2 = \sigma_p^2 + \sigma_\varepsilon^2 + \varepsilon_s \quad (3.22)$$

We can now see that the deviation of the predicted variance from the measured value of variance is the sum of the variance due to error terms and the error due to approximation of the sensitivities:

$$\sigma_{\bar{q}2}^2 - \sigma_p^2 = \sigma_\varepsilon^2 + \varepsilon_s \quad (3.23)$$

Both of these error terms can then be grouped into total variance error,  $\varepsilon_v$  such that:

$$\varepsilon_v = \sigma_\varepsilon^2 + \varepsilon_s = \sigma_{\bar{q}2}^2 - \sigma_p^2 \quad (3.24)$$

The definitions of bias (3.17) and variance error (3.24) apply throughout this text.

### 3.5 Manufacturing Process Tolerance Threshold

As discussed in Chapter 1, there is an important distinction between tolerance and variation. Tolerance represents the amount of allowable variation on a given quality characteristic and is set by the designer, usually with regards to performance specifications. Variation, on the other hand, is a function of the process inputs and the process itself. As was shown in Figure 1.1, the probability that a produced part will meet its tolerance specifications is a function of both the process variation and the bias. In this section we will focus on the process variation alone, implicitly assuming that the process is on target.

Ideally, designers should take process variation into account when determining product tolerances, in order to ensure their feasibility. We have found that this is rarely the case; tolerances are usually based entirely on performance requirements or on in-house guidelines. For example, part design engineers at one major aerospace manufacturer tolerance all sheet metal parts to either 10 thousandths or 30 thousandths of an inch, depending on their judgement of the part's "importance." The manufacturing engineers at this company are then forced to develop processes capable of meeting these largely arbitrary tolerances, often resulting in long development times and high cost. A more cost-effective approach would involve determining the minimum variation inherent in a process, and incorporating this information into the tolerance design process. Tolerances which are set without consideration of minimal process variation can lead to high costs due to more complex process development, longer processing times, and higher scrap and rework rates.

In this section we present the concept of the *Tolerance Threshold*, a lower bound on the process variation inherent in a manufacturing operation with no process control. This quantity has been termed "process capability" by Kalpakjian (1995), but will be renamed here to differentiate it from the tolerance-based Process Capability Indices such as  $c_p$ ,  $c_{pk}$ , and  $C$ . As discussed in Chapter 2, tolerance-based indices are commonly used in industry to numerically evaluate the ability of a process to meet a given set of tolerances. The use of these indices presumes that part tolerances are pre-existing, and independent of the process. The indices themselves indicate *process* capability, which implies that the process must be adjusted to produce parts that meet some pre-determined tolerances.

The Tolerance Threshold, on the other hand, is the predicted output variation of a given operation, based on input variation and process sensitivities. It is evaluated at a given operating point. The Tolerance Threshold value can be used to either guide tolerancing or to evaluate the feasibility of existing tolerances. Unlike the indices discussed previously, the Tolerance Threshold value is predicted through modeling, rather than being predicated upon measurements of variation in an existing system. As such, it can be used to guide the tolerancing of parts during design, prior to any actual production.

To determine the Tolerance Threshold of an operation, we propagate variances with ranges rather than distributions. These ranges are bilateral limits around a nominal value, each specified according to a  $3\sigma$  yield criterion (99.7%). If the proposed or actual

tolerances on a quality characteristic are smaller than the Threshold value for that characteristic, more than 0.3% of parts will fail to meet specifications. If, on the other hand, the tolerances are larger than the Threshold value, the process is capable of producing 99.7% acceptable parts.

When calculating the Tolerance Threshold value, variation inherent to the operation is shown as a standard deviation of the random variable vector  $\bar{x}$ , which contains nominal values of process parameters. Variation on the incoming material or work-in-process is considered to be within some known tolerance band  $\bar{T}_{q_1}$ . The range of output variation for the given operation can be determined through one of two methods: worst-case stack up or root-sum squares (RSS). The former is a very conservative estimate, assuming that all random variables are at their  $3\sigma$  limits, and add together. The RSS approach is based upon the statistical combination of distributions, and provides a more accurate estimate. Both methods are developed below.

### 3.5.1 Worst Case Tolerance Threshold Determination

The worst case stack-up approach is based on equation (3.5), the linearized representation of a generalized operation. To determine the Tolerance Threshold, the distributions in (3.5) are bounded with bilateral tolerance limits at  $\pm 3\sigma$ . This gives:

$$\frac{\tau_{q_2,i}}{2} = \sum_j \left| \frac{\partial F_i}{\partial x_j} \right| 3\sigma_{x_j} + \sum_k \left| \frac{\partial F_i}{\partial q_{1,k}} \right| \frac{T_{q_{1,k}}}{2} + 3\sigma_{\bar{\varepsilon}_i} + \bar{\varepsilon}_s \quad (3.25)$$

which can be written more compactly as:

$$\bar{\tau}_{q_2} = 6 \left[ \left[ F_{\bar{x}} \right] \right]_{q^*, \bar{x}^*} \bar{\sigma}_x + \left[ \left[ F_{\bar{q}} \right] \right]_{q^*, \bar{x}^*} \bar{T}_{q_1} + 6\bar{\sigma}_{\bar{\varepsilon}} + \bar{\varepsilon}_s \quad (3.26)$$

where  $\left[ \left[ F_{\bar{x}} \right] \right]_{q^*, \bar{x}^*}$  and  $\left[ \left[ F_{\bar{q}} \right] \right]_{q^*, \bar{x}^*}$  are the matrices of absolute values of each sensitivity coefficient, as in equation (3.9),  $\bar{T}_{q_1}$  are the tolerances on the work-in-process entering the operation, and  $\bar{\tau}_{q_2}$  is the vector of Tolerance Threshold values for the final product. The worst-case approach quickly becomes unreasonable for operations with more than two output variables. A more accurate approach is the root-sum squares determination, discussed in the next section.

### 3.5.2 RSS Tolerance Threshold Determination

A more accurate method is the root-sum squares approach. This method requires bounding the distributions in (3.9) with tolerance limits at  $\pm 3\sigma$ . In this case:

$$\bar{\tau}_{q_2}^2 = 36 \left[ \left[ F_{\bar{x}}^2 \right] \right]_{q^*, \bar{x}^*} \bar{\sigma}_x^2 + \left[ \left[ F_{\bar{q}}^2 \right] \right]_{q^*, \bar{x}^*} \bar{T}_{q_1}^2 + 36\bar{\sigma}_{\bar{\varepsilon}}^2 + \bar{\varepsilon}_s^2 \quad (3.27)$$

This method works well with normal independent data and reasonably linear systems. In other cases, the integral in equation (3.3) can be used with normal distributions on  $\bar{q}_1$  and with  $\pm 3\sigma$  limits on  $\bar{T}_{q_1}$ .

### 3.6 Serial Systems

Having outlined two methods for determining the output quality characteristic variance of a single operation, we now examine variation propagation through a *system* composed of multiple operations. Figure 3.2 illustrates a simple system, comprised of two operations in series.

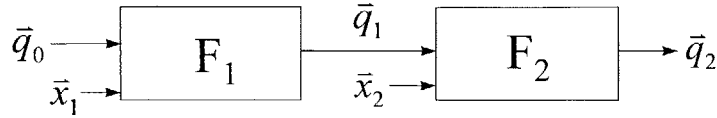


**Figure 3.2: A two operation serial system.**

As with single operations,  $F_1$  and  $F_2$  represent the mapping between input and output vectors, such that:

$$\bar{q}_2 = F_2(\bar{q}_1, \bar{x}_2), \quad (3.28)$$

$$\bar{q}_1 = F_1(\bar{x}_1, \bar{q}_0). \quad (3.29)$$

From the preceding section, we know that the variation of the end-of-line quality characteristics,  $\bar{\sigma}_{\bar{q}_2}$ , will be a function of both the input variation to each operation and the process sensitivities. End-of-line variance is then:

$$\sigma_{\bar{q}_2}^2 = \left[ F_{2\bar{q}_1}^2 \right]_{\bar{q}_1, \bar{x}_2} \bar{\sigma}_{\bar{q}_1}^2 + \left[ F_{2\bar{x}_2}^2 \right]_{\bar{q}_1, \bar{x}_2} \bar{\sigma}_{\bar{x}_2}^2 + \bar{\epsilon}_{v_2} \quad (3.30)$$

where

$$\sigma_{\bar{q}_1}^2 = \left[ F_{1\bar{q}_0}^2 \right]_{\bar{q}_0, \bar{x}_1} \bar{\sigma}_{\bar{q}_0}^2 + \left[ F_{1\bar{x}_1}^2 \right]_{\bar{q}_0, \bar{x}_1} \bar{\sigma}_{\bar{x}_1}^2 + \bar{\epsilon}_{v_1} \quad (3.31)$$

as before. Substituting (3.31) into (3.30) gives an expression for the end-of-line variance in terms of the variance of all system inputs:

$$\bar{\sigma}_{\bar{q}_2}^2 = \left[ F_{2\bar{x}_2}^2 \right]_{\bar{q}_1, \bar{x}_2} \bar{\sigma}_{\bar{x}_2}^2 + \left[ F_{2\bar{q}_1}^2 \right]_{\bar{q}_1, \bar{x}_2} \left[ F_{1\bar{q}_0}^2 \right]_{\bar{q}_0, \bar{x}_1} \bar{\sigma}_{\bar{q}_0}^2 + \left[ F_{2\bar{q}_1}^2 \right]_{\bar{q}_1, \bar{x}_2} \left[ F_{1\bar{x}_1}^2 \right]_{\bar{q}_0, \bar{x}_1} \bar{\sigma}_{\bar{x}_1}^2 + \left[ F_{2\bar{q}_1}^2 \right]_{\bar{q}_1, \bar{x}_2} \bar{\epsilon}_{v_1} + \bar{\epsilon}_{v_2} \quad (3.32)$$

It is useful to generalize (3.32) to describe the output variance of the  $i^{\text{th}}$  operation of a series system:

$$\sigma_{\bar{q}_i}^2 = \left[ F_{i, \bar{q}_{i-1}}^2 \right]_{\bar{q}_{i-1}^*, \bar{x}_i^*} \bar{\sigma}_{\bar{q}_{i-1}}^2 + \left[ F_{i, \bar{x}}^2 \right]_{\bar{q}_{i-1}^*, \bar{x}_i^*} \bar{\sigma}_{\bar{x}_i}^2 + \bar{\varepsilon}_{v_i}. \quad (3.33)$$

Similarly, we can derive generalized iterative relationships for the Tolerance Threshold of the  $i^{\text{th}}$  operation in a series, similar to (3.26) and (3.27). For the worst-case stack-up approach:

$$\bar{\tau}_i = 6 \left[ F_{i, \bar{x}} \right]_{\bar{q}_{i-1}^*, \bar{x}_i^*} \bar{\sigma}_{\bar{x}_i} + \left[ F_{i, \bar{q}_{i-1}} \right]_{\bar{q}_{i-1}^*, \bar{x}_i^*} \bar{T}_{i-1} + 6 \bar{\sigma}_{\bar{\varepsilon}_i} + \bar{\varepsilon}_{s_i} \quad (3.34)$$

and for the RSS analysis,

$$\bar{\tau}_i^2 = 36 \left[ F_{i, \bar{x}}^2 \right]_{\bar{q}_{i-1}^*, \bar{x}_i^*} \bar{\sigma}_{\bar{x}_i}^2 + \left[ F_{i, \bar{q}_{i-1}}^2 \right]_{\bar{q}_{i-1}^*, \bar{x}_i^*} \bar{T}_{i-1}^2 + 36 \bar{\sigma}_{\bar{\varepsilon}_i}^2 + \bar{\varepsilon}_{s_i} \quad (3.35)$$

These equations can be used to determine the accumulated variation or Tolerance Threshold value at any stage of a transfer line.

### 3.7 Parallel Operations

While many common manufacturing systems are transfer lines composed of operations linked in series, there are also a number of systems where the outputs of several independent processes become inputs to a single process. We term these *parallel operations*. One example is assembly, in which multiple parts and sub-assemblies are brought together in a single operation. Figure 3.3 depicts the simple case of two operations which feed into a single, third operation.

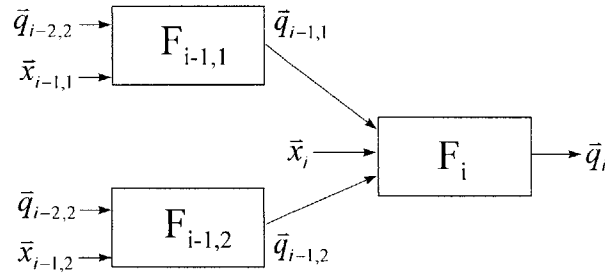


**Figure 3.3: Parallel Operations.**



The framework we have outlined for serial operations is directly applicable to parallel operations by simply adding inputs to the  $i^{\text{th}}$  operation. Thus if there are  $n$  parallel operations feeding into operation  $i$ , the output variance of operation  $i$  will be:

$$\bar{\sigma}_{\bar{q}_i}^2 = \left[ F_{\bar{x}_i}^2 \right]_{\bar{q}_i^*, \bar{x}_i^*} \bar{\sigma}_{\bar{x}_i}^2 + \bar{\varepsilon}_{v_i} + \sum_n \left( \begin{array}{l} \left[ F_{\bar{q}_{i,n}}^2 \right]_{\bar{q}_{i-1}^*, \bar{x}_i^*} \left[ F_{\bar{q}_{i-1,n}}^2 \right]_{\bar{q}_{i-2,n}^*, \bar{x}_{i-1,n}^*} \bar{\sigma}_{\bar{q}_{i-2,n}}^2 \\ + \left[ F_{\bar{x}_{i,n}}^2 \right]_{\bar{q}_{i-1}^*, \bar{x}_i^*} \left[ F_{\bar{x}_{i-1,n}}^2 \right]_{\bar{q}_{i-2,n}^*, \bar{x}_{i-1,n}^*} \bar{\sigma}_{\bar{x}_{i-2,n}}^2 + \bar{\varepsilon}_{v_{i-1,n}} \end{array} \right) \quad (3.36)$$

Similarly one can calculate the Tolerance Threshold value for a parallel system using a worst case analysis as:

$$\bar{t}_i = \left[ F_{i,\bar{x}} \right]_{\bar{q}_{i-1}^*, \bar{x}_{i-1}^*} 6\bar{\sigma}_{\bar{x}_i} + 6\bar{\sigma}_{\bar{\varepsilon}_i} + \bar{\varepsilon}_{s_i} + \sum_n \left( \left[ F_{i,\bar{q}_{i-1,n}} \right]_{\bar{q}_{i-1}^*, \bar{x}_i^*} \bar{T}_{i-1,n} \right) \quad (3.37)$$

And by the RSS method as,

$$\bar{t}_i^2 = 36 \left[ F_{i,\bar{x}}^2 \right]_{\bar{q}_{i-1}^*, \bar{x}_{i-1}^*} \bar{\sigma}_{\bar{x}_i}^2 + 36\bar{\sigma}_{\bar{\varepsilon}_i}^2 + \bar{\varepsilon}_{s_i} + \sum_n \left( \left[ F_{i,\bar{q}_{i-1,n}}^2 \right]_{\bar{q}_{i-1}^*, \bar{x}_i^*} \bar{T}_{i-1,n}^2 \right) \quad (3.38)$$

### 3.8 Integrated System Model

The *Integrated System Model (ISM)* is a framework for evaluating variation propagation through a manufacturing system. Composed of linked mathematical models of each operation, the ISM allows easy identification of the major sources of variation in the system, and serves as a platform for evaluating variation reduction strategies.

Traditional approaches to the analysis of manufacturing operations have involved the development of mathematical models that predict nominal output values based on nominal input values. We call these *predictive models*; they can be either physics-based or statistical. Predictive models alone are not sufficient for evaluating the effects of variation in manufacturing systems. Also necessary are models linking input variations and noise to output quality characteristic variations. These *variational models* are derived from the predictive models through sensitivity analysis or Jacobians. They contain matrices of local sensitivities (linearized partial derivatives) relating input and output variations.

To evaluate the effects of variation within manufacturing systems, we couple predictive and variational models of each operation within the system. When linked together with any feedback or feed-forward control loops existing in or between the actual processes, the resulting large-system model is called an “Integrated System Model.” The ISM is shown in schematic form in Figure 3.4, and discussed in detail through the rest of this section. An example ISM is developed in Chapter 5.

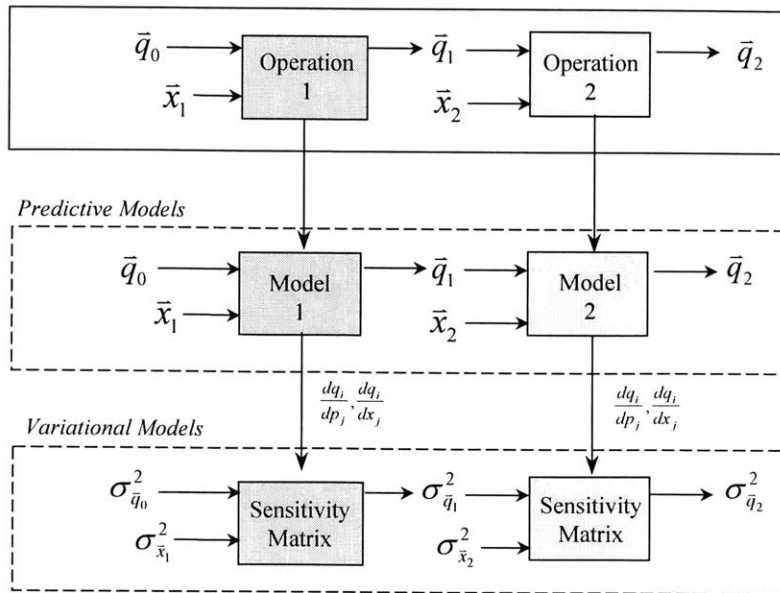


**Figure 3.4: Integrated System Model.**

### 3.8.1 Predictive Models

A predictive model is defined as a mathematical mapping between nominal input values and nominal output values. This type of model can range in complexity from a closed-form analytical expression to a complex numerical simulation. As indicated by its name, the predictive model must be able to predict the values of desired output quantities, given the relevant input parameters. For the purposes of this discussion, we will consider models of a generalized manufacturing operation in which two classes of input variable are mapped to one class of output variable, as shown in Figure 3.4.

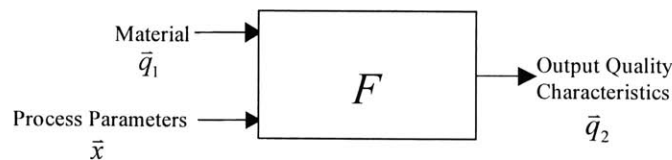


**Figure 3.4: Generalized Manufacturing Operation.**

As outlined previously, there are two input vectors to this operation. The vector  $\bar{q}_1$  represents either raw material or the output of a previous operation (work-in-process), while the vector  $\bar{x}$  accounts for process parameters unique to this operation. The vector of output quality characteristics,  $\bar{q}_2$ , contains information about material properties or geometric characteristics describing the processed part. This vector may act as an input to a successive operation, giving rise to serial and parallel systems.

It is important to validate each predictive model. Output predictions must be compared to measured output values in order to ensure that the model is an adequate representation of the physical process. While many manufacturing processes are non-linear through their process space, it is often reasonable to assume linearity in a small region around a given operating point. To ensure validity, the predictive model must be evaluated at every operating point of interest.

### 3.8.2 Variational Models

The second major component of the ISM is the variational model. Just as the predictive model maps nominal input values to predicted nominal output values, the variational model serves as a mapping between the variances of the inputs and predicted variances of the outputs. The variances are related through sensitivity matrices, composed of partial derivatives. A variational model for a generalized operation is shown in schematic form in Figure 3.5. The rest of this section discusses the variational model in detail.

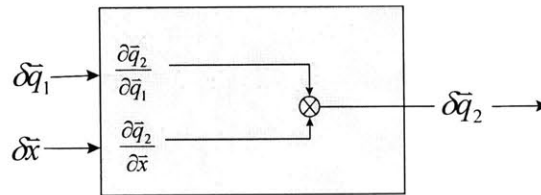


**Figure 3.5: Variational Model.**

#### 3.8.2.1 Derivation of Sensitivity Matrices

As mentioned previously, the sensitivity matrices are derived from predictive models. The type of predictive model determines the best method for deriving the sensitivity matrices. Methods associated with several types of predictive model are discussed in this section.

##### *Closed-Form Analytic Expressions*

A closed form predictive model is ideal. The sensitivity matrices can be directly derived from this model by taking partial derivatives of each output with respect to each input. The most advantageous feature of closed-form predictive models is the fact that the partial derivatives will be valid over the entire model space, not just in a localized region around the operating point.

##### *Numerical Simulation*

When the predictive model is a numerical process simulation that runs quickly with little computational effort, one method for deriving the sensitivity matrices is through Monte Carlo analysis. A Monte Carlo simulation package such as *Crystal Ball* can numerically determine the effect of each input variable on each output variable. Accuracy depends on the number of trials, which is in turn a function of the speed of the process simulation.

### *Complex Numerical Simulation*

Some predictive models consist of numerical simulations that are both complex and computationally intensive. Many finite-element based models fit into this category. In these situations it is often impossible to run many simulations, necessitating some approximation technique. We suggest the use of a localized response surface, centered on the operating point of interest. In situations where a number of operating points must be considered, we implement an approximate response surface of the entire parameter space, supplemented by more accurate localized response surfaces where necessary. This is similar to the method described by Guo and Sachs (1993), except that we use both the localized and generalized surfaces in conjunction. We now briefly discuss Response Surface Methods and their development through designed experiments.

### *Response Surface Methods*

According to Montgomery, “Response surface methodology, or RSM, is a collection of mathematical and statistical techniques that are useful for the modeling and analysis of problems in which a response of interest is influenced by several variables and the objective is to optimize this response” (Montgomery, 1984). In essence, a response surface is a multi-dimensional contour map of the output of a function, plotted over the possible values of its inputs. The response surface usually approximates the actual function through a low-order polynomial, in the region of interest.

The parameters required to fit the response surface can be obtained from the actual system (in this case the numerical model) in several ways. The most common method is through a designed experiment over the model space. Design of Experiments is discussed in the following section.

### *Design of Experiments*

Design of Experiments (DoE) is an efficient method for determining the effects of several input parameters on a single output parameter. It involves constructing and running an experiment composed of a series of trials, each with a different pre-determined combination of parameter settings. The results of each trial are analyzed together in order to determine the effect of each parameter and parameter combination on the output parameter. The use of designed experiments can significantly reduce the number of trials necessary to determine parameter effects and interactions.

In DoE terminology, the input parameters of interest are known as *factors*. Each factor is tested at several different settings, or *levels*. It is common to use either two levels (high and low), or three levels (high, medium, low). The levels are chosen such that they span the region of interest of each input parameter. A designed experiment can be designated by an exponential, in which the number of levels is raised to the number of factors. For example, consider an experiment with 3 factors and 2 levels (a  $2^3$  experiment). Evaluating every combination of factors and levels (called a *full-factorial* experiment) would require a total of 8 different trials. Using designed experiment techniques, however, we can run a  $2^3$  *partial-factorial* experiment, requiring only 4 trials. This partial-factorial experiment can then be analyzed to determine all parameter effects and two-parameter interaction effects. More detailed treatments of the Design of

Experiments methodology can be found in (DeVor, Chang et al. 1992) and (Phadke 1989).

### 3.8.3. Linking the ISM

As discussed previously, the ISM is composed of linked predictive and variational models for each operation within a system. Having discussed the form of predictive models and the successive derivation of variational models for individual operations, we now describe the linking process.

Models for each operation must be linked within some overarching environment. For our implementation, we have chosen to use a spreadsheet software package. The spreadsheet contains a number of separate “process sheets,” one for each operation within the system, and a “control sheet” listing the values and variations of the initial system inputs (characteristics of the stock material) and end-of-line outputs. Each process sheet contains a table of sensitivities for a given operation. These sensitivities are linked in two ways: as a linearized model of the operation around a given operating point (using equation 3.5) and as an RSS variational model of the operation (using equation 3.9). Implementation of a worst-case variational model is straightforward, requiring only that each sensitivity term be multiplied by the corresponding input variation and then summed with all others.

The process sheets are then linked together by setting the values of the input variables  $\bar{q}_i$  on the process sheet for operation  $i$ , equal to the values in the output cells  $\bar{q}_i$  from the process sheet for operation  $i-1$ . As such, the output of one operation is effectively passed to another operation as if it were work-in-process. Inputs to the first operation in the system are contained on the control sheet, and end-of-line nominal values and variations are reported there as well. This spreadsheet implementation can be used to propagate variation analytically through a system, to evaluate the effect of parameter changes on end-of-line variation, and as a system model for Monte Carlo simulation.

## 3.9 System-Level Parameter Design

One important use of the ISM is system-level parameter design. Most traditional parameter design methods aim to increase robustness on an operational level. They make the implicit assumption that if each operation is optimized for minimum output variation, the entire system will then also be optimized for minimum output variation. What is often overlooked is the fact that the output variation, and by default, the sensitivity matrices as well, are localized values, contingent on the nominal operating point of an operation. This operating point is, in turn, determined by the target values of the end-of-line quality characteristics and by the operating points of other operations in the system. Not only will the sensitivity of each operation to input variation likely change between operating points, but each system has the potential for a number of operating point combinations that will result in the target end-of-line characteristic values. As such, a system-level parameter design method is needed to evaluate each of these combinations

and choose the one that allows the product to meet end-of-line specifications while also resulting in the lowest variation.

The advantage of a system model incorporating both nominal values and variation is that we can quickly search through all of the possible operating point combinations, to find the one with both the desired output values and the lowest end-of-line variation. This state may require that a given operation be set at a non-optimal point if this setting then allows an upstream or downstream operation to operate under conditions which are much more robust.

In this section, we develop an approach to system-level robustness. Strictly speaking this is not “optimization,” since we are obtaining a localized minimum through a simple gradient search on an approximate response surface modeling the actual system. The same problem formulation could be used with other search methods to guarantee a global minimum over the model space, if desired.

### 3.9.1 Variation in the Presence of Adjustments

In this section we first re-work the variation propagation equations derived previously, in order to isolate *adjustable variables*: process parameters whose values can be changed between parts or batches. We then develop a method for choosing the values of these parameters, in order to both meet end-of-line quality characteristic tolerances while reducing end-of-line variation. In Chapter 4 we will discuss the use of real-time changes to the adjustable variables to implement feed-forward or feedback process control.

#### 3.9.1.1 Propagation Equations With Adjustable Variables

In Figure 3.6, we present a schematic representation of a generalized manufacturing operation with adjustable input variables. This diagram is similar to Figure 3.1, but with an additional input vector  $\bar{p}$ . This vector contains the nominal values of adjustable process parameters; these are inputs that can easily be changed between parts or batches. Examples of adjustable parameters include machine settings and critical times. The vector  $\bar{x}$  still represents process parameters unique to this operation, with fixed nominal values. Vectors  $\bar{q}_1$  and  $\bar{q}_2$  contain material properties and geometry of the incoming and outgoing material as before.

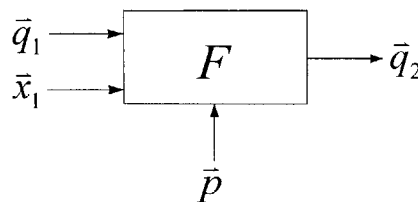


**Figure 3.6: Operation with Adjustable Variables.**

Like the other input parameters, the adjustable variables have both a nominal set-point value, and some variation about this nominal, which contributes to the end-of-line product variation. The variation due to adjustable variables can easily be incorporated into the previously derived propagation equations through the addition of an extra term. For a single operation, the Taylor series expansion of equation (3.4) becomes:

$$\bar{q}_2 \approx \bar{F}(\bar{x}^*, \bar{q}_1^*) + \left( \frac{\partial \bar{F}}{\partial \bar{x}} \right)_{\bar{x}^*, \bar{q}_1^*, \bar{p}^*} (\bar{x} - \bar{x}^*) + \left( \frac{\partial \bar{F}}{\partial \bar{q}_1} \right)_{\bar{x}^*, \bar{q}_1^*, \bar{p}^*} (\bar{q}_1 - \bar{q}_1^*) + \left( \frac{\partial \bar{F}}{\partial \bar{p}} \right)_{\bar{x}^*, \bar{q}_1^*, \bar{p}^*} (\bar{p} - \bar{p}^*) + H.O.T.$$

which can be written compactly as:

$$\bar{q}_2 = \bar{q}_2^* + [F_{\bar{x}}]_{\bar{q}^*, \bar{x}^*, \bar{p}^*} \Delta \bar{x} + [F_{\bar{q}_1}]_{\bar{q}^*, \bar{x}^*, \bar{p}^*} \Delta \bar{q}_1 + [F_{\bar{p}}]_{\bar{q}^*, \bar{x}^*, \bar{p}^*} \Delta \bar{p} + \bar{b} \quad (3.39)$$

Note that the sensitivity matrices  $[F]$  are now dependent on an operating point defined by  $(\bar{q}_1^*, \bar{x}^*, \bar{p}^*)$ . This operating point will be represented by the symbol “\*” through the rest of this thesis. The Root-Sum Squares output variation of this operation is:

$$\bar{\sigma}_{\bar{q}_2}^2 = [F_{\bar{x}}^2]_{\bar{q}^*, \bar{x}^*, \bar{p}^*} \bar{\sigma}_{\bar{x}}^2 + [F_{\bar{q}_1}^2]_{\bar{q}^*, \bar{x}^*, \bar{p}^*} \bar{\sigma}_{\bar{q}_1}^2 + [F_{\bar{p}}^2]_{\bar{q}^*, \bar{x}^*, \bar{p}^*} \bar{\sigma}_{\bar{p}}^2 + \bar{\varepsilon}_v \quad (3.40)$$

Similarly, we can extend the variation propagation equations to account for systems with adjustable parameters. A serial system with adjustable variables is shown in schematic form in Figure 3.7:

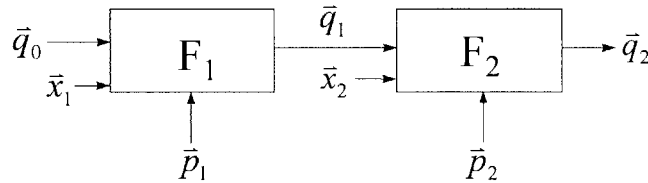


**Figure 3.7: System with Adjustable Variables.**

For a serial system with  $i$  operations, the end-of-line variation will be:

$$\sigma_{\bar{q}_i}^2 = [F_{i, \bar{q}_{i-1}}^2]_{\bar{q}^*, \bar{x}^*, \bar{p}^*} \bar{\sigma}_{\bar{q}_{i-1}}^2 + [F_{i, \bar{x}}^2]_{\bar{q}^*, \bar{x}^*, \bar{p}^*} \bar{\sigma}_{\bar{x}_i}^2 + [F_{i, \bar{p}}^2]_{\bar{q}^*, \bar{x}^*, \bar{p}^*} \bar{\sigma}_{\bar{p}_i}^2 + \bar{\varepsilon}_v \quad (3.41)$$

while for a system with  $n$  parallel operations which feed into a single operation  $i$ , end-of-line variation will be :

$$\bar{\sigma}_{\bar{q}_i}^2 = \left[ F_{\bar{x}_i}^2 \right] \bar{\sigma}_{\bar{x}_i}^2 + \left[ F_{\bar{p}_i}^2 \right] \bar{\sigma}_{\bar{p}_i}^2 + \bar{\varepsilon}_{v_i}^2 + \sum_n \left( \begin{array}{l} \left[ F_{\bar{q}_{i,n}}^2 \right] \left[ F_{\bar{q}_{i-1,n}}^2 \right]_{\bar{q}_{i-2}^*, \bar{x}_{i-1}^*, \bar{p}_{i-1}^*} \bar{\sigma}_{\bar{q}_{i-2}}^2 \\ + \left[ F_{\bar{x}_{i,n}}^2 \right] \left[ F_{\bar{x}_{i-1,n}}^2 \right]_{\bar{q}_{i-2}^*, \bar{x}_{i-1}^*, \bar{p}_{i-1}^*} \bar{\sigma}_{\bar{x}_{i-2}}^2 + \bar{\varepsilon}_{v_{i-1}}^2 \end{array} \right) \quad (3.42)$$

Equations (3.41) and (3.42) are similar to the equations derived previously for non-adjustable systems. The segregation of adjustable variables, however, allows for the evaluation of system performance at different operating points. In the following sections we develop a method for selecting the values of adjustable variables in order to decrease end-of-line variation and to determine allowable in-process tolerances.

### 3.9.2 System-Level Variation Reduction

In this section, we develop methods for selecting the values of adjustable variables  $\bar{p}$  in order to reduce end-of-line variation in a manufacturing system. We first determine the system operating point resulting in lowest end-of-line variation, assuming that adjustments are free. We then associate adjustment costs with each variable in order to find a system operating point that is both economical and robust. The problem formulations presented below can be implemented in practice with any standard optimization algorithm.

#### 3.9.2.1 Variation Reduction With No Adjustment Cost

Given a serial system with  $i$  operations, in which all adjustments are assumed equally costly, we restrict the adjustment variables  $\bar{p}_i$  to ranges  $\bar{P}_i$  where:

$$\bar{P}_i = [\bar{p}_{i,\min} \dots \bar{p}_{i,\max}]$$

such that:

$$\bar{p}_{i,\min} \leq \bar{p}_i \leq \bar{p}_{i,\max}$$

The system operating point that produces parts both meeting specifications and having lowest end-of-line variation can be found through:

$$\begin{array}{ll} \min & \|\bar{\sigma}_{\bar{q}_i}^2\| = \left[ F_{i,\bar{q}_{i-1}}^2 \right] \bar{\sigma}_{\bar{q}_{i-1}}^2 + \left[ F_{i,\bar{x}}^2 \right] \bar{\sigma}_{\bar{x}_i}^2 + \left[ F_{i,\bar{p}}^2 \right] \bar{\sigma}_{\bar{p}_i}^2 + \bar{\varepsilon}_v \\ \text{s.t.} & \bar{m}_i - \bar{\delta} \leq \bar{q}_i \leq \bar{m}_i + \bar{\delta}, \bar{q}_i = F(\bar{x}, \bar{q}_{i-1}, \bar{p}) \\ \text{over} & \bar{p}_i \in \bar{P}_i \\ & \text{where } \bar{x}_i, \bar{\sigma}_{\bar{x}_i}, \bar{\sigma}_{\bar{p}_i}, \bar{\varepsilon}_v \text{ are constant over } \bar{P}_i \end{array} \quad (3.43)$$



where  $\bar{m}_i$  is a vector of end-of-line quality characteristic target values, and  $\bar{\delta}_i$  is a vector containing allowable deviation from target. For each output quality characteristic,  $\delta_i$  should be chosen such that:

$$\delta_i + 3\sigma_{\bar{q}_i} \leq \bar{T}_{\bar{q}_i} \quad (3.44)$$

where  $\bar{T}_{\bar{q}_i}$  is the designer-set tolerance on that quality characteristic. In effect, (3.44) constrains the optimization in (3.43) to find the set of process parameter values that will produce parts with the least variation and a 99.7% chance of meeting tolerances. This is a precise restatement of the robust process design problem originally posed by Taguchi, and in fact, (3.43) reduces to Taguchi's method when examining one method with one quality characteristic.

Until now, we have assumed that all variables in  $\bar{p}_i$  can be adjusted freely within their ranges, and that all adjustments are equally costly. In reality, however, some adjustable variables are easier to change than others. We account for this in the next section.

### 3.9.2.2 Variation Reduction With Adjustment Costs

In this section, we develop a variation reduction method for a system in which process parameter adjustments have associated costs. This situation can occur when a manufacturing system is functioning at some operating point, and the operators choose to tune the system by adjusting various process parameters. The changes are likely to have different costs. Adjustments to machine settings, for instance, tend to be inexpensive or free, while changes to the process equipment or the process itself are likely to be costly. To evaluate the cost-savings of a process parameter change, we associate a cost savings with reduction in end-of-line variation, representing the increased quality of the final product. This savings will come from a decrease in the number of scrapped or reworked parts, or from a decrease in total quality loss. To determine an efficient operating point for the system, we seek to find process parameter settings such that the cost savings associated with improvement of the final product outweighs the cost of making necessary adjustments to the system. This problem can be stated as:

$$\begin{aligned} \min \quad & Cost(\bar{p}_i) = [C_q] \left[ \frac{\bar{\sigma}_{\bar{q}_i}^2 - \bar{\sigma}_{\bar{q}_i, p^*}^2}{\bar{m}_i} \right] + \sum_{n=1}^i [C_n] [\bar{p}_n - \bar{p}_{n,*}] \\ \text{s.t.} \quad & \bar{\sigma}_{\bar{q}_i}^2 = [F_{i, \bar{q}_{i-1}}]^2 \bar{\sigma}_{\bar{q}_{i-1}}^2 + [F_{i, \bar{x}}]^2 \bar{\sigma}_{\bar{x}_i}^2 + [F_{i, \bar{p}}]^2 \bar{\sigma}_{\bar{p}_i}^2 + \bar{\varepsilon}_v \\ & \bar{m}_i - \bar{\delta}_i \leq \bar{q}_i \leq \bar{m}_i + \bar{\delta}_i, \bar{q}_i = F(\bar{x}, \bar{q}_{i-1}, \bar{p}) \\ \text{over} \quad & \bar{p}_i \in \bar{P}_i \\ & \text{where } \bar{x}_i, \bar{\sigma}_{\bar{x}_i}, \bar{\sigma}_{\bar{p}_i}, \bar{\varepsilon}_v \text{ are constant over } \bar{P}_i \end{aligned} \quad (3.45)$$

Here the cost matrices  $[C]$  are diagonal, containing relative weightings of each adjustment factor in cost per unit change, and the cost savings due to reduced variation in

cost per percent of the target nominal value. This optimization problem can be solved using standard techniques. Extension of the problem statements in (3.43) and (3.45) to serial or parallel systems with more than 2 operations is straightforward.

Note that in both equations (3.43) and (3.45) above, the sensitivity matrices  $[F^2]$  are functions of a given operating point. As the adjustable parameters  $\bar{p}_i$  change, the terms in the sensitivity matrices will likely change as well. If the range  $\bar{P}_i$  is large, this change can be both significant and non-linear. As discussed previously, if the underlying predictive model is in closed form, the sensitivities will be based on partial derivatives that are valid over the entire space. If, on the other hand, the sensitivities have been derived through designed experiments or perturbation analysis on a computationally intensive predictive model, the terms will only be valid in a small region around the operating point. There are several methods for working around this problem. If the inputs are independent, one method is to conduct a designed experiment or perturbation analysis on the predictive model over the full range of possible  $\bar{P}_i$  values, and then approximate each input/output relationship with an interpolated function. The derivative of this function can be used as a continuous approximation for the actual sensitivity function. When a new “optimum” system operating point is located, a designed experiment, centered on this point, can be used to obtain more accurate localized sensitivities. The new sensitivity terms can then be used in the minimization to better determine the most robust operating point.

### 3.9.3 Approximating Sensitivities

Note that in both of the formulations above, the sensitivity matrices  $[F^2]$  are functions of a given operating point. As the adjustable parameters  $\bar{p}_i$  change, the values in the sensitivity matrices will likely change as well. If the range  $\bar{P}_i$  is large, this change can be both significant and non-linear. As discussed in the section on deriving variational models, if the underlying predictive model is computationally intensive, this problem can be addressed in several ways. One method is to do a designed experiment over the range of possible  $\bar{P}_i$  and interpolate a function through the points. The derivative of this function can then be used as a continuous approximation for the actual sensitivity function. When a new “optimum” system operating point is reached, a new localized designed experiment can be run at this point, to obtain a more accurate sensitivity. This localized sensitivity can then be used in the minimization to obtain a more accurate determination of the robust operating point.

### 3.9.4 Discussion of Related Work

The parameter design methods discussed in this section are related to the Evolutionary Operation (EVOP) method of (Box and Draper 1969). EVOP is essentially an ongoing series of designed experiments, in which plant process parameters are perturbed slightly

from their nominal values in order to determine the effect on a single output variable. The best input variable settings from one experiment are then used as nominal values for the next experiment. While the designed experiments in EVOP are conducted on the actual plant, our methods determine parameter settings off-line, through simulation. As with EVOP, we suggest using sequential designed experiments to refine set-point selection. The EVOP approach has one main advantage over our methods in that it tunes the actual system, thus eliminating the effect of modeling errors. EVOP can also account for changes in the system over time, which would require additional modeling in our approach. EVOP's main disadvantage is logistics; it is difficult or impossible to continuously change the settings of multiple input parameters for operations separated by time and space in a coordinated manner. In addition, EVOP is most effective on manufacturing systems with either continuous or high-volume production. Systems producing a small number of parts may not be able to furnish enough experiments to guide process changes.

Our parameter design methods are also similar to Taguchi's robust design methodology (Phadke 1989). Taguchi's P Diagram representation of a generic product/process, shown in Figure 3.8, is very similar to our schematic representation of a generalized manufacturing system (Figure 3.6).

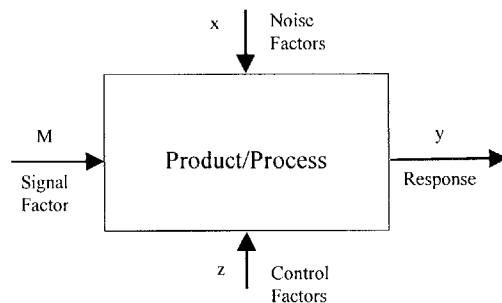


**Figure 3.8: Taguchi P Diagram.**

Our representation makes a clear distinction between incoming material characteristics and process parameters, but is similar to Taguchi's in that each input has both a signal component and a noise component. By seeking to minimize process variation while keeping nominal values on target, we are implicitly trying to maximize the S/N ratio. In effect, our parameter design approach is a multi-operation extension of Taguchi's. This extension requires new techniques; it is not generally possible, for instance, to conduct a designed experiment over an entire system due to logistical difficulties. We avoid this problem through the use of system models, which allow us to conduct matrix experiments and system-level parameter design with relative ease.

### 3.10 Selective Biasing

In the previous section we outlined a method for using the ISM to find the combination of operating points which allow the system to produce parts meeting specifications with minimum end-of-line variation. In this section we briefly outline another system-level

application of the ISM: using a process parameter in one operation to change the nominal output value of a downstream operation. This procedure is known as *selective biasing*.

To understand why we might need selective biasing, consider the simple two-operation system composed of stretch forming and chemical milling, shown in Figure 3.9. The two important end-of-line quality characteristics are final part radius and final part thickness. Suppose that we are producing parts with some target radius and thickness, and then for design reasons, wish to change the target radius value. There is no way to make a parameter change within the chemical milling operation that will change final part radius without also changing final part thickness.

This type of process parameter coupling is common in manufacturing operations. We can circumvent this problem by considering the system as a whole. The part radius after chemical milling is dependent on the stress state of the part after stretch forming, since chemical milling will relieve residual stresses, thus changing part contour. By altering a stretch forming process parameter such as pre-stretch, to change the stress state of the part, we can change the final radius without having any effect on thickness. This must be done, however, with some knowledge of the effects of the chemical milling operation, in order to determine the correct amount to change the process parameter setting.

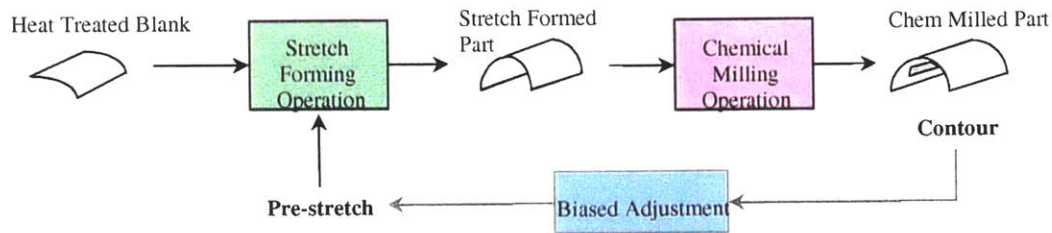


**Figure 3.9: Selective Biasing.**

Effectively we can use the system model to find a decoupled input parameter to change a given output parameter. Without detailed knowledge of the system, we might have tried to make the change solely in the chemical milling operation, which has only coupled parameters.

To determine whether a system can be selectively biased, we must examine the coupling between inputs and outputs. This can be done by taking the sensitivity matrices for each operation in the system, and assembling them into an “adjustment matrix” as shown in Figure 3.10.

$$\begin{bmatrix}
\frac{\partial q_{1,1}}{\partial p_{1,1}} & \frac{\partial q_{1,1}}{\partial p_{1,2}} & \dots & \frac{\partial q_{1,1}}{\partial p_{1,v}} & 0 & \dots & 0 \\
\frac{\partial q_{1,2}}{\partial p_{1,1}} & \frac{\partial q_{1,2}}{\partial p_{1,2}} & \dots & \frac{\partial q_{1,2}}{\partial p_{1,v}} & 0 & \dots & 0 \\
\vdots & \vdots & \ddots & \vdots & \ddots & \dots & \frac{\partial q_{i,j}}{\partial p_{i,s}} \\
\frac{\partial q_{1,j}}{\partial p_{1,1}} & \frac{\partial q_{1,j}}{\partial p_{1,2}} & \dots & \frac{\partial q_{1,j}}{\partial p_{1,v}} & \dots & \frac{\partial q_{i,j}}{\partial p_{i,s-1}} & \frac{\partial q_{i,j}}{\partial p_{i,s}} \\
\vdots & \vdots & \ddots & \vdots & \ddots & \vdots & \vdots \\
\frac{\partial q_{1,r}}{\partial p_{1,1}} & \frac{\partial q_{1,r}}{\partial p_{1,2}} & \dots & \frac{\partial q_{1,r}}{\partial p_{1,v}} & \dots & \frac{\partial q_{i,r}}{\partial p_{i,s-1}} & \frac{\partial q_{i,r}}{\partial p_{i,s}} \\
\frac{\partial q_{1,r}}{\partial p_{1,1}} & \frac{\partial q_{1,r}}{\partial p_{1,2}} & \dots & \frac{\partial q_{1,r}}{\partial p_{1,v}} & \dots & \frac{\partial q_{i,r}}{\partial p_{i,s-1}} & \frac{\partial q_{i,r}}{\partial p_{i,s}}
\end{bmatrix}$$

**Figure 3.10: Adjustment Matrix.**

The subscripts on each entry of the matrix represent respectively the operation number and the parameter number associated with each term. Thus each column in the matrix is associated with a specific process parameter, and each row in the matrix with a specific quality characteristic. The system represented by the matrix in Figure 3.9 has  $i$  operations, a total of  $r$  output quality characteristics, and  $s$  adjustable variables. The first operation has only  $v$  adjustable variables, resulting in the zero entries in the upper right hand side of the matrix.

To determine the coupling state within a given operation, we examine the columns of the sub-matrix associated with that operation. Any column with only one non-zero entry implies that the process parameter associated with that column only affects a single output for the given operation. This parameter is a candidate for selective biasing. Note that although the parameter is decoupled with respect to one operation, it may affect outputs in other operations. The entire system must be adjusted in a coordinated manner in order to ensure that any induced bias is corrected, and that the final product meets target specifications.

### 3.11 Chapter Summary

In this chapter, we showed how a generalized manufacturing operation could be represented as a transformation between input and output vectors. By linearizing this transformation, we were able to derive equations predicting output quality characteristic variation based on two methods, Root-Sum Squares and Worst-Case. We extended each method to predict end-of-line quality characteristic variation in a manufacturing system composed of multiple operations. We then used this analytical formulation as the basis of the Integrated System Model, a framework for understanding variation propagation in a system. We discussed two applications of the ISM: system-level parameter design, and selective biasing. System-level parameter design is a method for determining the set of

operating points which results in lowest end-of-line variation while still producing parts which meet specifications. Selective biasing is a means for adjusting a nominal output value in one operation by changing a process parameter in a previous operation. In the next chapter we will discuss additional applications of the ISM, including the formulation and evaluation of process control strategies.

## Chapter 4: Process Limits and Control

In the previous chapter, we derived equations for predicting process variation in operations and systems, and presented the concept of the Integrated System Model. In this chapter, we explore several applications of the ISM framework. We first use the ISM as a means for back-propagating end-of-line tolerances through a system, in order to determine the necessary limits on the output of each operation. We then discuss the use of these process limits in determining where control and measurement are required in a system. Finally we consider both feedback and feed-forward control strategies, and their impact on variation.

### 4.1. Process Limits

The variation propagation equations developed in Chapter 3 are process based, and independent of any product tolerances. As discussed in that chapter, we believe that process variation should be an important consideration during product tolerance design. In industry today, however, designers usually base tolerances completely on product specifications, with no consideration of the processes required to manufacture the product. This creates two major problems for the process engineers responsible for designing manufacturing systems. First, the processes required to manufacture a given part may not be capable of producing parts that meet a given set of tolerances. Second, although many parts are produced by multi-operation manufacturing systems, design tolerances only specify the characteristics and quality of the output of the final operation. As such, the process engineer must determine target values and allowable variation for each intermediary operation in a system. Until now, there has been no mathematical method to ensure that a manufacturing system is capable of producing a desired product. In this section we introduce the concept of *process limits*, the maximum allowable variation on each operation within a system that will guarantee that the final product meets design specifications. We first explain how to determine the process limits within a system, and then discuss the use of process limits in determining where control and measurement are required in a system.

In the previous chapter, we developed the concept of a “Tolerance Threshold,” which represents the minimum level of process variation in a manufacturing system. The Tolerance Threshold is a function of the variation of process inputs and the sensitivity of the process itself. A viable product tolerance must be larger than the Tolerance Threshold of the system used to manufacture the product. Since many designers determine tolerances without regard to process variation, it is not unlikely that a tolerance will be smaller than the Threshold value. In this situation, there are several options:

- 1) Produce some large number of parts that do not meet end-of-line specifications, and either scrap or rework these parts.
- 2) Identify those parts which will not meet end-of-line specifications at an early stage of the system, thus eliminating the wasted time and cost of processing them through other operations.

- 3) Remove variation from some step of the operation by adding process control to reduce the Threshold value.

It is common in industry to implicitly select the first option, and only evaluate quality against end-of-line specifications. It is much more cost-effective, however, to use options 2 or 3. We can use the concept of process limits to screen parts at intermediary operations or to determine where process control is needed in a system.

Process limits can be considered “intermediary tolerances” on a part. Based on process capability, they prescribe the maximum allowable output variation for each operation in a system, to ensure that produced parts will meet end-of-line specifications. One method for determining these limits is through back-propagation of the desired end-of-line tolerances through the system. In this section we develop this technique.

We will first determine the process limits in a simple serial system, using the Worst-Case method for calculating variation propagation. We begin with the expression for the Tolerance Threshold of the system, as derived in Chapter 3:

$$\bar{\tau}_i = 6 \left[ \left[ F_{i,\bar{x}} \right]_{\bar{q}_{i-1}^*, \bar{x}_i^*} \bar{\sigma}_{\bar{x}_i} + \left[ \left[ F_{i,\bar{q}_{i-1}} \right]_{\bar{q}_{i-1}^*, \bar{x}_i^*} \bar{T}_{i-1} + 6\bar{\sigma}_{\bar{\varepsilon}_i} + \bar{\varepsilon}_{\bar{x}_i} \right] \right] \quad (3.34)$$

In equation (3.34),  $\bar{\tau}_i$  is the Tolerance Threshold and  $\bar{T}_{i-1}$  is the tolerance on the incoming material or work-in-process. In order to determine the process limits on the  $(i-1)^{th}$  operation, we must solve a modified version of equation (3.34) for the allowable incoming variation  $\bar{T}_{i-1}$  that will allow the process to meet the desired output specifications. We can rewrite (3.34) by first changing the Tolerance Threshold value to a specified tolerance on operation  $i$ , and then changing the equality to an inequality in order to capture the fact that any quality characteristic values less than or equal to the target tolerance are acceptable. This gives:

$$\bar{T}_i \geq 6 \left[ \left[ F_{i,\bar{x}} \right]_{\bar{q}_{i-1}^*, \bar{x}_i^*} \bar{\sigma}_{\bar{x}_i} + \left[ \left[ F_{i,\bar{q}_{i-1}} \right]_{\bar{q}_{i-1}^*, \bar{x}_i^*} \bar{T}_{i-1} + 6\bar{\sigma}_{\bar{\varepsilon}_i} + \bar{\varepsilon}_{\bar{x}_i} \right] \right] \quad (4.1)$$

To avoid confusion, we will designate the process limits,  $\bar{T}_{i-1}$ , for operation  $i$  as  $\bar{\lambda}_i$ . The process limits  $\bar{\lambda}_i$  thus represent the maximum level of input variation allowable for the  $i^{th}$  operation in order to ensure that output variation is smaller than  $\bar{T}_i$ . They simultaneously prescribe the maximum allowable output variation for operation  $i-1$ . With this new notation, equation (4.1) becomes:

$$\bar{T}_i \geq 6 \left[ \left[ F_{i,\bar{x}} \right]_{\bar{q}_{i-1}^*, \bar{x}_i^*} \bar{\sigma}_{\bar{x}_i} + \left[ \left[ F_{i,\bar{q}_{i-1}} \right]_{\bar{q}_{i-1}^*, \bar{x}_i^*} \bar{\lambda}_i + 6\bar{\sigma}_{\bar{\varepsilon}_i} + \bar{\varepsilon}_{\bar{x}_i} \right] \right]$$



We solve this for the process limits by first grouping the process-specific variations ( $\bar{\sigma}_{\bar{x}_i}$  and  $\bar{\sigma}_{\bar{\varepsilon}_i}$ ) into a vector of constants,  $\bar{K}$ :

$$\bar{K} = 6 \left[ F_{i,\bar{x}} \right]_{\bar{q}_{i-1}^*, \bar{x}_i^*} \bar{\sigma}_{\bar{x}_i} + 6 \bar{\sigma}_{\bar{\varepsilon}_i} + \bar{\varepsilon}_{\bar{x}_i}.$$

We can now write:

$$\left[ F_{i,\bar{q}_{i-1}} \right]_{\bar{q}_{i-1}^*, \bar{x}_i^*} \bar{\lambda}_i \leq \bar{T}_i - \bar{K}. \quad (4.2)$$

Equation (4.2) defines the feasible space of process limits  $\bar{\lambda}_i$  guaranteeing that the final product variation will fall within specifications  $\bar{T}_i$ . The boundaries of this space enclose an  $n$ -dimensional convex polytope. This is represented for the two-dimensional case in Figure 4.1, which shows a polygonal feasible space bounded by two active constraints. In  $n$ -space, the feasible polytope could be bounded by up to  $n$  active constraints, not including the axes.

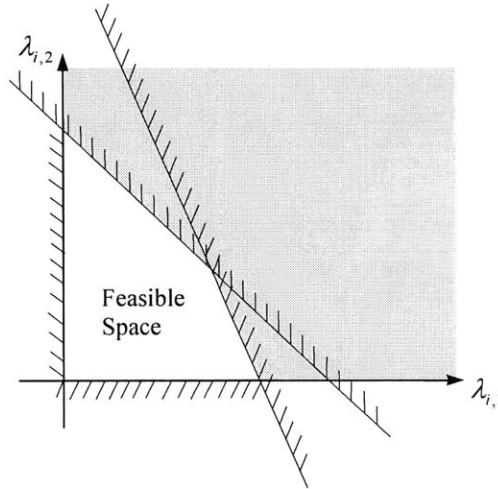


**Figure 4.1: Feasible Limit Space in 2 Dimensions.**

The process limits will be the maximum acceptable set of  $\bar{\lambda}_i$ . With bilateral tolerances, it is not practical to use the space bounded by the polytope itself, since this may be non-rectangular, such as that shown in Figure 4.1. A non-rectangular limit region would require a multivariate approach to tolerancing (the tolerance on dimension A is a function of the variation on dimension B), which generally adds excessive complexity to the manufacturing process. We can instead determine a rectangular subset of the acceptable space, which ensures that any process limit within its boundary is acceptable.

#### 4.1.1 Bounding the Process Limits

To determine conservative process limits, we can identify the largest hyper-rectangle completely contained within the feasible space. This rectangular “limit space” will contain only feasible solutions, but will exclude some feasible values. There are an infinite number of such hyper-rectangles, based on the relative magnitudes of the  $\bar{\lambda}_i$

components. In the 2 dimensional case, one vertex of the hyper-rectangle must lie somewhere along the boundary of the feasible region, shown in Figure 4.2.

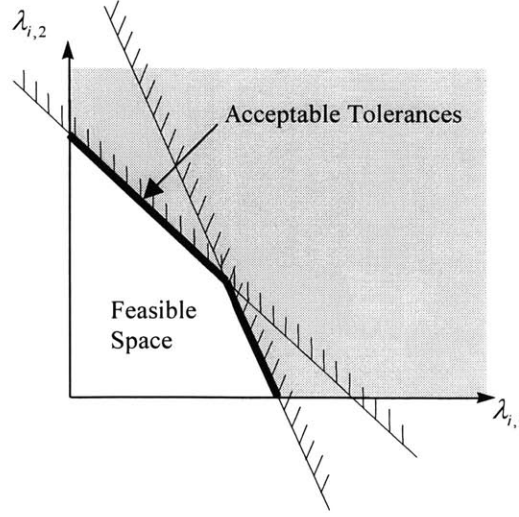


**Figure 4.2: Conservative Bound Acceptable Limits.**

One approach to selecting a single process limit  $\bar{\lambda}_i$  from the infinite set is to first determine the relative costs of holding limits on the variation of each input. We can then maximize a norm of the relative cost weighted limits:

$$\max_{\bar{\lambda}_i} \|W\bar{\lambda}_i\| \quad (4.3)$$

subject to the output tolerances being satisfied:

$$\left[ F_{i,\bar{q}_{i-1}} \right]_{\bar{q}_{i-1}^*, \bar{x}_i^*} \bar{\lambda}_i \leq \bar{T}_i - \bar{K}. \quad (4.4)$$

The  $W$  matrix in (4.3) is a diagonal matrix where each  $w_{kk}$  coefficient is the reciprocal of relative cost, and one reference  $w_{kk}$  term has a value of 1. Any vector norm such as the one-norm (addition) can be used. We restrict the space to positive values:

$$\bar{\lambda}_i \geq \bar{\delta} \quad (4.5)$$

where each  $\bar{\delta}$  is a reasonable minimum tolerance given the process capability. We can reduce (4.5) to a single dimension by requiring that all of the input tolerances on an operation be the same. This is often useful for assembly operations, which involve a number of identical fasteners or welds. In this case:

$$\lambda_{i,1} = \lambda_{i,2} = \dots = \lambda_{i,n}. \quad (4.6)$$

The constraints of (4.6) can be thought of as a ray emanating from the origin at a 45° hyper-angle, and intersecting each constraint hyperplane of (4.4). This is illustrated for the two-dimensional case by Figure 4.3, which shows the new constraint (4.6) and the boundaries of the square that becomes the limit region.

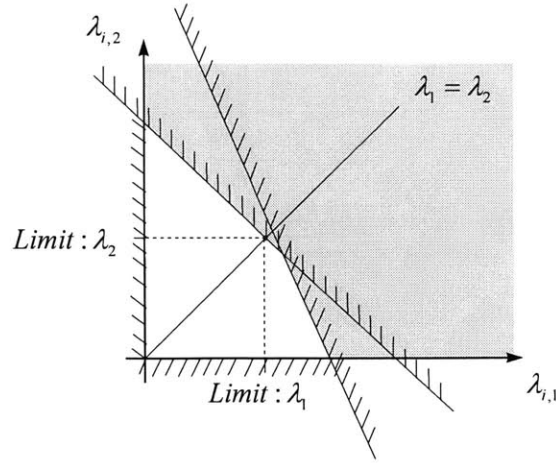


**Figure 4.3: Determination of Limit Region.**

Again, there is no reason that the tolerance region need be a hypercube. It is very likely, in fact, that the different quality characteristics on a product will require different tolerances. We can choose a different bounding polytope by replacing the constraint (4.6) with a weighted version:

$$w_{11} \cdot \lambda_{i,1} = w_{22} \lambda_{i,2} = \dots = w_{mm} \lambda_{i,n}, \quad (4.7)$$

in which  $w_{kk}$  is a component of a diagonal relative cost matrix as before. The maximization itself can be done using one of the standard optimization techniques, or simply by solving for the intersection of (4.7) with each hyperplane contained in the constraint system:

$$\left[ F_{i,\bar{q}_{i-1}} \right]_{\bar{q}_{i-1}^*, \bar{x}_i^*} \bar{\lambda}_i \leq \bar{T}_i - \bar{K}$$

The first plane intersected will be the active constraint. Note that in general, one active constraint will limit the size of the hyper-rectangle. The output tolerance associated with this constraint is a “key characteristic” of the system, since it restricts the magnitude of all other quality characteristic values. If this one tolerance is satisfied, all others will be as well. If this constraint is relaxed sufficiently, a different output tolerance constraint will become active. In this way, we can rank the importance of various output dimensions.

The back-propagation method outlined in this section can also be used with the RSS formulation by simply changing (3.35) to the form of (4.2). In this case, we use the constraint system:

$$\left[ F_{i,\bar{q}_{i-1}}^2 \right]_{\bar{q}_{i-1}^*, \bar{x}_i^*} \bar{\lambda}_i^2 \leq \bar{T}_i^2 - \bar{K} \quad (4.8)$$

where:

$$\bar{K} = 36 \left[ F_{i,\bar{x}}^2 \right]_{\bar{q}_{i-1}^*, \bar{x}_i^*} \bar{\sigma}_{\bar{x}_i}^2 + 36 \bar{\sigma}_{\bar{\epsilon}_i}^2 + \bar{\epsilon}_{s_i} \quad (4.9)$$

#### 4.1.2. Parallel Operations

Back propagation of tolerances in systems containing parallel operations is quite similar to that for serial operations, with the extension that the tolerances must be weighted not only within each operation, but among the parallel operations as well. To develop this method, we begin with a variant of (3.38):

$$\bar{T}_i^2 \geq 36 \left[ F_{i,\bar{x}}^2 \right]_{\bar{q}_{i-1}^*, \bar{x}_i^*} \bar{\sigma}_{\bar{x}_i}^2 + 36 \bar{\sigma}_{\bar{\epsilon}_i}^2 + \bar{\epsilon}_{s_i} + \sum_n \left( \left[ F_{i,\bar{q}_{i-1},n}^2 \right]_{\bar{q}_{i-1}^*, \bar{x}_i^*} \bar{T}_{i-1,n}^2 \right)$$

Rather than using the Tolerance Threshold,  $\bar{\epsilon}_i$ , we now have some desired final tolerance  $\bar{T}_i$ , and wish to determine input tolerances  $\bar{T}_{i-1,1}$  through  $\bar{T}_{i-1,n}$ . This expression can first be re-written as:

$$\sum_n \left( \left[ F_{i,\bar{q}_{i-1},n}^2 \right]_{\bar{q}_{i-1}^*, \bar{x}_i^*} \bar{\lambda}_{i,n}^2 \right) \leq \bar{T}_i^2 - 36 \left[ F_{i,\bar{x}}^2 \right]_{\bar{q}_{i-1}^*, \bar{x}_i^*} \bar{\sigma}_{\bar{x}_i}^2 + 36 \bar{\sigma}_{\bar{\epsilon}_i}^2 + \bar{\epsilon}_{s_i} \quad (4.10)$$

One method for solving this equation is to append the  $n$  matrices  $\left[ F_{i,\bar{q}_{i-1},n}^2 \right]_{\bar{q}_{i-1}^*, \bar{x}_i^*}$  together, and also append the  $n$  vectors  $\bar{\lambda}_{i,n}^2$ . This will give us a single new sensitivity matrix  $\left[ F_{i,\bar{q}_{i-1}}^2 \right]_{\bar{q}_{i-1}^*, \bar{x}_i^*}$  and process limit vector  $\bar{\lambda}_i^2$ :

$$\left[ F_{i,\bar{q}_{i-1}}^2 \right]_{\bar{q}_{i-1}^*, \bar{x}_i^*} \bar{\lambda}_i^2 \leq \bar{T}_i^2 - 36 \left[ F_{i,\bar{x}}^2 \right]_{\bar{q}_{i-1}^*, \bar{x}_i^*} \bar{\sigma}_{\bar{x}_i}^2 + 36 \bar{\sigma}_{\bar{\epsilon}_i}^2 + \bar{\epsilon}_{s_i} \quad (4.11)$$

This relation can now be reduced to the form of (4.4)

$$\left[ F_{i,\bar{q}_{i-1}}^2 \right]_{\bar{q}_{i-1}^*, \bar{x}_i^*} \bar{\lambda}_i^2 \leq \bar{T}_i^2 - \bar{K} \quad (4.12)$$

and then solved in a similar way. The only difference will be in determining the constraints (4.7)

$$w_{11} \cdot \lambda_{i,1} = w_{22} \lambda_{i,2} = \dots = w_{mm} \lambda_{i,n}$$

where the weighting factors  $w_{kk}$  will contain relative weightings among the parallel operations as well as within them.

#### 4.1.3 Application of Process Limits

Once process limits have been determined for each operation within a system, they can be used to guide system improvement. Process limits have two main applications:

- To allow early identification of those parts which will not meet end-of-line specifications. This eliminates the wasted time and cost of leaving them in the manufacturing system.
- To identify points in the system requiring measurement and control

The first of these applications is straightforward. Process limits are effectively “intermediary tolerance” specifications on the output of each operation within a system. By inspecting the output of a given operation and evaluating it against the process limits for that operation, those parts with quality characteristic values exceeding the process limits can be removed from the system. Since it is impossible for these parts to meet end-of-line tolerances, leaving them in the system is a waste of resources.

Process limits can also be used in conjunction with the Tolerance Threshold values of each operation in a system, to determine where measurement and control are needed. As discussed in the previous section, process limits are back-propagated through the system from end-of-line specifications. We can simultaneously forward-propagate the Tolerance Threshold values for each operation, based on the known variations of process parameters and incoming material quality characteristics. The output of each operation will then be associated with both a Tolerance Threshold value and a process limit. Beginning with the next-to-last operation in a system and moving towards the first operation in the system, we can compare the process limit values with the Tolerance Threshold values. This situation is depicted in Figure 4.4.

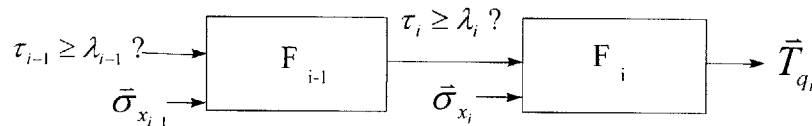


**Figure 4.4: Comparison of Tolerance Threshold with process limits.**

If the process limit is greater than the Tolerance Threshold value:

$$\lambda_i \geq \tau_i$$

then every part produced by that operation is capable of meeting the end-of-line tolerances. If, however, the Tolerance Threshold is larger than the process limit, then some parts are being produced that cannot meet end-of-line tolerances. In other words, when:

$$\lambda_i < \tau_i$$

either the output of operation  $i$  needs to be screened in order to remove those parts from the system that cannot meet final specifications, or some form of process control is needed in the system. If the latter approach is chosen, the Tolerance Threshold values of each operation can be recalculated accounting for the effects of control, to ensure that all process limits are satisfied. We discuss the use of process control to reduce variation in the next section. An example of the use of process limits in a manufacturing system is presented in Chapter 5.

## **4.2 Process Control**

In Chapter 3, we discussed one method for reducing end-of-line variation: system-level parameter design. A second approach is to reduce the actual source variation of key input parameters. If neither of these methods is cost-effective or sufficient, we can apply process control to our system.

Process control can take many forms within manufacturing systems. Many machine parameters incorporate feedback loops, to ensure that they reach and maintain a desired setting. Some processes utilize feed-forward control, in which a material parameter is measured as it enters an operation, and this value is used to determine the value of a process parameter in that operation. Part-to-part feedback can also be found in the manufacturing domain. This method involves measuring the product of an operation and using the measurement to change process parameter settings that govern production of the next part. These control strategies are not necessarily planned; in some cases they may be incidental, due to operator intervention.

In this section we will discuss methods for using adjustable process parameters to decrease end-of-line variation. We will develop analytical expressions predicting the effect of feed-forward control, and discuss the use of feedback control. In Chapter 5, we evaluate both methods through numerical simulation, and present experimental validation of a feed-forward control strategy.

### **4.2.1 Feed-Forward Control**

Feed-forward process control can be a useful manufacturing strategy for systems with good measurement capability and/or a low production rate. This approach involves first measuring the geometry or material properties of a workpiece as it enters an operation, and then using the measurement to set the value of some adjustable process parameter in that operation. The output variation in an operation controlled in this way is directly related to the accuracy of the measurements, controller, and actuators. In this section we derive equations predicting the output variation of operations involving feed-forward control.

#### 4.2.1.1 Feed-Forward and Variation

Figure 4.5 depicts a single operation with a feed-forward loop measuring some subset of the inputs  $\bar{q}_i$  and  $\bar{x}$ , and changing some subset of the adjustable variables  $\bar{p}$ .

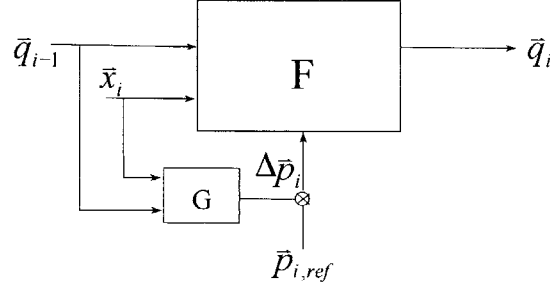


**Figure 4.5: Feed-Forward Control Loop.**

We can write the generalized equation for this operation as:

$$\bar{q}_i = F(\bar{q}_{i-1}, \bar{x}_i, \bar{p}_i) \quad (4.13)$$

where:

$$\bar{p}_i = \bar{p}_{i,ref} - \Delta \bar{p}_i = \bar{p}_{i,ref} - G(\bar{q}_{i-1}, \bar{x}_i) \quad (4.14)$$

In equation (4.14),  $G$  is the controller model that links the measured values of input variations to changes in the values of the adjustable variables. We can find the function  $G$  by using a Taylor series to linearize the system around an operating point  $(\bar{q}_{i-1}^*, \bar{x}_i^*, \bar{p}_i^*)$ :

$$\bar{q}_i \approx F(\bar{q}_{i-1}^*, \bar{x}_i^*, \bar{p}_i^*) + \left( \frac{\partial F_i}{\partial \bar{x}_i} \right)_{\bar{q}_{i-1}^*, \bar{p}_i^*, \bar{x}_i^*} \Delta \bar{x}_i + \left( \frac{\partial F_i}{\partial \bar{p}_i} \right)_{\bar{q}_{i-1}^*, \bar{p}_i^*, \bar{x}_i^*} \Delta \bar{p}_i + \left( \frac{\partial F_i}{\partial \bar{q}_{i-1}} \right)_{\bar{q}_{i-1}^*, \bar{p}_i^*, \bar{x}_i^*} \Delta \bar{q}_{i-1} + H.O.T. \quad (4.15)$$

This can be rewritten as:

$$\bar{q}_i = \bar{q}_i^* + [F_p]_i^* \Delta \bar{p}_i + [F_x]_i^* \Delta \bar{x}_i + [F_q]_i^* \Delta \bar{q}_{i-1} + \bar{b}_i \quad (4.16)$$

where the symbol “\*” indicates evaluation at a given nominal operating point. Now, to determine the adjustable variable change  $\Delta \bar{p}_i$  required to offset variations  $\Delta \bar{x}_i$  and  $\Delta \bar{q}_{i-1}$  in the input variables, we can divide through by  $[F_p]_i^*$  and re-arrange to get:

$$\Delta \bar{p}_i = [F_p]_i^{-1} \bar{m}_i - [F_p]_i^{-1} \bar{q}_i^* - [F_p]_i^{-1} [F_x]_i^* \Delta \bar{x}_i - [F_p]_i^{-1} [F_q]_i^* \Delta \bar{q}_{i-1} \quad (4.17)$$

where  $\bar{m}_i$  is the vector of target output values for operation  $i$ . If we assume that the feed-forward control loop is without bias, the nominal output values  $\bar{q}_i^*$  will be equal to the target output values  $\bar{m}_i$ , allowing both of these terms to drop out of (4.17).

The inverse matrices in (4.17) must be generalized inverses, since the sensitivity matrices are not likely to be square. We have chosen to use the weighted generalized inverse  $F^{-1*}$  of a matrix  $F$ , given by:

$$F^{-1*} = W^{-1} F^T (F W^{-1} F^T)^{-1} \quad (4.18)$$

where  $W$  is a diagonal matrix, containing the relative weights of each column of  $F$ . This means that  $w_{kk}$  is a measure of the relative cost of adjustment for each process parameter  $\bar{p}_i$ . These costs represent the difficulty involved in making a unit change to each variable.

If the weighting matrix  $W$  is set to identity, (4.18) will seek to minimize the norm of the vector originally paired with matrix  $F$ . In other words, the method will seek input tolerances that are equally minimized in bandwidth relative to their sensitivity. For a square non-singular matrix, equation (4.18) reduces to the standard matrix inverse:

$$F^{-1*} = F^{-1}$$

All inverse matrices in this thesis are assumed to be generalized inverses according to (4.18).

The controller derived in equation (4.17) presumes perfect measurement and system modeling, and provides a theoretically correct adjustment to the operation. In reality, there are several sources of error, most notably measurement error, modeling error, and actuation error. We can incorporate these errors into (4.17) by writing:

$$\Delta \bar{p}_i = [F_p]_i^{-1} \bar{k}_i - [F_p]_i^{-1} [F_x]_i^* (\Delta \bar{x}_i + \bar{\varepsilon}_{\bar{x}}) - [F_p]_i^{-1} [F_q]_i^* (\Delta \bar{q}_{i-1} + \bar{\varepsilon}_{\bar{q}}) - \bar{\varepsilon}_m - \bar{\varepsilon}_a \quad (4.19)$$

In equation (4.19),  $\bar{\varepsilon}_{\bar{x}}$  represents error in measuring the values of  $\bar{x}_i$ ,  $\bar{\varepsilon}_{\bar{q}}$  is error in measuring  $\bar{q}_i$ ,  $\bar{\varepsilon}_m$  represents modeling error, and  $\bar{\varepsilon}_a$  accounts for actuation error (the limits of accuracy on the setting of the adjustments themselves). The error terms  $\bar{\varepsilon}$  are all random variables. Depending on the situation, they may follow a normal distribution with a mean of zero, or a uniform distribution. Since the process matrices  $[F]$  are functions of  $\bar{p}_i$ , they must be evaluated at some operating point  $(\bar{q}_{i-1}^*, \bar{x}_i^*, \bar{p}_i^*)$  for use in the controller. The error term  $\bar{\varepsilon}_m$  incorporates differences between  $[F]$  and  $[F]^*$ . Naturally not all input variables will be measured; in these cases, the value of  $\bar{\varepsilon}_{\bar{x}}$  or



$\bar{\varepsilon}_{\bar{q}}$  associated with the unmeasured variable will simply be the input standard deviation associated with that variable.

If we substitute (4.19) into (4.16) we can predict the actual output values  $\bar{q}_i$  in terms of the target output values  $\bar{m}_i$  and the measurement, modeling, and actuation errors:

$$\bar{q}_i = \bar{m}_i - [F_x]_i^* \bar{\varepsilon}_x - [F_q]_i^* \bar{\varepsilon}_q - [F_p]_i^* \bar{\varepsilon}_m - [F_p]_i^* \bar{\varepsilon}_a \quad (4.20)$$

The variation of  $\bar{q}_i$  can be determined from (4.20) through a Monte Carlo simulation for errors with either normal or uniform distributions. If the errors are independent, we can calculate the output variance by the RSS method as:

$$\bar{\sigma}_{\bar{q}_i}^2 = [F_x^2]_i^* \bar{\sigma}_{\bar{\varepsilon}_x}^2 + [F_q^2]_i^* \bar{\sigma}_{\bar{\varepsilon}_q}^2 + [F_p^2]_i^* \bar{\sigma}_{\bar{\varepsilon}_m}^2 + [F_p^2]_i^* \bar{\sigma}_{\bar{\varepsilon}_a}^2 \quad (4.21)$$

We can also obtain a worst-case estimate of the range of the output values  $\bar{q}_i$  by substituting the  $3\sigma$  values of the random variable error terms in (4.21):

$$range[\bar{q}_i] = \bar{m}_i \pm \left( -[F_x]_i^* 3\bar{\sigma}_{\bar{\varepsilon}_x} - [F_q]_i^* 3\bar{\sigma}_{\bar{\varepsilon}_q} - [F_p]_i^* 3\bar{\sigma}_{\bar{\varepsilon}_m} - [F_p]_i^* 3\bar{\sigma}_{\bar{\varepsilon}_a} \right) \quad (4.22)$$

#### 4.2.1.2 Feed-Forward With Adjustment Limits

Equations (4.20) through (4.22) are based on the assumption that the adjustable variables  $\bar{p}_i$  can take on any values, and thus control any amount of work-in-process variation. In practice, however, there will be some interval of adjustment:

$$\bar{P}_i = [\bar{p}_{i,\min} \cdot \bar{p}_{i,\max}]$$

such that:

$$\bar{p}_{i,\min} \leq \bar{p}_i \leq \bar{p}_{i,\max}$$

which will limit the amount of correction possible through feed-forward control. In a system with adjustment limits, we can determine the maximum controllable work-in-process input variation as:

$$\begin{aligned}
& \max \quad \|\bar{\sigma}_{\bar{q}_{i-1}}\| \\
& \text{s.t.} \quad [F_q]_i^* \bar{\sigma}_{\bar{q}_{i-1}} = \frac{1}{3} [F_p]_i^* \Delta \bar{p}_i - [F_x]_i^* \bar{\sigma}_{x_i} \\
& \text{over} \quad \bar{p}_i \in \bar{P}_i \\
& \text{where} \quad \Delta \bar{p}_i = (\bar{p}_{i,\min} - \bar{p}_i) \text{ if } (\bar{p}_{i,\min} - \bar{p}_i) < \frac{\bar{p}_{i,\max} - \bar{p}_{i,\min}}{2} \\
& \quad \quad \Delta \bar{p}_i = (\bar{p}_{i,\max} - \bar{p}_i) \text{ otherwise} \\
& \quad \quad \bar{\sigma}_{\bar{x}_i} \text{ is constant over } \bar{P}_i
\end{aligned} \tag{4.23}$$

The formulation (4.23) is derived from (4.16) by replacing  $\Delta \bar{x}_i$  and  $\Delta \bar{q}_{i-1}$  with their maximum or minimum possible values, based on  $\pm 3\sigma$  limits. The conditional definition of  $\Delta \bar{p}_i$  accommodates the possibility that the parameters  $\bar{p}_i$  are not centered in their adjustment ranges.

We can also determine a new probability density function for the “controlled” variable. As shown in (Soyucayli and Otto 1998), if we are controlling some variable  $q_{i-1}$  with a variance  $\bar{\sigma}_{q_{i-1}}^2$ , we can estimate the controlled variance  $\bar{\sigma}_c^2$  as:

$$\sigma_c^2 = \Delta_q^2 + \sigma_{q_{i-1}}^2 - 2\sqrt{\frac{2}{\pi}} \sigma_x \Delta_q \tag{4.24}$$

where  $\Delta_q$  is the range of output quality characteristic values based on the range  $\Delta_p$  of the controllable input parameters  $\bar{p}_i$ :

$$\Delta_q = \left| \frac{\partial y}{\partial t} \right| \Delta_p \tag{4.25}$$

Equation (4.24) can be used as another method for evaluating the effect of feed-forward control on end-of-line variation. The controlled output variation calculated through this equation can be substituted into a system model, replacing the original variance associated with the incoming material quality characteristic  $q_{i-1}$  in the controlled operation. This will simulate the effect of the control loop, and show the impact of control on end-of-line variation.

#### 4.2.1.3 Modeling Error in the Controller

As mentioned previously, modeling error in the feed-forward controller can introduce significant variation into the controlled system. We can use equation (4.21) to evaluate

the impact of modeling error in a given system. If the magnitude of measurement and actuation errors are known (this is likely since they are both hardware dependent), we can calculate the upper limit on modeling error  $\bar{\epsilon}_m$  that will still ensure that the output variation of a controlled operation is smaller than the process limit.

If  $\bar{\lambda}_i$  is the set of process limits for the controlled operation, the maximum allowable modeling error will be:

$$\begin{aligned}
& \max \quad \left\| \bar{\sigma}_{\bar{\epsilon}_m}^2 \right\| \\
& \text{s.t.} \quad \left[ F_p^2 \right]_i^* \bar{\sigma}_{\bar{\epsilon}_m}^2 \leq \frac{\bar{\lambda}_i^2}{36} - \left[ F_x^2 \right]_i^* \bar{\sigma}_{\bar{\epsilon}_x}^2 - \left[ F_q^2 \right]_i^* \bar{\sigma}_{\bar{\epsilon}_q}^2 - \left[ F_p^2 \right]_i^* \bar{\sigma}_{\bar{\epsilon}_p}^2 \\
& \text{over} \quad \bar{\sigma}_{\bar{\epsilon}_m} \geq 0 \\
& \text{where} \quad \left[ F_p \right] \left[ F_q \right] \left[ F_x \right], \bar{\lambda}_i, \bar{\sigma}_{\bar{\epsilon}_x}, \bar{\sigma}_{\bar{\epsilon}_q}, \bar{\sigma}_{\bar{\epsilon}_p} \text{ are constant}
\end{aligned} \tag{4.26}$$

Once again, errors are assumed to be random variables with normal distributions, and process limits define the width of the acceptable tolerance band ( $6\sigma$ ). Equation (4.26) can be used to determine the necessary accuracy of a control model for a given operation.

#### 4.2.1.4 Application of feed-forward

Use of the analytical expressions derived in this chapter for feed-forward control are demonstrated on an example system model in Chapter 5. In that chapter we also present the results of a feed-forward experiment conducted on the factory floor. The experimental data shows that feed-forward control can be effective in reducing end-of-line variation in a production environment.

### 4.2.2 Feedback Control

Many manufacturing processes utilize some form of feedback control. In the context of manufacturing, feedback can take one of two forms: machine feedback and part-to-part feedback. In machine feedback, a control loop regulates the value of an input parameter to improve accuracy and reduce variation. Some examples of controlled parameters include injection pressure and polymer temperature on injection molding machines, and spindle speed and feed rate on CNC lathes. Part-to-part feedback, on the other hand, involves producing and measuring a single part, and then using the measurement data to adjust process parameter settings prior to production of the next part. Part-to-part feedback is often a consequence of operator practice, rather than a deliberate control strategy. This situation can occur when an operator makes frequent adjustments to process parameter settings based on visual inspection of the parts being produced. Part-to-part feedback has many variant forms, with differing numbers of parts being produced and measured before any adjustments are made. One such approach is run-by-run control

(Boning, Moyne et al. 1996), in which data gathered from one batch of parts is used to make parameter changes for the next batch of parts.

While machine feedback reduces the variation of the controlled parameters, part-to-part feedback can actually increase variation in manufacturing systems. This situation occurs when the system is not allowed to equilibrate, or when the time constant of the variation is much smaller than the time constant of the feedback loop. The first condition is prevalent in large systems, in which there is a time delay in reaching equilibrium after process parameter changes. Jaikumar (1996) relates a situation he encountered at a manufacturing plant, where the operators were making constant process parameter adjustments with no improvement in product quality. He found that the plant was not allowed to reach equilibrium after each change, and that the operators were effectively making random changes to the process parameter settings. When the operators were told to stop making “improvements,” end-of-line variation actually decreased (Jaikumar 1996).

Operator adjustment can also lead to an increase in variation when the time constant of workpiece variation is smaller than the time constant of the feedback loop. An example of this situation is part-to-part control of an operation in which variation is primarily the result of chance causes. Since the quality characteristics of each part vary randomly around their nominal values, any changes made to the system based on the characteristics of a single produced part will have no correlation with the quality characteristic values of the next workpiece. Making parameter adjustments after producing single or multiple parts thus actually adds a source of random variation to the system. This increases end-of-line variation over the uncontrolled value.

Despite causing an increase in variation in some situations, part-to-part control is useful for correcting mean shifts and reducing the effects of variation due to assignable causes. Since it is quite complicated to derive general analytical expressions for the effects of feedback control on variation, we will limit ourselves to numerical simulation. In Chapter 5, we compare various forms of machine feedback and part-to-part feedback through Monte Carlo simulation on an example system model.

### **4.2.3 Controllability**

In classical control engineering, the term controllability refers to the ability of an unconstrained control vector to transfer a system from its initial state to any other state in a finite amount of time (Ogata 1990). Mantipragada and Whitney (1997) discuss the controllability of assembly systems, represented by “State Transition Models.” They seek to understand the impact of different assembly sequences on variation. Their transition model representation is similar to the concept of variation propagation presented in Chapter 3; in our notation, the state transition equation for a system with adjustable variables is exactly (3.27).

Following the example set by Mantipragada (1997), we can view (3.27) as a state equation, in which the work-in-process variations change with each operation, rather than

with time. We can then apply Kalman's controllability criteria (Ogata 1990), to show that the system will be output controllable if:

$$\text{rank} \left[ YF_{\bar{p}} \mid YIF_{\bar{p}} \mid YI^2F_{\bar{p}} \mid \cdots \mid YI^{n-1}F_{\bar{p}} \right] = M \quad (4.27)$$

where  $I$  is the identity matrix,  $[F_{\bar{p}}]$  is the sensitivity matrix relating output quality characteristics to adjustable variables,  $[Y]$  is a vector of 0's and 1's determining the measured outputs,  $\bar{q}_m$ , from the total set of outputs,  $\bar{q}$  as:

$$\bar{q}_m = [Y] \cdot \bar{q} \quad (4.28)$$

and  $M$  is the number of measured output variables. This means that the system is controllable if the rows of the sensitivity matrix  $[F_{\bar{p}}]$ , linking the outputs to the adjustable variables, are linearly independent.

### 4.3 Chapter Summary

In this chapter, we explored several applications of the Integrated System Model framework. We first presented the concept of process limits, which act as intermediary tolerances within a system. Derived from end-of-line specifications, the limits guide process engineers in determining the maximum allowable output variation for each operation in a system. They can also be used to identify the need for measurement or control of an operation. In cases where process control is needed, we suggested the use of either feed-forward or feedback process control. We derived a number of analytical expressions predicting the effects of feed-forward control on output variation, and discussed several forms of feedback control. Finally we presented an expression for determining the controllability of a manufacturing operation. The concepts developed within this chapter are demonstrated on an example system model in Chapter 5.

## Chapter 5: Sheet Stretch-Forming Example

In Chapters 3 and 4 of this thesis, we presented a number of tools for the prediction and reduction of variation in manufacturing systems. In this chapter we demonstrate the use of these techniques on an actual sheet stretch-forming manufacturing system. We follow the variation reduction method presented in Chapter 1. This approach consists of the following procedure:

- 1) Develop an Integrated System Model of the manufacturing system
  - Build predictive models of each operation
  - Derive variational models of each operation
  - Link the models into an ISM
  - Validate system predictions against measured data
- 2) Identify major sources of variation in the system
- 3) Conduct system-level parameter design
- 4) Evaluate the need for measurement or control in a system
- 5) Formulate several variation reduction strategies
  - Source reduction
  - Feed-forward control
  - Feedback control
- 6) Evaluate strategies in simulation using the ISM
- 7) Implement the most promising strategy

We begin by presenting the example system, a sheet stretch-forming system used to form aircraft skin components for a major aerospace manufacturer. We construct predictive and variational models of the two operations in this system: heat treatment and stretch-forming. The models are linked into an ISM, validated against production data, and used to identify major sources of variation in the system. This information is used to formulate several variation reduction strategies that are then compared in simulation. One promising strategy, inter-operation feed-forward, is selected for evaluation. We present data from a shop floor test of this method, showing that it was successful in reducing end-of-line variation.

The manufacturing system modeled in this chapter is located at Northrop-Grumman Corporation's Commercial Aircraft facility, near Dallas, Texas. For this example, we focus on a specific part modeled through two operations: heat treatment and stretch forming. The target part and each of these operations are described in more detail in the following sections.

### 5.1 Target Part

The sheet stretch-forming manufacturing system outlined in this chapter is used to produce aircraft skin components with complex curvatures. The specific part we will model for this example is a double-curvature nacelle doubler, shown in Figure 5.1. This component fits on the inside of an assembly consisting of two similar pieces, bonded together for strength. The assembly itself forms the top half of a nacelle (engine housing)

on a large cargo aircraft. The nacelle doubler, known hereafter as the “target part,” is formed from 0.05” thickness stock aluminum 2024-O.



**Figure 5.1: Nacelle Doubler.**

## **5.2 System Overview**

The target part is formed through a series of operations, which transform incoming sheet stock into products with the desired shape and material properties. In this section we will describe the process used to manufacture the target part, and discuss some important modeling considerations.

### **5.2.1 Process Description**

The target part is formed through a series of three major operations: heat treatment, stretch forming, and trimming. Stock material arrives at the shop floor as flat sheet, and is rolled into coils by the heat treatment operators. Ten to twelve coils are lined up next to one another on a carrier for heat treatment (Figure 5.2). Batch sizes larger than twelve are subdivided into two smaller batches for heat treatment.



**Figure 5.2: Coils Stacked on Carrier.**

The heat treatment process for the target part consists of solution heating followed by a rapid quench. During solution heating, the carrier containing the coils is loaded into salt

bath heated to approximately 920°F, and allowed to “soak” for at least 25 minutes. Both temperature of the salt bath and time in the oven are constantly monitored. When the desired soak time is reached, the salt bath doors are opened and the carrier is quickly transferred to a tank containing quenchant at room temperature. The coils remain in the tank for 2 minutes, and are then removed and transferred by hand to a freezer. Freezer temperature is kept at approximately -10°F to retard natural aging. The amount of time the coils remain in the freezer varies based on the forming schedule; this can be as short as a few minutes or as long as 24 hours. Just prior to forming, a batch of 3-5 coils is removed from the freezer and the coils are straightened between a set of rollers (see Figure 5.3).



**Figure 5.3 Sheet Being Uncoiled.**

The flattened sheets are then carried to the stretch forming press, where they are formed one after another (Figure 5.4)



**Figure 5.4: Sheet Mounted on Stretch Press.**

Once all of the parts have been formed, they are degreased with hot water and a solvent, and are then carried to a trimming station. Each part is placed on a trimming fixture and is hand routed to shape (Figure 5.5). The trimmed parts are then sent to a bonding facility, where they each become part of a doubler assembly.





**Figure 5.5: Part Being Trimmed.**

### **5.2.2 Modeling Considerations**

The Integrated System Model developed in this chapter is composed of two operations: heat treatment and stretch forming. We omit two of the actual processing steps—uncoiling of the sheet, and trimming. The amount of plastic deformation added to the sheet during coiling and uncoiling is very small, and we assume that the effects of work-hardening are insignificant in comparison with the effects of natural aging. The model validation, discussed later in this chapter, supports this assumption. Trimming is an important operation for some parts; leading edges, for example, exhibit significant post-trim springback (Parris 1996). As such, we took detailed measurements of the parts after trim, and implemented a finite-element based model of the trimming operation. Our measurements revealed that the amount of material removed from the target part during trim is sufficient to virtually eliminate post-trim springback. Since the trimming operation does not affect either of the two output variables of interest in this example (thickness and strain), we omit the trimming operation from the ISM, and from this discussion.

## **5.3 Integrated System Model**

This section outlines development of the stretch-forming system model. We discuss each constituent operation in turn, first describing the operation and its process parameters, and then detailing the predictive and variational models. We then link the operational models together into a system model, which is validated against production data.

### **5.3.1 Heat Treatment**

#### 5.3.1.1 Process Overview

Heat treatment is an important part of the stretch-forming manufacturing system. This operation is used to increase the strength of the stock material, stabilize mechanical or physical properties, and relieve residual stresses (Van Horn 1967). Through controlled heat treatment, the resistance to deformation of some alloys can be varied by a factor of 5 or 6. Although heat treatment is often thought of as a single operation, it is really

composed of three separate steps: solution heat treatment, quenching, and age hardening. Of these three steps, quenching is usually considered the most important in determining the material's final properties. Since alloys are softer and more ductile immediately after quenching than after aging, many forming operations are conducted between these two steps. A typical process plan will involve solution heating and quenching stock material, forming it into a desired shape, and then aging the formed part. Each step of the heat treatment process is discussed in more detail below.

### **Solution Heat Treating**

The first step in heat treatment is *solution heat treat*, which involves “soaking” the blank at an elevated temperature for a given time. This procedure forces the soluble hardening elements in the alloy (such as Cu, Mg, Si, and Zn) into solution (Davis 1993). The solute atoms form coherent clusters surrounded by strain fields, due to the size mismatch between solvent and solute atoms. The particles and strain fields obstruct the movement of dislocations through the material, thus increasing its strength.

The soak temperature must be below the melting point of the material, but above the temperature at which complete solution occurs. The material is heated to the soak temperature in an air furnace or salt bath. Soak time depends on the material microstructure before heat treat. For a part in a salt bath, the soak time is the time that the part is immersed in the batch. For a part in an air furnace, soak time begins when all instruments have returned to their original set temperature.

There are several sources of variation in solution heating. Most notably, the furnace temperature can vary by  $\pm 10^{\circ}\text{F}$  from nominal soak temperature during heating (Davis 1993). Uniform heating of the part is also a concern; this is generally controlled by means of racking spacing. Commercial rule of thumb is that parts should be spaced 2” apart to allow for air flow and even heating.

### **Quenching**

*Quenching* is often considered to be the most critical step in heat treatment (Davis 1993). Through rapid cooling, the quench creates a supersaturated solution which preserves the solid solution formed during solution heating. Quenching retains solute atoms in solution, and maintains a minimum number of vacant lattice sites, which can support low temperature diffusion. The rate of cooling during quench is important, since any solute atoms which diffuse to grain boundaries or any vacancies which migrate to disordered regions during cooling will not be able to contribute towards material hardening (Van Horn 1967). Rapid quench rates are thus proportional to high strength, toughness, and corrosion-resistance. Cooling rate effects are most significant in the range 530-750°F. For 7075 aluminum, for instance, cooling rates on the order of 540°F/s are necessary to obtain maximum strength.

#### *Modeling Considerations*

The heat transfer coefficient during quench is affected by the part geometry and local process factors (Tiryakioglu and Menguc 1996). This leads to variations in cooling

patterns between different parts and between different sections of the same part. Heat transfer to the quenchant is characterized by a surface heat transfer coefficient and an associated surface heat flux. This heat transfer coefficient is not constant during quenching, which complicates attempts to model the quenching process.

There are 4 different stages of cooling during quench:

1) Initial liquid contact

The initial liquid contact stage is very short (~0.25 s) and is characterized by intense boiling and a very high cooling rate at the part surface (Fletcher 1989). This stage lasts only until sufficient vapor has been generated to coat the part.

2) Vapor Blanket Stage

Vapor from the previous step forms a “blanket” between the part and the quenchant, which exists as long as the supply of heat from the metal surface exceeds the amount of heat needed to maintain maximum vapor per unit area. During vapor blanket stage, heat is transferred at a slow rate through the high thermal resistance of the vapor layer. This is primarily a conduction process. Heat that reaches the surface of the liquid is then removed by convection. The vapor blanket is stable for  $\Delta T$  (temperature differential between the part and the quenchant) in the range 400-1000°F. When  $\Delta T > 1000^\circ\text{F}$ , radiation effects become significant (Rohsenow and Choi 1961).

3) Nucleate Boiling

When the vapor blanket collapses, there is contact between the part and quenchant, and some violent boiling. This is the nucleate boiling stage, which has the fastest rate of heat removal from the part. Nucleate boiling involves 2 separate processes: bubble formation and growth and motion of the bubbles.

4) Convective Cooling

When the temperature of the part-quenchant interface approaches the liquid boiling point, the surface heat transfer coefficient decreases significantly (Tiryakioglu and Menguc 1996). Laminar convection becomes the primary mode of heat transfer

The cooling rate in each stage of quench is dependent on a number of parameters, including the temperatures of the material and bath, the quench medium, and the part geometry. We briefly discuss each of these factors below.

*Quench Delay*

In order to ensure that the part does not cool too much before being quenched, limits are placed on the amount of time allowed for transporting the material from furnace or salt bath to quench tank. This time is called the *quench delay*, and is measured from the moment when the furnace door is opened or the first corner of the workpiece emerges from the salt bath, until the moment when the last corner of the workpiece is immersed in the quench tank. Increasing the quench delay is similar to reducing the cooling rate.

### *Quench Media*

The choice of quench medium is dependent on the desired rate of cooling. Water and a variety of polymer solutions are the most commonly used quenchants. Water is a very effective medium, producing a faster quench rate than most polymers. This can lead to distortion in the final part; the cooling rate can thus be reduced by adding glycol to the water bath or by using a coating on the material. The vapor blanket stage in water is very short and sometimes non-existent (Fletcher 1989). The nucleate boiling stage, on the other hand, is prolonged.

### *Part Characteristics*

Quench rate is also dependent on part characteristics. Since heat transfer during quench is limited by the thermal resistance at the surface in contact with the quenchant, the cooling rate is a function of the ratio of surface area to volume. Cooling rate is also very sensitive to the surface condition of the part. It has been shown empirically that the lowest cooling rate is on parts with freshly machined, clean surfaces (Davis 1993). Oxide films and coatings tend to increase the cooling rate.

### *Residual Stress*

The temperature of the cooling bath naturally has an effect on the cooling rate: the higher the bath temperature, the lower the cooling rate. The effects of this parameter are mixed however, since the greater the temperature differential between the part and the bath, the more chance of residual stresses in the part. These stresses are caused by differential thermal expansion. Sudden cooling and contraction of the workpiece surface generates tensile stresses at the surface and compressive stresses near the part center. The magnitude of these stresses is proportional to the temperature difference between the surface and the interior of the part. During cooling, as the temperature of the surface approaches that of the quenchant, the rate of cooling at the surface is slower than that at the part center. This results in a stress reversal, in which the residual stresses become compressive at the surface and tensile at the center (Tiryakioglu and Menguc 1996). This stress field can cause problems in post-processing, since material removal operations can expose the tensioned material or create an asymmetric residual stress field. Warpage during quench is a significant problem in sheet material. Warpage is very dependent on racking conditions, symmetry during cooling, and on the amount of impact when the material enters the bath.

### *Additional Factors*

There are several additional parameters influencing quench behavior. Agitation during quench is an important factor, as it decreases vapor blanket stability. The immersion conditions of the part are also significant; these include part orientation, direction and velocity of quenchant flow, and immersion velocity of the part (Tiryakioglu and Menguc 1996). Finally, initial part temperature is directly proportional to the stability of the vapor blanket.

## Age Hardening

The final step in the heat treatment process is *age hardening*. This procedure allows additional strengthening of the material, through the formation of precipitate zones and vacancy migration. There are two types of aging: natural, in which the material is allowed to strengthen at room temperature, and artificial, in which aging occurs at some elevated temperature. In many cases, it is desirable to suspend natural aging after quench, until the part can be formed. Aging can be slowed significantly by freezing the material at a temperature below 0°F.

### *Natural Aging*

There are no microstructural changes during natural aging; hardening effects are due to the formation of zone structures in the material (Van Horn 1967). In 2024 aluminum, most natural aging occurs in the space of 24 hours. 7075 aluminum, on the other hand, hardens indefinitely at room temperature (although the hardening rate eventually decreases to the point of being negligible). While material strength increases during natural aging, electrical and thermal conductivities decrease.

### *Artificial Aging*

Heating the quenched material to 200-400°F accelerates precipitation effects. Artificial aging does not just increase the reaction rate however, there are structural changes in the material as well (Van Horn 1967). This process relaxes some quenching stresses by 10-35%.

#### 5.3.1.2 Modeling Strategy

At the Northrop-Grumman Commercial Aircraft facility, it is common practice to solution heat treat and quench stock material in batches. The variation between parts prior to age hardening is thus comparatively minimal, even across batches. After quench, the material is moved to a freezer until forming. Although this transfer occurs quickly for the material used to form our target part (approximately 6 minutes), the process specifications used by the heat treatment operators prescribe a window of 30 minutes to move material from quench to freezer. This large process window is necessary for some parts, which are carried to freezers in other buildings.

As mentioned previously, it is standard procedure for the operators to remove 3-5 aluminum sheets from the freezer at one time, and to then form them sequentially. The time each part is out of the freezer (and naturally aging) can vary by up to 45 minutes. The operators report that in the winter they will remove up to 5 parts from the freezer at a time, while in the summer they can usually only remove and form 3 parts at a time before too much hardening sets in.

Our process models indicate that natural aging begins after a part has been out of the freezer for approximately 15 minutes. The time required in practice to transport the coiled material from quench to freezer is approximately 6 minutes, and the time to straighten 4 coils of material is also approximately 6 minutes. It is likely, therefore, that each workpiece begins to strengthen prior to forming, and that material yield strength at

the time of forming varies significantly within each group of parts removed together from the freezer. While freezer temperature is set at  $-10^{\circ}\text{F}$ , the freezer door is often left open for long periods of time, allowing the internal temperature to climb as high as  $32^{\circ}\text{F}$ . It is not known what effect these temperature spikes will have on aging.

In developing a model of the heat treatment process, we first assumed that all parts were solution heated to saturation. This decision was supported by measurements of the salt bath temperature and saturation time. We then used one model to simulate the effects of quench, and a second model to evaluate the impact of aging time. These models are described in detail in the next section.

### 5.3.1.3 Heat Treatment Models

To determine the effects of quench, we used a model that relates material yield strength to quench parameters, developed at ALCOA (Kinnear 1998). Model inputs and outputs are shown in schematic form in Figure 5.6. The quench model predicts final yield strength of the quenched material, based on initial material geometry and properties and quenching process parameters. We then derived a second model, to predict the effects of aging time from the empirical data shown in Figure 5.7. The input and output parameters of this model are also shown in schematic form in Figure 5.6. The natural aging model first determines the part *aging time*: the amount of time each part spends out of the freezer between quench and forming. Calculation of aging time is based on the number of parts removed from the freezer at the same time, the time required to form the first part, and the time required to form each successive part. The model then uses the aging time to predict material yield strength.

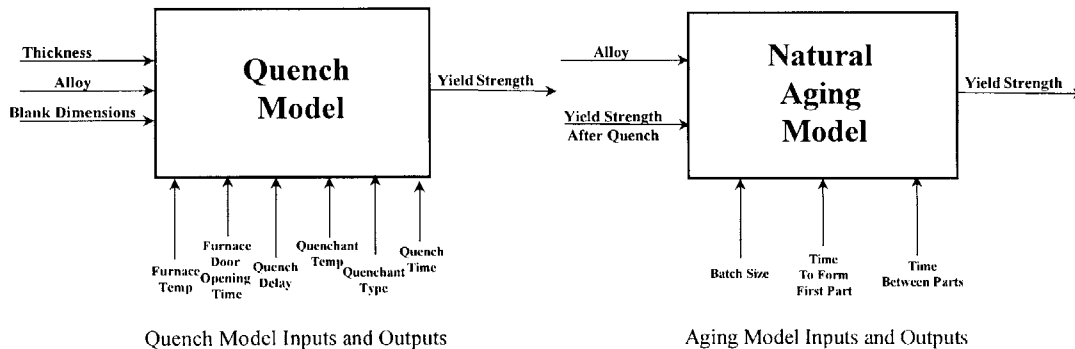


**Figure 5.6: Heat Treatment Model Parameters.**

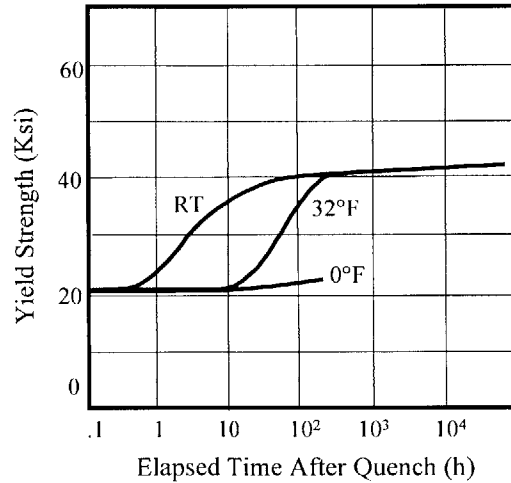


**Figure 5.7: Yield Strength vs. Aging Time (Van Horn 1967).**

In order to derive the natural aging model, we first fit a polynomial to the room-temperature aging curve in Figure 5.7, over the region of interest (15 minutes to 60 minutes). We then calibrated this polynomial, using a measured value of material yield strength at a typical aging time. The calibration point was obtained from tensile tests conducted on heat treated specimens of 2024 aluminum. These specimens were found to have a mean yield strength value of 131.6 MPa at a mean time out of freezer of 24 minutes. The calibrated aging time curve is:

$$Y_s = 0.3469t + (Y_s - 6.25) \quad (5.1)$$

where  $t$  is time out of freezer in minutes, and  $Y_s$  is the yield strength immediately after quench, which was found to be 129.52 MPa. Ambient temperature is a potential source of error in this model. Temperature on the factory floor varies between 50° and 100°F from winter to summer, and also changes depending on the time of day. The ambient temperature may affect both the time required for the onset of aging and the aging rate. Some additional calibration of this curve may thus be necessary to make the model more robust to plant conditions.

#### 5.3.1.4 Variational Models

To derive a variational model for quench, we first perturbed the predictive model inputs through their  $\pm 3\sigma$  ranges, based on in-plant measurements of input variations. Within the tested ranges, the model predicted no variation in output yield strength. We then spoke to an expert at ALCOA who explained that due to the fast quench in this case, noticeable yield strength variation from batch to batch is unlikely (Kinnear 1998). We thus focused on natural aging as the primary source of yield strength variation. The variational model for natural aging was derived by simply taking partial derivatives of equation (5.1) such that:

$$\frac{\partial Y_s}{\partial t} = 0.3469 \quad (5.2)$$

and

$$\frac{\partial Y_s}{\partial Y_{s_i}} = 1 \quad (5.3)$$

### 5.3.2 Stretch-Forming

#### 5.3.2.1 Process Overview

Stretch-forming is a manufacturing process commonly used in the aerospace industry to transform flat sheet metal into curved shapes. There are two basic types of stretch forming: stretch-wrap forming and drape forming. In stretch-wrap forming, a sheet is first stretched until it just becomes plastic, and is then wrapped over a die. The pre-stretch significantly reduces the amount of post-forming springback. In drape forming, a sheet is clamped around its edges, and is then simultaneously bent and stretched over a die. Usually the jaws are held fixed during drape forming, and the die moves to impart the stretch (Parris 1996). When the die is removed, the sheet springs back slightly, relieving internal stresses.

Our target part is formed using the drape forming process on a Cyril-Bath hydraulic press (Figure 5.8). Two operators are generally required during forming; one runs the machine while the other stands on top of the die table and watches the part and machine to spot problems.

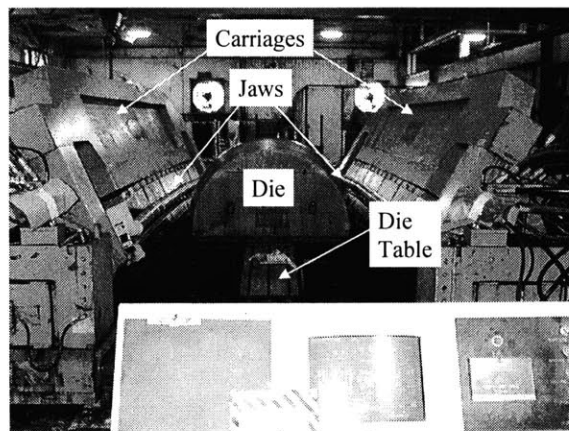


**Figure 5.8: Stretch-Forming Press.**

The first step in drape forming a part is to secure a flat blank in the jaws. The carriages (on which the jaws are mounted) are adjusted somewhat, and the die table is moved up until it contacts the sheet. The press operator continues to manipulate both table and carriages until the sheet is “snugged.” In the snug condition, the sheet is wrapped around the die, but without enough force to induce plastic strain. After the operator is satisfied with the snug, he moves the table up into the sheet. Displays on the machine report both table force (in tons) and die table height. The operator uses one of several possible



control strategies to determine when the part is formed. When we first visited the plant, the operator would stop forming at his discretion, based on visual inspection of the part. On the second trip, the operators were using a form of displacement control, in which they raised the die table to a specific table height (read off the display), based on prior experience. This change in control strategy was due to the work of (Parris 1996), who showed that displacement control can significantly reduce variation over visual inspection. The target part can also be formed using either force control or strain control, both of which will be discussed in more detail later in this chapter. Forming can be halted at any time, if the operator who is standing on top of the die table detects a problem. Potential problems include imminent tearing of the part and slippage in the jaws.

### 5.3.2.2 Modeling

The stretch-forming simulation is based on a Finite-Element Analysis (FEA) model of drape forming, developed by Socrates and Boyce within the commercial package *Abaqus* (Socrates and Boyce 1996). Their original model simulated the forming of a thin strip of material over a cylindrical die. We modified this model, to simulate the actual forming conditions of the target part. We describe the finite-element model in detail in this section; a full listing of the *Abaqus* input deck is provided in Appendix A.

#### *Aluminum Sheet*

The FEA simulation models one-half of the blank, with a line of symmetry running through the axis of the die. The full sheet measures 36" (w) by 136" (l), and is 0.05" thick. The material is 2024-W aluminum. The sheet is modeled in *Abaqus* using 4 node shell elements, which are commonly used in sheet forming simulations. The FEA sheet representation is meshed variably, with fine meshing near the point of initial contact with the die, and coarser mesh towards the side. A schematic of the sheet layout is shown in Figure 5.9 below. The diagram shows the node numbers at the corners of the sheet, the labeling of the axes, and the different mesh sizes.

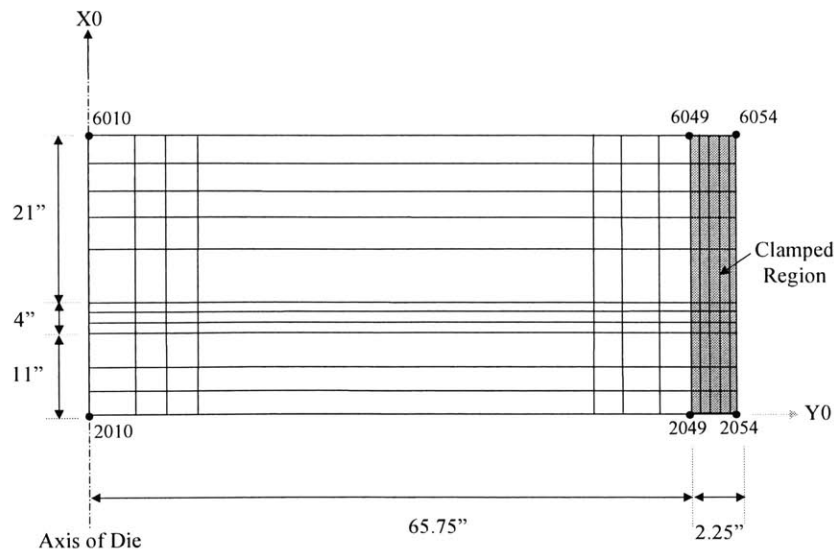


**Figure 5.9: Layout of Sheet.**

### *Die Geometry*

The die geometry used in the FEA model is derived from a CAD file of the actual die. Northrop-Grumman provided us with an IGES surface representation of the die geometry, converted from the *Catia* solid-modeler (Figure 5.10). We initially attempted to import the IGES file directly into *Abaqus*, using the *Houdini* software package developed by Algor Inc. We were unable to mesh the geometry correctly with *Houdini*; the software could interpret some surfaces, but not others. We then used the package *Abaqus Pre*, which was able to both read and mesh all surfaces. We imported the mesh generated by *Pre* into *Abaqus* as a rigid body. This seemed to work successfully, and *Abaqus* was able to display and utilize the rigid body die. We discovered, however, that forming invariably failed to converge, at a point roughly 20% of the way through the forming step. This problem was somehow related to the rigid body representation, and the only successful solution proved to be a different geometric representation. We were able to use the node points along the top edge of the meshed die representation to form the profile of a surface of revolution. This surface was then generated internally within *Abaqus*. After this modification, the FEA simulation successfully completed the forming step. The support engineers at HKS, the developers of *Abaqus*, were unable to explain this geometric discrepancy.



**Figure 5.10: Die Geometry.**

### *Material Properties*

The blank material is 2024-W aluminum, an unstable form due to heat treatment. As discussed previously, this material begins to naturally age when removed from the freezer, and thus the actual yield strength and stress strain curve change during forming. We initially used a stress-strain curve from Al 2024-O, with the yield strength scaled to agree with the output of the ALCOA quench model. This characterization allowed us to get the FEA model working, and provided a reasonable approximation of the production data. During our second trip to Northrop-Grumman, we conducted tensile tests on several specimens of 2024-W, which had been heat treated, quenched, and then placed in the freezer. The mean time out of the freezer was 24 minutes, and the mean yield strength was 131.6 MPa. We used this yield strength to calibrate the material model. The strain hardening coefficient we derived from the tensile tests was much larger than that found for 2024-O, and caused the simulation to diverge. We thus used the yield strength from the tensile tests in conjunction with the strain hardening coefficient for

2024-O. As will be shown in the validation section later in this chapter, this hybrid material model was sufficient to generate good predictions.

### *Coefficient of Friction*

The frictional coefficient,  $\mu$ , between the die and the sheet was set to a value of 0.1 based on previous research and best fit. Studies done by other authors have shown that the value of the frictional coefficient in stretch forming varies from 0.1 to 0.3 (Azushima 1995; Parris 1996). Within that range, the trends predicted by the model were closest to the trends found in the measurements at a value of  $\mu=0.1$ .

### *Jaws*

The jaws are simulated by constraining the set of nodes forming a 2.5” wide strip along the edge of the sheet (see Figure 5.9). The degrees of freedom of these nodes are linked by a user subroutine so that the entire strip moves as one unit during forming. While this approach simulates the clamping effects of the jaw, it fails to account for the slippage in the transverse and lateral directions found in the actual machine. Without this slippage, the simulated sheet begins to neck at a lower value of forming force than the actual sheet.

### *Wrap Angle*

The wrap angle parameter is an artifact of the *Abaqus* implementation. In reality, the die table moves up into the sheet, until the table reaches a given height. In the model, the edge of the sheet is being pulled down while the die remains stationary. To determine how far down the edge needs to move, we calculate a “wrap angle” based on the table height, carriage positions, and die radius. A simple schematic outlining the geometry of this situation is shown in Figure 5.11.

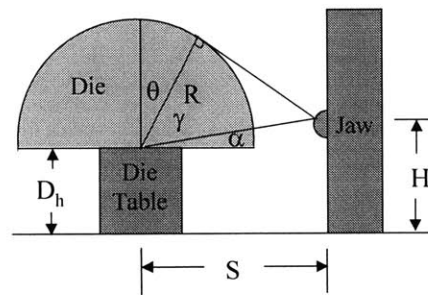


**Figure 5.11: Wrap Angle Geometry.**

To calculate the wrap angle,  $\theta$ , we can perform a series of simple calculations:

$$\alpha = \arctan\left(\frac{H - D_h}{S}\right) \quad (5.4)$$

$$\gamma = \arctan\left(\frac{\sqrt{S^2 + (H - D_h)^2} - R}{R}\right) \quad (5.5)$$

$$\theta = \frac{\pi}{2} - \gamma - \alpha \quad (5.6)$$

The actual measured values for each of these variables are listed in Table 5.1.

**Table 5.1: Forming Geometry.**

Variable	Measured Value
Table Height at Max. Force ( $D_h$ )	36.0625"
Jaw Height (H)	38.375"
Distance from Table Centerline to Jaw (S)	33.375"
Die Radius at Widest Point (R)	33.588"

Substituting these values into equations (5.4) through (5.6) results in a wrap angle of  $86^\circ$  when the sheet is completely formed. It was not possible to accurately determine the wrap at snug, but from visual inspection this angle was between  $50^\circ$  and  $70^\circ$ . Having calculated the final wrap angle, we can determine the Z-displacement of the edge of the sheet that is necessary to bend the sheet sufficiently. We use a simple algorithm to determine Z-displacement, based on sheet and die geometry. This algorithm is composed of the following calculations:

$$\zeta = R - R \cos \theta \quad (5.7)$$

$$s = R \theta \quad (5.8)$$

$$\Delta = \Lambda - s \quad (5.9)$$

$$Z = \Delta \sin \theta + \zeta \quad (5.10)$$

In these equations,  $\zeta$  is the vertical distance shown in Figure 5.12,  $Z$  is the displacement of the edge of the sheet from its original height,  $R$  is die radius,  $\theta$  is the wrap angle, and  $A$  is the total initial length of the sheet. These quantities are all depicted graphically in Figure 5.12. Equations (5.7) through (5.10) first determine the length of sheet wrapped around the die at the given wrap angle  $\theta$ , and then derive the location of the end of the sheet assuming that it will be tangent to the die at the last point of contact.

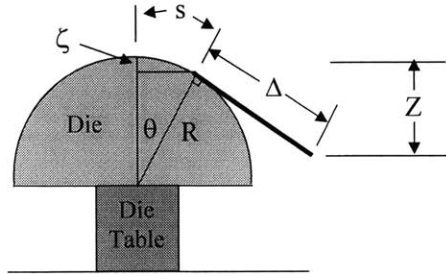


**Figure 5.12: Additional Wrap Angle Geometry.**

#### *Forming Force*

The maximum force during forming was recorded from the display on the forming press. This value is the measured force on the die table as the die is pushed into the sheet. A simple geometric relation can be used to adjust this value to the modeling framework, where the jaws pull down on the sheet. As shown in Figure 5.13, force on the sheet from the jaws will be:

$$F = \frac{\text{Die Table Force}}{2 \cdot \sin \theta} \quad (5.11)$$

where the factor of 2 is used to account for the fact that the simulation only models  $\frac{1}{2}$  of the sheet. Application of equation (5.11) gives a forming force of 238,412.8 N for the model, based on a measured average forming force of 53.3 tons. The same formula can be applied to determine the force at snug. We used a wrap angle at snug of  $53^\circ$ , which provided the best fit to measured data of all angles within the acceptable range. Based on a measured mean snug force of 18 tons, the snug force used in the model was 100,249 N.

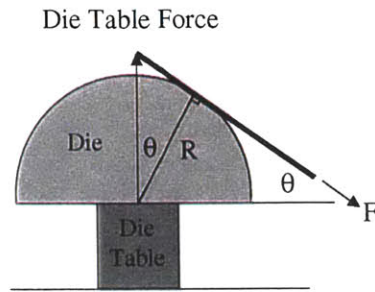


**Figure 5.13: Force Adjustment Geometry.**

### *Forming Steps*

The complete FEA simulation has 13 steps, including forming and relaxation. Figure 5.14 shows the main steps in graphical form. In this section, we provide a detailed explanation of each step. The full *Abaqus* input deck is listed in Appendix A.

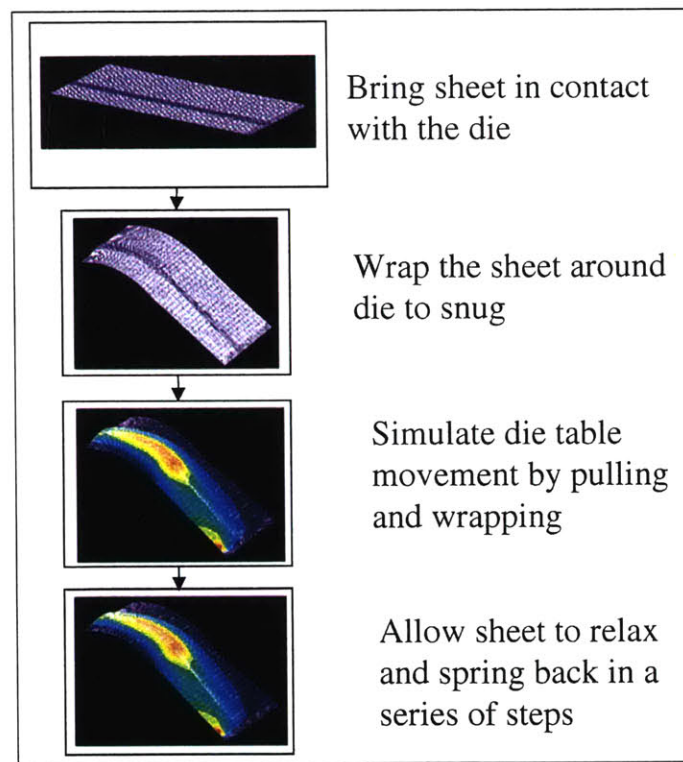


**Figure 5.14: Basic Steps of Forming Model.**

### *Step 1*

The model contains two rows of dashpot elements, attached at one end to nodes in the clamped region, and at the other end to ground. One row of dashpots is attached to nodes at the very edge of the sheet (node numbers 2054 to 6054), while the other row is

attached to nodes along the edge of the clamped region (a line parallel to the Y axis, composed of nodes numbered 2049 to 6049). The dashpot elements are used to aid in stress relaxation after forming. Although they must be included in the model definition, they are removed immediately in this step, and are then replaced in step 8, after forming.

#### *Step 2*

The blank is subject to tension by a force producing a stress across the entire sheet, equivalent to 0.5% of the material yield strength. Sheet boundaries are constrained to be symmetric about both the X and Y axes, and the entire sheet is constrained in the Z direction so that it remains flat during pre-stretch. During this step, the sheet is located slightly above the die in space.

#### *Step 3*

The edge of the sheet, constrained to simulate clamping conditions, is lowered by an amount equal to the sheet thickness. This brings the sheet into contact with the die. The sheet edges are kept constrained by symmetry conditions, and the sheet is still in tension.

#### *Step 4*

This step simulates snug. During actual forming, the die is raised into the sheet during snug, inducing a wrap angle between  $50^\circ$  and  $70^\circ$ . Later, during stretch, the die is raised an additional amount, bringing the wrap angle to its final value of  $86^\circ$ . In this model, the sheet is fully wrapped around the die during the snug step, while the stretch step only applies a tangential force to the sheet. This change was a modeling necessity; when stretch and wrap were combined into a single step, the finite-element code failed to apply the full load to the sheet. Instead, the step terminated at full wrap with only partial loading. We thus separate stretch and wrap into two different steps. Although this is an abstraction, it serves to accurately reproduce the strain field across the formed sheet.

During the snug step, the sheet is only restricted by symmetry about the Z axis, leaving its free edges unconstrained. The clamped edge is displaced in the Z direction by a value determined from equation (5.10), resulting in the desired wrap angle. Force on the sheet is increased to the mean value measured from the forming press at snug, translated to the model geometry through equation (5.11).

#### *Step 5*

The grips are rotated to allow force transmission at the proper angle. This is an artifact of the modeling geometry; during actual forming, this angle changes dynamically as the table height is increased. In the model, grip rotation is simulated by rotating the clamped edge (designated by the "PULL" node set) about the Y axis, by the wrap angle. The sheet is still constrained to be symmetric about the X axis, and an additional boundary condition is added to constrain it in the Y direction. This keeps the sheet from slipping off the die.

#### *Step 6*

This is the forming step. While maintaining the boundary conditions established in step 5, a force is applied to the clamped node set in the local (rotated) X direction. This force

is based on the measured maximum forming force, transformed to the model geometry through equation (5.11). During this step the sheet experiences significant plastic deformation. As discussed previously, in actual forming there is slippage between the sheet and jaws. Lack of slippage in the model results in increased edge wrinkling and an earlier onset of necking than is found in practice.

#### *Step 7*

In this step, the sheet is rigidly constrained in space while the die is removed from the model.

#### *Step 8*

Here the dashpot elements are reintroduced into the model. Forming of the target part is severe enough to induce significant wrinkling of the clamped edges. As the boundary constraints are removed, *Abaqus* must determine the final configuration of the relaxed wrinkled edge. The dynamics of unloading make it difficult for the program to identify the correct final edge geometry, resulting in convergence problems. Through experiment, we found that the addition of dashpot elements to the edge nodes allows convergence. These elements effectively “slow” relaxation, making it easier for *Abaqus* to determine the final geometry.

#### *Step 9*

This is the first relaxation step. The clamped region is kept constrained, and is prevented from rotating about the Y axis. Membrane stress in the sheet is allowed to relax over a time step of 1 second.

#### *Step 10*

Here the constraints on the PULL node set are relaxed, allowing for independent motion of the edge, excepting rotation about the Y axis. Membrane stress in the sheet is allowed to relax over a time step of 2220 seconds. This value was empirically determined to be long enough to allow all dashpot forces to decrease to negligible values. We found that two relaxation steps (9 and 10) are necessary for convergence. In the case of a single, longer, time step, *Abaqus* quickly increased the allowable time increment during bulk movement of the sheet, and was then unable to reduce it sufficiently to deal with edge wrinkling. The addition of a second relaxation step forces the program to restart with a much smaller time increment, avoiding this problem.

#### *Step 11*

In this step, the sheet is constrained rigidly in space and the dashpots are removed for the last time.

#### *Step 12*

The sheet is constrained to be symmetric about the X axis, and a single point is fixed in both the X and Y directions. This point, the site of initial contact with the die, is effectively “grounded,” which provides the sheet with a reference point fixed in space. The PULL node set is still constrained from rotation about the Y axis. The “Amplitude”



command, which controls the rate that the loads are removed, is essential for convergence of this step.

### *Step 13*

The constraint prohibiting rotation of the PULL node set around the Y axis is removed, allowing the sheet to unload to its final shape. The “Amplitude” command is necessary for convergence of this step as well.

#### 5.3.2.3 Modeling Notes

The *Abaqus* drape-forming model, listed in full in Appendix A, simulates forming of the target part shape under a range of process parameters. The model should work with other die shapes as well, although this was not tested. The two major assumptions in the model involve the frictional coefficient value and clamping at the edge of the sheet.

The results of our FEA model are quite sensitive to the value of the frictional coefficient governing contact between the sheet and die. From the forming literature, it seems likely that the frictional coefficient is not constant during forming (Azushima 1995). We were unable, however, to implement a dynamic frictional coefficient in the model, and thus assume that the value of this parameter is constant. In addition, the actual value, or range of values, for the frictional coefficient is unknown. As mentioned previously, studies done by other authors have shown that the value of the frictional coefficient in stretch forming varies from 0.1 to 0.3 (Azushima 1995; Parris 1996). Within that range, the trends predicted by the model were closest to the trends found in the measurements at a value of  $\mu=0.1$ .

We also assumed that there is no slippage between the sheet and the jaws. As described above, edge clamping was simulated by constraining the movement of nodes along the edge of the sheet. This clamping model does not allow for the slippage in both the lateral and transverse directions found in the actual system. Slippage between the sheet and the jaws would both reduce the edge wrinkling seen in the model results, and delay the onset of necking. Since the measurement locations for both outputs of interest (strain and thickness) were far from the clamped region, this assumption does not significantly affect the results.

#### 5.3.2.4 Variational Model

The first step in deriving the variational model from the *Abaqus* predictive model was to identify those process parameters most likely to contribute to output variation. Based on discussions with stretch-forming engineers and the work of Parris (1996), we determined that the most significant parameters contributing to variation in this operation were maximum force, material yield strength, sheet thickness, carriage position, and table height. Carriage position and table height do not appear explicitly in the model; they are instead combined into the “wrap angle” parameter. This leaves 4 input parameters for study.

The second step in developing the variational model was a designed experiment to determine parameter sensitivities. We considered only first-order effects, and ran a simple sensitivity analysis in which each input parameter was perturbed individually to values of  $\pm 1.5\sigma$  and  $\pm 3\sigma$ , where  $\sigma$  is the measured standard deviation of the value of the input variable. The output variables of interest (strains at three locations and thickness at 9 locations) were predicted at each input variable setting, and we interpolated a polynomial through each output/input combination. The derivative of this polynomial was then used to approximate the partial derivative of the output variable with respect to the input variable, in a region around the operating point. The set of partial derivatives serves as the variational model for stretch-forming. This method of calculating the sensitivities assumes that there are no second order interactions between the variables. This assumption was reasonable, since statistical analysis of the production data showed no significant correlation between input variables.

### 5.3.3 Assembling the ISM

The variational models for heat treatment and stretch-forming were linked together within a Microsoft *Excel* spreadsheet. The model was composed of four linked worksheets, one listing all system inputs and outputs, and three containing process sensitivities. On each worksheet, the sensitivities were used to form both linearized predictive models as in equation (3.5), and to predict output sensitivities through equations (3.33) and (3.34). The top-level worksheet, titled “Control,” listed all system inputs and outputs. Input values entered on this worksheet were simultaneously entered on the process worksheets. The first process worksheet was called “Heat Treatment,” and contained both the localized aging model from equation (5.1) and process sensitivities, derived from (5.2) and (5.3). Inputs to this worksheet were linked to the listing on the “Control” worksheet, and the process output, yield strength, became an input to the next two worksheets. The second process worksheet was titled “Thickness.” This sheet contained all of the thickness sensitivities derived from the stretch-forming predictive model. These sensitivities were linked together into a linearized predictive model of thickness at 9 locations on the part, and into both RSS and Worst-Case variational models of thickness variation. Outputs from this worksheet were reported on the “Control” sheet. The third process sheet was titled “Strain.” This worksheet contained all of the strain sensitivities derived from the stretch-forming model. Again, all process inputs except yield strength were obtained from the Control worksheet. Yield strength came from the Heat Treatment sheet. The Strain worksheet calculated output strain nominal values and variations at three locations on each part. These values were then reported on the Control worksheet.

By linking the inputs and outputs of each worksheet, the entire system model could be evaluated from the top-level Control worksheet. Changes to any input parameter were immediately propagated through the system, resulting in changes to the end-of-line nominal values and variations reported on the Control sheet. This spreadsheet implementation of the ISM allowed for easy implementation of system-level robustness and simulation of process control strategies. These applications will be discussed through the rest of this chapter.

## 5.4 Modeling Validation

The ISM predictions were validated by comparison with measured production data. Measurements were taken on a batch of 12 parts, produced at the Northrop-Grumman facility in October 1997. During production of these parts, the stretch-press was run in manual control, with forming being stopped based on operator discretion. In this section we discuss our measurement techniques, and list the measured values used as inputs to the system model. We then compare the model predictions to measured values of part strains and thickness.

### 5.4.1 Measured Parameters

#### *Thickness*

We measured sheet thickness before and after forming with a “Mighty-Mike” Hall-effect thickness gauge. This device consisted of a magnetic probe placed on one side of the sheet, and a ball bearing placed on the other. The distance between the tip of the probe and the bearing was displayed on a portable unit. Prior to forming, each sheet was measured in four locations, 1” in from each corner, in order to determine mean batch thickness and variation. After forming, sheet thickness was measured at nine locations on the part, as shown in Figure 5.15.

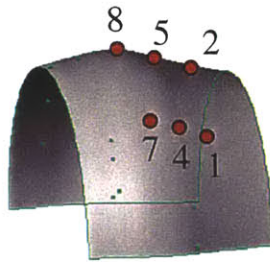


**Figure 5.15: Thickness Measurement Locations.**

Note that the part is axially symmetric, and thus locations 3, 6 and 9 are symmetrically opposite locations 1, 4, and 7, respectively. The thickness gauge measurements tended to drift, forcing frequent recalibration of the device. For this reason, we estimate measurement error to be 0.0005”.

#### *Force*

Both snug force and maximum force during forming were read off the machine display during operation. Previous calculations by (Parris 1996) suggest that the force readings on this machine can be inaccurate by up to  $\pm 10\%$  of the actual force. Our own experience has shown that bias in the force reading can be much higher—up to 100% of the actual force at times. Based on the stress-strain curve of the material, operator

model predictions, we estimate that our measured force values were within  $\pm 5\%$  of the actual force.

#### *Table Height*

Table height is displayed on the machine control panel. To determine the wrap angle, this table height reading was correlated with an absolute measurement of table height above ground. The table height reading appears to be quite accurate.

#### *Carriage Location*

Carriage location is also displayed on the control panel, and was also correlated to an absolute measurement of distance between the center of the die table and the edge of the jaw.

#### *Sheet Strain*

Strain on the sheet was measured through the separation of “strain marks,” inscribed on the sheet prior to forming. While this is not the most accurate means of determining strain, it proved to be the most reliable on the shop floor. Use of strain gauges was limited since we could not attach them in any way that might damage the surface finish of the sheet. We tested several methods, but were unable to find a dependable means of keeping gauges attached to the sheet during forming. We inscribed strain marks along both the X and Y axes of the sheet (as defined in Figure 5.9) at three measurement locations, shown in Figure 5.16.

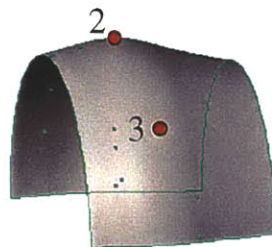


**Figure 5.16: Strain Measurement Locations.**

The marks were applied with a pencil and were exactly 10” apart, with the center points at the locations shown in Figure 5.16. A calibrated rule, with slots cut for marking, was used to place the marks accurately. Strain measurement error can come from two sources: inaccuracy in reading the separation between strain marks from the ruler, and misalignment of the strain marks themselves. The error on measuring stretch from the ruler is estimated to be  $\pm 0.03125$ ”. The maximum skew of any of the strain marks is estimated to be  $2.87^\circ$ . Over the total separation length of 10” this leads to a potential measurement error of  $\pm 0.00627$ . The total strain measurement error is thus  $\pm 0.00219$ .

#### *Contour*

Following the work of Parris (1996), we measured the springback of the part from the die after forming. Unlike the leading edges measured in that work, the nacelle doubler has little springback after forming, and virtually none after trim. To measure springback at

the front of the part (the left side of the part shown in Figures 5.15 and 5.16), we measured the distance from one corner to the other corner at the base of the die with a measuring tape. We then subtracted the diameter of the die from this reading. At the back of the part, the die protruded from the sheet. In this case we used a small scale to measure separation of the sheet from the die at each side. Due to the small amount of springback and the large measurement error, the springback measurements are not discussed further in this thesis.

#### **5.4.2 Measured Values**

The tables below list the measured values of inputs and outputs for the batch of 12 parts measured during the first trip. The operator made adjustments to the carriage displacement and table height settings after each of the first two parts. Because of these changes, and the fact that the first part tore during forming, we only present data for the last 10 parts in the batch. In the table, these are renumbered as parts 1-10. Table 5.2 lists the measured values of thickness for each part prior to forming. As discussed previously, these measurements were taken at each corner of the blank. Table 5.3 lists the values of machine parameters, read from the press display, at snug and at stop.

**Table 5.2: Sheet Thicknesses Before Forming.**

Part Number:	Thickness	Part Averages
1	0.0499	
	0.0502	
	0.0497	
	0.0496	0.04985
2	0.0509	
	0.0506	
	0.0499	
	0.0505	0.050475
3	0.05	
	0.0502	
	0.0501	
	0.0504	0.050175
4	0.05	
	0.0497	
	0.0502	
	0.0503	0.05005
5	0.0508	
	0.0509	
	0.0503	
	0.05044	0.05061
6	0.0504	
	0.0505	
	0.0507	
	0.0502	0.05045
7	0.0503	
	0.0504	
	0.0498	
	0.0497	0.05005
8	0.05	
	0.0503	
	0.0503	
	0.0503	0.050225
9	0.05	
	0.0499	
	0.0502	
	0.05	0.050025
10	0.0497	
	0.0498	
	0.0502	
	0.0506	0.050075
<b>Average:</b>	<b>0.0502</b>	<b>0.0502</b>
<b>Standard Dev:</b>	<b>0.00034</b>	
<b>% Std. Dev</b>	<b>0.6757</b>	

**Table 5.3 Machine Parameters During Forming**

Part #	Table Height at Snug (in)	Force at Snug (tons)	Table Height at Stop (in)	Force at Stop (tons)
1	52.6	18	57.53	53
2	52.46	18	57.6	55
3	52.15	17	57.71	53
4	52.41	17	57.01	54
5	52.91	20	57.69	54
6	52.84	17	57.76	52
7	52.86	20	57.66	54
8	52.66	18	57.51	50
9	52.76	17	57.72	55
10	52.0	17	57.72	53
Average	52.6	18	57.58	53.18
Standard Deviation	0.59	1.18	0.194	1.47

Carriage position is not listed in Table 5.3, as its value remained constant for these 10 parts. The position of the left carriage was set at 31.53", and the position of the right carriage was set at 31.55". Left and right are defined according to an operator standing at the control panel and looking at the stretch press. The next two tables list the value of output measurements. Table 5.4 lists sheet thickness at the 9 measurement points on each part after forming. Table 5.5 reports stretches (separation between two strain marks originally 10" apart) and strains at the three strain measurement locations on each part. The notation XX refers to measurements in the circumferential direction, and YY to measurements in the axial direction. These are based on the definitions of the sheet X and Y axes, from Figure 5.9.

**Table 5.4 Sheet Thickness After Forming.**

Part #	1	2	3	4	5	6	7	8	9
1	0.0479	0.048	0.0478	0.0469	0.0472	0.0465	0.0487	0.0481	0.0486
2	0.0478	0.0474	0.0477	0.0467	0.0472	0.0465	0.0487	0.0482	0.0485
3	0.0473	0.0481	0.0476	0.0466	0.0473	0.047	0.0482	0.0485	0.0478
4	0.0474	0.0483	0.0481	0.0474	0.0471	0.0471	0.0487	0.0493	0.0483
5	0.048	0.0482	0.0479	0.0465	0.0476	0.047	0.0481	0.0482	0.0479
6	0.0483	0.0482	0.048	0.0474	0.0479	0.0468	0.0488	0.0492	0.0488
7	0.0476	0.0474	0.0475	0.0467	0.0471	0.0464	0.048	0.0483	0.0476
8	0.0475	0.0483	0.0476	0.0473	0.0471	0.0465	0.0481	0.0485	0.0484
9	0.0474	0.0483	0.0477	0.047	0.0474	0.0467	0.0481	0.0492	0.049
10	0.0484	0.0485	0.0479	0.0479	0.048	0.047	0.0495	0.0481	0.0475
Average	0.04776	0.04807	0.04778	0.04704	0.04739	0.04675	0.04849	0.04856	0.04824
Std. Dev.	0.00039	0.00038	0.00019	0.00045	0.00033	0.00026	0.00047	0.00049	0.00051

**Table 5.5 Sheet Stretches and Strains at Each Location.**

Stretches: (in inches)	Measurement Pt. 2		Measurement Pt. 3		Measurement Pt. 1	
Part #	Top XX	Top YY	Left XX	Left YY	Right XX	Right YY
3	10.906	9.750	11.156	9.750	11.063	9.719
4	11.047	9.656	11.0469	9.75	11.047	9.750
5	11.000	9.813	11.172	9.813	11.094	9.813
6	11.047	9.719	11.156	9.750	11.063	9.688
7	11.047	9.688	11.031	9.688	11.125	9.719
8	11.032	9.719	11.031	9.688	11.063	9.719
9	11.063	9.719	11.031	9.750	11.125	9.719
10	11.000	9.734	11.000	9.750	11.125	9.750
11	11.000	9.719	11.094	9.719	11.078	9.641
12	11.031	9.688	11.094	9.719	11.188	9.688
Strains:	Measurement Pt. 2		Measurement Pt. 3		Measurement Pt. 1	
Part #	Top XX	Top YY	Left XX	Left YY	Right XX	Right YY
3	0.091	-0.025	0.116	-0.025	0.106	-0.028
4	0.105	-0.034	0.105	-0.025	0.105	-0.025
5	0.1	-0.019	0.117	-0.019	0.109	-0.019
6	0.105	-0.028	0.116	-0.025	0.106	-0.031
7	0.105	-0.031	0.103	-0.031	0.113	-0.028
8	0.103	-0.028	0.103	-0.031	0.106	-0.028
9	0.106	-0.028	0.103	-0.025	0.113	-0.028
10	0.1	-0.027	0.1	-0.025	0.113	-0.025
11	0.1	-0.028	0.109	-0.028	0.108	-0.036
12	0.103	-0.031	0.109	-0.028	0.119	-0.031
AVG	0.102	-0.028	0.108	-0.026	0.110	-0.028
STDEV	0.0045	0.0042	0.0062	0.0037	0.0043	0.0046



### 5.4.3 System Model Predictions

#### 5.4.3.1 Nominal Values

The system model was used to predict output strains and sheet thickness. Strains were predicted at 3 locations on each of the 10 parts, and thickness was predicted at 9 locations on each part. The predicted strains are shown in comparison with measured strain values in Figure 5.17. Each of the measurement points on the graph is the average of ten measurements, one for each part.

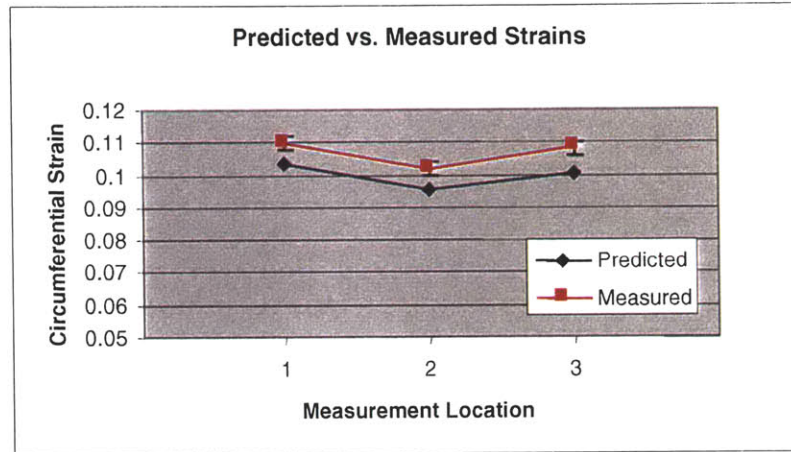


**Figure 5.17: Predicted and Measured Strain Values.**

The model is clearly a good predictor of the trend of the data, with predicted values offset from the measured values by less than 6%. The bias differs from location 1 to location 3 by just over 1%. The measured and predicted values at each point are listed in Table 5.6.

**Table 5.6: Measured and Predicted Strain Values.**

Strain	Measured	Predicted	Error
Location 1	0.1097	0.1034	5.74%
Location 2	0.1017	0.0957	5.9%
Location 3	0.1081	0.1006	6.94%

While the error is quite reasonable for a finite-element forming simulation, it may be due in part to uncertainty in the input parameter values. As discussed previously, the value of forming force read from the machine display could differ from the actual forming force by as much as 10%. An increase in forming force of less than 5% in the system model results in predicted values within 1% of measured values. Similarly, a decrease in the initial material yield strength of less than 3% gives predictions that match the measurements within 1%. It seems quite possible that the actual value of one or both of these input parameters differed slightly from the measured value.

Figure 5.18 shows the measured and predicted values of thickness at each of the nine measurement locations on each part. Again, each of the predicted values on the graph is the average of ten measurements, one per part.

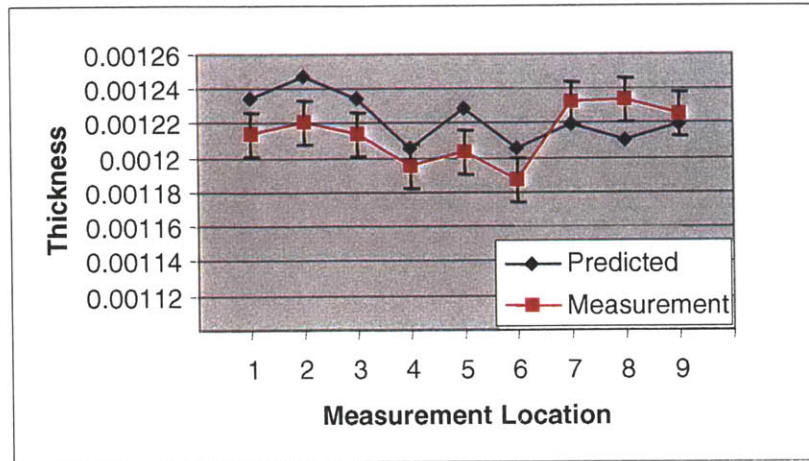


**Figure 5.18: Predicted and Measured Thickness Values.**

Figure 5.18 shows that the model follows thickness trends well from points 1 through 6; the model under-predicts thickness at points 7, 8, and 9. Maximum error between the predicted and measured values is just over 2%. Referring back to Figure 5.15, locations 7-9 are near the initial contact point with the die, and in the region of greatest plastic strain. Any bias in the model will have its greatest effects in this area. The ISM predicts greater thinning at these points than is seen in the measured data. This could be due to the effects of slippage at the jaws or to a frictional coefficient lower than that used in the simulation. In either case, the error at this point is less than 2%. Actual and predicted values for thickness at each of the nine measurement points are listed in Table 5.7.

**Table 5.7: Measured and Predicted Average Thickness Values.**

Thickness	Measured Value (m)	Predicted Value (m)	% Error
Location 1	0.001213	0.001202	1.8
Location 2	0.001221	0.001198	2.2
Location 3	0.001214	0.001202	1.8
Location 4	0.001195	0.001209	0.9
Location 5	0.001204	0.001231	2.0
Location 6	0.00119	0.001209	1.5
Location 7	0.001232	0.001255	1.0
Location 8	0.001233	0.001265	1.9
Location 9	0.001225	0.001255	0.5

### 5.4.3.2 Variations

As discussed in Chapter 3, a system can have multiple operating points that produce parts with identical nominal quality characteristic values, but with different amounts of variation. It is therefore insufficient to validate the predicted nominal output values of the ISM; we must also establish the accuracy of the predicted variations. We can predict end-of-line variance of a two-operation system using equation (3.32):

$$\bar{\sigma}_{\bar{q}_2}^2 = \left[ F_{2\bar{x}}^2 \right]_{\bar{q}_1^* \bar{x}^*} \bar{\sigma}_{\bar{x}_2}^2 + \left[ F_{2\bar{q}_1}^2 \right]_{\bar{q}_1^* \bar{x}_2^*} \left[ F_{1\bar{q}_0}^2 \right]_{\bar{q}_0^* \bar{x}_1^*} \bar{\sigma}_{\bar{q}_0}^2 + \left[ F_{2\bar{q}_1}^2 \right]_{\bar{q}_1^* \bar{x}_2^*} \left[ F_{1\bar{x}}^2 \right]_{\bar{q}_0^* \bar{x}_1^*} \bar{\sigma}_{\bar{x}_1}^2 + \left[ F_{2\bar{q}_1}^2 \right]_{\bar{q}_1^* \bar{x}_2^*} \bar{\varepsilon}_{v_1} + \bar{\varepsilon}_{v_2} \quad (3.32)$$

For the sheet stretch-forming system, end-of-line variance can be calculated as:

$$\begin{bmatrix} \sigma_{\varepsilon_1}^2 \\ \sigma_{\varepsilon_2}^2 \\ \sigma_{\varepsilon_3}^2 \\ \sigma_{h_f}^2 \end{bmatrix} = \begin{bmatrix} \frac{\partial \varepsilon_1}{\partial f} & \frac{\partial \varepsilon_1}{\partial \theta} \\ \frac{\partial \varepsilon_2}{\partial f} & \frac{\partial \varepsilon_2}{\partial \theta} \\ \frac{\partial \varepsilon_3}{\partial f} & \frac{\partial \varepsilon_3}{\partial \theta} \\ \frac{\partial h_f}{\partial f} & \frac{\partial h_f}{\partial \theta} \end{bmatrix}^2 \begin{bmatrix} \sigma_f^2 \\ \sigma_\theta^2 \end{bmatrix} + \begin{bmatrix} \frac{\partial \varepsilon_1}{\partial h_i} \\ \frac{\partial \varepsilon_2}{\partial h_i} \\ \frac{\partial \varepsilon_3}{\partial h_i} \\ \frac{\partial h_f}{\partial h_i} \end{bmatrix}^2 \bar{\sigma}_{h_i}^2 + \begin{bmatrix} \frac{\partial \varepsilon_1}{\partial Y_s} \\ \frac{\partial \varepsilon_2}{\partial Y_s} \\ \frac{\partial \varepsilon_3}{\partial Y_s} \\ \frac{\partial h_f}{\partial Y_s} \end{bmatrix}^2 \left[ \frac{\partial Y_s}{\partial Y_{s_i}} \right]^2 \bar{\sigma}_{Y_{s_i}}^2 + \begin{bmatrix} \frac{\partial \varepsilon_1}{\partial Y_s} \\ \frac{\partial \varepsilon_2}{\partial Y_s} \\ \frac{\partial \varepsilon_3}{\partial Y_s} \\ \frac{\partial h_f}{\partial Y_s} \end{bmatrix}^2 \left[ \frac{\partial Y_s}{\partial t} \right]^2 \bar{\sigma}_t^2 \quad (5.12)$$

where:

- $\varepsilon_1$ : Strain at measurement location 1
- $\varepsilon_2$ : Strain at measurement location 2
- $\varepsilon_3$ : Strain at measurement location 3
- $h_f$ : Average thickness after forming (across all 9 points)
- $h_i$ : Average thickness of the incoming material
- $Y_{s_i}$ : Yield strength of the incoming material
- $Y_s$ : Yield strength after heat treatment and aging
- $f$ : Maximum forming force
- $\theta$ : Wrap angle
- $t$ : Natural aging time

Equation (5.12) is a reduced version of the actual variational model used to determine the tolerance threshold of the system. The full model contains very large sensitivity matrices linking each input with each of the nine output thicknesses, and with 10 different strain measurements that combine into the average output strain at each measurement location. The values of each sensitivity term were derived from the *Abaqus* model through perturbation analysis, as discussed in Chapter 3. The full sensitivity matrices are presented in Appendix B. In order to reduce the complexity of the examples in this

chapter, we will write equations as if there is a single thickness sensitivity term, and 3 sensitivity terms for strain (one at each measurement location). For the purposes of example, we also neglect the error terms in each equation.

The predicted end-of-line variation predictions, obtained through use of the full sensitivity matrices, are compared with measured output variations in Table 5.8.

**Table 5.8: Measured and Predicted End-of-Line Standard Deviation.**

Output Standard Deviations	Measured	Predicted Value (RSS)	Predicted Value (Worst Case)	% Error Between Measured and RSS
Strain (mark 1)	.004345	.006304	.009325	45.1
Strain (mark 2)	.004507	.004731	.008107	4.97
Strain (mark 3)	.006241	.006614	.009428	5.98
Thickness	$9.82 \cdot 10^{-6}$ m	$9.38 \cdot 10^{-6}$ m	$1.29 \cdot 10^{-5}$ m	4.48

Table 5.8 shows that the predicted values of end-of-line variation are very close to the measured values for three of the four output variables. Only strain variation at measurement location 1 shows significant error. Measurement locations 1 and 3 are symmetric reflections of one another; the slightly different values of the predictions come from machine asymmetries captured in the model. Due to this relationship, the measured value at location 1 should be nearly identical to the measured value at location 3. Were the measured value at location 1 equal to that at location 3, for instance, the error between measurement and prediction would be under 1%. The discrepancy between measurements at locations 1 and 3 indicates that the error at location 1 is likely the result of either measurement error or some asymmetry in the machine that is not reflected in the model.

Having generated and validated the stretch-forming ISM, we now demonstrate the formulations developed in Chapters 3 and 4. In the following sections, we determine the major sources of variation in the stretch forming system, develop several variation reduction strategies, and compare these strategies in simulation. We also conduct system-level parameter design, and calculate process limits for each operation.

## 5.5 Major Sources of Variation

The second step of the variation reduction method outlined at the beginning of this chapter is to determine the major sources of variation in the system. We can do this for each input parameter by first measuring its variation, multiplying this value by each relevant process sensitivity, and then dividing by the total end-of-line variation, calculated using the Worst-Case method. For example, the percentage contribution of forming force to strain at measurement location 1 is calculated as:

$$\% \text{ Contribution} = \frac{\left(\frac{\partial \varepsilon_1}{\partial f}\right) \cdot \sigma_f}{\sigma_{\varepsilon_1}} \quad (5.13)$$

where  $\sigma_f$  is the measured input force variation, and  $\sigma_{\varepsilon_1}$  is the total strain variation at location 1, calculated using the worst-case method as follows:

$$\sigma_{\varepsilon_1} = \left[ \frac{\partial \varepsilon_1}{\partial f} \quad \frac{\partial \varepsilon_1}{\partial \theta} \right] \cdot \begin{bmatrix} \sigma_f \\ \sigma_\theta \end{bmatrix} + \left[ \frac{\partial \varepsilon_1}{\partial h_i} \right] \cdot \sigma_{h_i} + \left[ \frac{\partial \varepsilon_1}{\partial Y_s} \right] \cdot \left[ \frac{\partial Y_s}{\partial Y_{s_i}} \right] \cdot \sigma_{Y_{s_i}} + \left[ \frac{\partial \varepsilon_1}{\partial Y_s} \right] \cdot \left[ \frac{\partial Y_s}{\partial t} \right] \cdot \sigma_t \quad (5.14)$$

For the sheet stretch-forming system, the percentage contributions of each input to each output are listed in Table 5.9.

**Table 5.9: Major Sources of Variation in the Stretch-Forming System.**

Percent Contribution of Inputs to End-of-line Variation		Process Variables				
		Heat Treatment		Stretch Forming		
		Initial Yield Strength	Aging Time	Forming Force	Wrap Angle	Initial Thickness
Output Quality Characteristi	Strain (1)	16	23.3	49.7	.7	10.6
	Strain (2)	18.3	26.3	35.7	3.5	16.2
	Strain (3)	12.1	17.5	58.2	.9	11.3
	Thickness	6.2	8.8	18.7	.4	65.9

Table 5.9 clearly shows that process parameters are the major sources of strain variation. Forming force variation has the largest effect, followed by variation in aging time. The third process parameter, wrap angle, has a very small effect. Variations in the incoming material are responsible for 20-30% of end-of-line variation. This implies that the most effective means of reducing strain variation are process changes, rather than

improvements in the stock material. Each operation has a significant impact on end-of-line variation. Thickness variation is just the opposite. The major source of end-of-line thickness variation is the thickness variation of the incoming material. This is followed by variation in the forming force. The heat treatment operation only causes about 15% of final thickness variation, and the effect of wrap angle variation is very small. These results indicate that the best way to decrease end-of-line thickness variation is to specify and purchase stock material with tighter thickness tolerances.

## 5.6 System-Level Robustness

Now that we have identified the major sources of variation in the system, we seek to reduce output sensitivity to these input variations. As discussed in section 3.9, the ISM can be used to conduct system-level parameter design, in order to find the operating point producing lowest end-of-line variation. In Chapter 3, we presented the following formulation for system-level parameter design:

$$\begin{aligned}
\min \quad & \left\| \bar{\sigma}_{\bar{q}_i} \right\|^2 = \left[ F_{i, \bar{q}_{i-1}} \right]^2 \bar{\sigma}_{\bar{q}_{i-1}}^2 + \left[ F_{i, \bar{x}} \right]^2 \bar{\sigma}_{\bar{x}_i}^2 + \left[ F_{i, \bar{p}} \right]^2 \bar{\sigma}_{\bar{p}_i}^2 + \bar{\varepsilon}_v \\
\text{s.t.} \quad & \bar{m} - \bar{\delta} \leq \bar{q}_i \leq \bar{m} + \bar{\delta}, \bar{q}_i = F(\bar{x}, \bar{q}_{i-1}, \bar{p}) \\
\text{over} \quad & \bar{p}_i \in \bar{P}_i \\
\text{where} \quad & \bar{x}_i, \bar{\sigma}_{\bar{x}_i}, \bar{\sigma}_{\bar{p}_i}, \bar{\varepsilon}_v \text{ are constant over } \bar{P}_i
\end{aligned} \tag{3.43}$$

where  $m$  is the vector of end-of-line targets, and  $\delta$  is some acceptable deviation from that target such that:

$$\delta \leq \frac{T_i}{3}$$

This ensures that the quality characteristic values of the produced parts will be within their toleranced values. The formulation of (3.43) can be executed within the Microsoft *Excel* spreadsheet environment containing the ISM. We seek to minimize a vector norm of output variables:

$$\left\| \bar{\sigma}_{\bar{q}_i} \right\| = \sqrt{\left| \sigma_{q_1} \right|^2 + \left| \sigma_{q_2} \right|^2 + \cdots + \left| \sigma_{q_n} \right|^2} \tag{5.15}$$

For this example, we consider 4 output variables: strain variation at the three measurement locations  $(\sigma_{\varepsilon_1}, \sigma_{\varepsilon_2}, \sigma_{\varepsilon_3})$ , and average thickness variation,  $\sigma_{h_f}$ . The system has a total of 5 input variables: initial yield strength,  $Ys_i$ , aging time,  $t$ , forming force,  $f$ , wrap angle,  $\theta$ , and initial thickness,  $h_i$ . Three of these inputs are adjustable parameters: aging time, forming force, and wrap angle.

These adjustable variables are limited to the following ranges:

$$15 \text{ min} \leq t \leq 45 \text{ min}$$

$$200 \text{ KN} \leq f \leq 275 \text{ KN}$$

$$80^\circ \leq \theta \leq 90^\circ$$

The lower bound on aging time is 15 minutes, which is the minimum practical time out of freezer required to form a part. The upper limit is set at 45 minutes, which is the maximum usually seen in practice, although it is feasible that the parts could be allowed to age even longer. Force is bounded over a range of values slightly larger than the  $\pm 3\sigma$  range seen in practice. All parts formed with force values within this range in the plant were judged acceptable. Similarly, the bounds on the wrap angle contain the range of values used to manufacture acceptable parts in practice.

We also need output target values and tolerances, in order to limit the number of possible operating points. Actual specifications were not available for this part, and would not have been prescribed for strains in practice. For the purposes of this example, we dictate an end-of-line nominal target strain value of 0.1, with a tolerance of  $\pm 0.02$ . These values are based upon the range of strains measured on acceptable production parts. We also prescribe the minimum allowable output thickness to be 0.045", which is 90% of the stock thickness. This value is based on standard aerospace tolerances.

We define the system operating point by the values of the three adjustable variables: aging time, forming force, and wrap angle. The original operating point is:

$$t = 24 \text{ min}$$

$$f = 238412.8 \text{ N}$$

$$\theta = 86^\circ$$

which results in an output norm value of:

$$\|\bar{\sigma}_{\bar{q}_i}\| = 0.0103$$

In this example, we use the Microsoft *Excel* solver (a Generalized Reduced Gradient search algorithm) to minimize this norm, subject to the constraints outlined above. We first assume that:

$$\delta = 0$$

which constrains the predicted nominal output values to be identical to the target output values. Using the formulation in (3.43), the solver suggests a slightly more robust operating point with an output norm value:

$$\|\bar{\sigma}_{\bar{q}_i}\| = 0.00992$$

This operating point is defined by:

$$t = 15 \text{ min}$$

$$f = 236146.9 \text{ N}$$

$$\theta = 83^\circ$$

At this point, end-of-line variation is reduced by 4%, with no change in the target output values. The new operating point requires nominal aging time to decrease by 9 minutes. For this to be feasible, the operators must remove and form each part from the freezer individually. This requires additional effort on their part, but is relatively easy to implement. In addition, forming force must decrease by 1% (about 0.5 tons), and wrap angle must decrease by 3%. Both of these changes are minor, and can be implemented by the operator controlling the stretch press with no additional effort.

By allowing some deviation from the original target specifications, we can reduce end-of-line variation even more. If we constrain the nominal output values to remain within  $3\sigma$  of the original tolerance limits:

$$\delta = \frac{T_i}{3} = 0.0067$$

the solver finds an improved norm value of:

$$\|\bar{\sigma}_{\bar{q}_i}\| = 0.00784$$



at the operating point defined by:

$$t = 15 \text{ min}$$

$$f = 225210.6 \text{ N}$$

$$\theta = 83^\circ$$

At this operating point, end-of-line variation is reduced by 24% of its original value. This operating point differs from the previous one only in that forming force has now been reduced to 95% of its original value. This change is easy to implement in practice, and requires no additional effort from the operator. Although the nominal values of the output quality characteristics have shifted from the original target values, they will still meet tolerances with a 99.7% probability. The nominal values of strain and thickness at these settings are shown in Table 5.10.

**Table 5.10: Predicted Strain and Thickness After Parameter Design**

Variable	Nominal Value	Variation
Strain at Location 1	0.1035	0.0042
Strain at Location 2	0.0933	0.0053
Strain at Location 3	0.0984	0.0040
Thickness	0.001224 m	$9.34 \cdot 10^{-6}$ m

The nominal strain values shown in Figure 5.10 are reasonable, based on our measurements of acceptable production parts. Note that in this example, we simultaneously changed the operating points of two different operations in order to get the lowest end-of-line variation. This can be more effective than considering each operation separately. Had we followed the latter approach, aging time in the heat treatment operation would have remained fixed since aging time sensitivity is a constant. As such, we would have attempted to optimize the stretch forming operation based on an input nominal aging time of 24 minutes. Using this value, the *Excel* solver suggests a new operating point defined by:

$$f = 232230.8 \text{ N}$$

and

$$\theta = 80^\circ$$

The output norm value at this operating point is:

$$\|\bar{\sigma}_{\bar{q}_i}\| = 0.00884$$

This is a 14% reduction in variation over the original settings, significantly less than the 24% improvement gained by considering the entire system. As shown by this example, system-level parameter design can be a highly effective variation reduction technique. In some situations, however, additional improvement is desired. In the following sections we consider the use of measurement and process control to reduce end-of-line variation. To prevent confusion, we will evaluate the system at the original operating point, not the more robust point found in this section.

## 5.7 Tolerance Threshold

The next step in our variation reduction method is to evaluate whether there is a need for measurement or process control in a system. To do this, we compare the Tolerance Threshold values of each operation with the process limits. In this section we determine the Threshold of the heat treatment operation.

As discussed in section 3.5, the Tolerance Threshold of an operation represents the minimum process variation inherent in that operation. Table 5.8 lists the predicted Threshold values for the example system, along with measured values of process variation. We can also calculate the Tolerance Threshold of the heat treatment operation alone, using either the Worst-Case stackup method:

$$\bar{t}_{q_2} = 6 \left[ \left[ F_{\bar{x}} \right]_{q^*, \bar{x}^*} \bar{\sigma}_x + \left[ \left[ F_{q_1} \right]_{q^*, \bar{x}^*} \bar{T}_{q_1} + 6 \bar{\sigma}_{\bar{e}} + \bar{e}_s \right] \right] \quad (3.26)$$

or the RSS method:

$$\bar{t}_{q_2}^2 = 36 \left[ \left[ F_{\bar{x}}^2 \right]_{q^*, \bar{x}^*} \bar{\sigma}_x^2 + \left[ \left[ F_{q_1}^2 \right]_{q^*, \bar{x}^*} \bar{T}_{q_1}^2 + 36 \bar{\sigma}_{\bar{e}}^2 + \bar{e}_s^2 \right] \right] \quad (3.27)$$

The output for this operation is material yield strength after aging, a quantity that cannot be measured in-process. Our model of heat treatment involves a single input process parameter, aging time, and one input material property, initial yield strength. Since the heat treatment operation is modeled as a closed-form equation in the region of interest, the heat treatment sensitivities can be represented analytically as:

$$\frac{\partial Y_s}{\partial t} = 0.3469 \quad (5.2)$$

and

$$\frac{\partial Y_s}{\partial Y_{s_i}} = 1 \quad (5.3)$$

Equations (3.14) and (3.15) can then be re-written as:

$$\tau_{Y_S} = 6 \left[ \left[ \frac{\partial Y_S}{\partial t} \right]_* \sigma_t + \left[ \left[ \frac{\partial Y_S}{\partial Y_{S_i}} \right]_* T_{Y_{S_i}} \right] + 6\sigma_{\varepsilon} \right] \quad (5.16)$$

and

$$\tau_{Y_S}^2 = 36 \left[ \left[ \frac{\partial Y_S}{\partial t} \right]_*^2 \sigma_t^2 + \left[ \left[ \frac{\partial Y_S}{\partial Y_{S_i}} \right]_*^2 T_{Y_{S_i}}^2 + 36\sigma_{\varepsilon}^2 \right] \right] \quad (5.17)$$

Substituting the measured variations for both  $\sigma_t$  and for  $T_{Y_{S_i}}$  (which properly speaking is a tolerance on the incoming material, but for our purposes will be identical to the known input variation of the incoming material) into equations (5.16) and (5.17) gives:

$$\tau_{Y_S} = 6 \cdot (0.3469) \cdot (5) + (1.2) + 6\sigma_{\varepsilon} \quad (5.18)$$

and

$$\tau_{Y_S}^2 = 36 \cdot (0.3469)^2 \cdot (5)^2 + (1.2)^2 + 36\sigma_{\varepsilon}^2 \quad (5.19)$$

If we neglect the error terms, the Tolerance Threshold value calculated by the Worst-case method is:

$$\tau_{Y_S} = 11.61 \text{ MPa}$$

And the Threshold value using the RSS method is:

$$\tau_{Y_S} = 10.48 \text{ MPa}$$

These values are the minimum levels of  $6\sigma$  process variation inherent in the heat treatment operation. Any feasible tolerance on output yield strength must be larger than these values. In the following section we calculate process limits for the heat treatment operation and compare them with these Threshold values.

## 5.8 Process Limits

As discussed in Chapter 4, process limits can be used to identify the need for measurement or process control within a system. We now derive process limits for the heat treatment and stretch forming operations, based upon a set of end-of-line tolerances. The problem of determining process limits can be formulated as:

$$\begin{aligned}
 & \max \quad \|W\bar{\lambda}_i\| \\
 & \text{s.t.} \quad \left\| F_{i, \bar{q}_{i-1}} \right\|_{q_{i-1}^*, \bar{x}_i^*} \bar{\lambda}_i \leq \bar{T}_i - \bar{K} \\
 & \text{over} \quad \bar{\lambda}_i \geq \bar{\delta} \\
 & \text{where} \quad \bar{K} = 6 \left\| F_{i, \bar{x}} \right\|_{q_{i-1}^*, \bar{x}_i^*} \bar{\sigma}_{\bar{x}_i} + 6\bar{\sigma}_{\bar{\varepsilon}_i} + \bar{\varepsilon}_{s_i}
 \end{aligned} \tag{5.20}$$

Equation (5.20) is a straightforward Linear Programming (LP) problem, and can be solved using traditional LP techniques. In this section, we first determine the process limits of the stretch-forming operation by back-propagating end-of-line tolerances. We then use the stretch-forming process limits to generate process limits for the heat treatment operation.

### 5.8.1 Stretch-Forming Process Limits

Process limit analysis begins with the last operation in the manufacturing system. In our two-operation example system, this is the stretch-forming operation. The inputs and outputs of this operation are shown in schematic form in Figure 5.19.

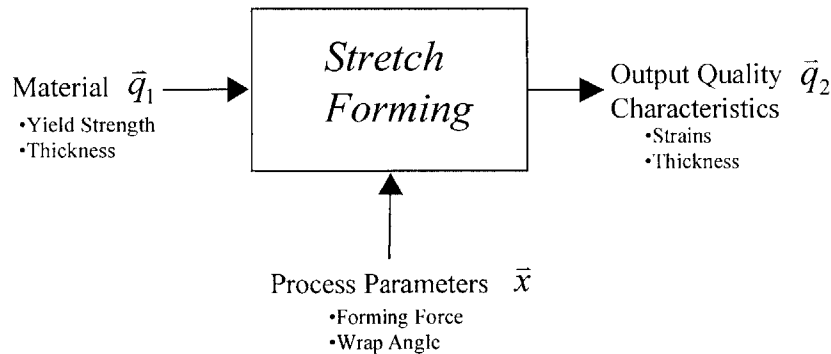


**Figure 5.19: Stretch Forming Inputs and Outputs**

The output quality characteristics of the stretch-forming operation are also the end-of-line quality characteristics of the system. End-of-line tolerances are thus constraints on strains and final thickness. In practice, it is unlikely that strains would be toleranced; some other criterion would be used to evaluate contour. For the purpose of this example, however, we will dictate specifications on strain based on measurements of production parts.

As shown in Figure 5.19, the vector of process parameters,  $\bar{x}$ , is composed of two variables: forming force and wrap angle. The vector of incoming material characteristics,  $\bar{q}_1$ , also includes two variables: yield strength, and thickness. The output vector  $\bar{q}_2$  contains four variables: strain at three measurement locations, and average output thickness. These vectors can be written as:

$$\bar{x} = \begin{bmatrix} F \\ \theta \end{bmatrix} \quad \bar{q}_1 = \begin{bmatrix} Ys \\ h_i \end{bmatrix} \quad \bar{q}_2 = \begin{bmatrix} \varepsilon_1 \\ \varepsilon_2 \\ \varepsilon_3 \\ h_f \end{bmatrix}$$

Using these input and output vectors, the LP formulation of (5.20) can be re-written for this example. The process vector  $\bar{K}$  (defined in section 4.1) will be:

$$\bar{K} = 6 \cdot \begin{bmatrix} \frac{\partial \varepsilon_1}{\partial f} & \frac{\partial \varepsilon_1}{\partial \theta} \\ \frac{\partial \varepsilon_2}{\partial f} & \frac{\partial \varepsilon_2}{\partial \theta} \\ \frac{\partial \varepsilon_3}{\partial f} & \frac{\partial \varepsilon_3}{\partial \theta} \\ \frac{\partial h_f}{\partial f} & \frac{\partial h_f}{\partial \theta} \end{bmatrix} \cdot \begin{bmatrix} \sigma_f \\ \sigma_\theta \end{bmatrix} \quad (5.21)$$

and the constraint on allowable input tolerances (4.2) is:

$$\begin{bmatrix} \frac{\partial \varepsilon_1}{\partial Ys} & \frac{\partial \varepsilon_1}{\partial h_i} \\ \frac{\partial \varepsilon_2}{\partial Ys} & \frac{\partial \varepsilon_2}{\partial h_i} \\ \frac{\partial \varepsilon_3}{\partial Ys} & \frac{\partial \varepsilon_3}{\partial h_i} \\ \frac{\partial h_f}{\partial Ys} & \frac{\partial h_f}{\partial h_i} \end{bmatrix} \cdot \begin{bmatrix} \lambda_{Ys} \\ \lambda_{h_i} \end{bmatrix} \leq \begin{bmatrix} T_{\varepsilon_1} \\ T_{\varepsilon_2} \\ T_{\varepsilon_3} \\ T_{h_f} \end{bmatrix} - 6 \cdot \begin{bmatrix} \frac{\partial \varepsilon_1}{\partial f} & \frac{\partial \varepsilon_1}{\partial \theta} \\ \frac{\partial \varepsilon_2}{\partial f} & \frac{\partial \varepsilon_2}{\partial \theta} \\ \frac{\partial \varepsilon_3}{\partial f} & \frac{\partial \varepsilon_3}{\partial \theta} \\ \frac{\partial h_f}{\partial f} & \frac{\partial h_f}{\partial \theta} \end{bmatrix} \cdot \begin{bmatrix} \sigma_f \\ \sigma_\theta \end{bmatrix} \quad (5.22)$$

The full LP problem can then be restated as:

$$\begin{aligned}
 & \max \quad T_{Y_s} + T_{h_i} \\
 & \text{s.t.} \quad \begin{matrix} \left| \frac{\partial \varepsilon_1}{\partial Y_s} & \frac{\partial \varepsilon_1}{\partial h_i} \right| \\ \left| \frac{\partial \varepsilon_2}{\partial Y_s} & \frac{\partial \varepsilon_2}{\partial h_i} \right| \\ \left| \frac{\partial \varepsilon_3}{\partial Y_s} & \frac{\partial \varepsilon_3}{\partial h_i} \right| \\ \left| \frac{\partial h_f}{\partial Y_s} & \frac{\partial h_f}{\partial h_i} \right| \\ \left| \frac{\partial Y_s}{\partial Y_s} & \frac{\partial h_i}{\partial h_i} \right| \end{matrix} \cdot \begin{matrix} \lambda_{Y_s} \\ \lambda_{h_i} \end{matrix} \leq \begin{matrix} T_{\varepsilon_1} \\ T_{\varepsilon_2} \\ T_{\varepsilon_3} \\ T_{h_f} \end{matrix} - 6 \cdot \begin{matrix} \left| \frac{\partial \varepsilon_1}{\partial f} & \frac{\partial \varepsilon_1}{\partial \theta} \right| \\ \left| \frac{\partial \varepsilon_2}{\partial f} & \frac{\partial \varepsilon_2}{\partial \theta} \right| \\ \left| \frac{\partial \varepsilon_3}{\partial f} & \frac{\partial \varepsilon_3}{\partial \theta} \right| \\ \left| \frac{\partial h_f}{\partial f} & \frac{\partial h_f}{\partial \theta} \right| \\ \left| \frac{\partial f}{\partial f} & \frac{\partial \theta}{\partial \theta} \right| \end{matrix} \cdot \begin{matrix} \sigma_f \\ \sigma_\theta \end{matrix} \\
 & \text{over} \quad T_{Y_s}, T_{h_i} \geq \delta
 \end{aligned} \tag{5.23}$$

In order to solve this problem, we must consider two issues of dimension. The first involves the dimensions of the sensitivity matrices themselves. While the sensitivity terms in equation (5.23) represent the required relationships between outputs and inputs, the full sensitivity matrices contained in the ISM include 10 different strain terms at each of the three strain measurement locations, and 9 different thickness terms, one for each thickness measurement location. The full sensitivity matrices are thus significantly larger than the 4x2 matrices above. For the purposes of clarity, we will simplify this example by using average sensitivities for both strain and thickness in the matrices of (5.23). The value of the sensitivity term:

$$\frac{\partial h_f}{\partial Y_s}$$

in equation (5.23) will thus be the average of 9 different values, each of which relates one thickness measurement location to the incoming yield strength. The strain sensitivities will be handled in the same way.

The second dimensional issue involves the fact that the two input variables, yield strength and thickness, have values that are different orders of magnitude. This generates a feasible tolerance space that is very wide along one axis, and very narrow along another. This situation is represented in Figure 5.20.

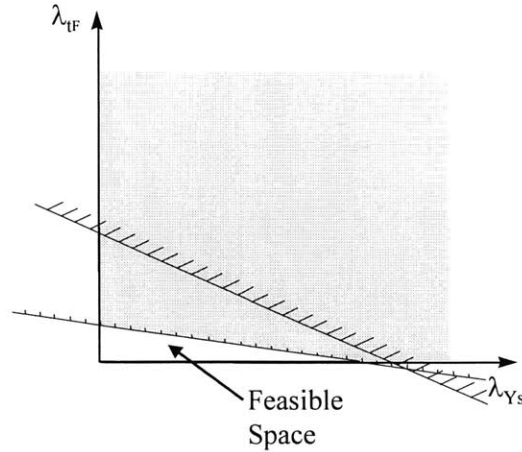


**Figure 5.20: Feasible Space (not to scale).**

In a case like this, the choice of  $\bar{\delta}$ , the minimum allowable input tolerances, is very important, since one component of the vector will be an active constraint, determining the size of the tolerancing polytope in the feasible region. In this example, the minimum tolerance on thickness will be active, and will determine the allowable tolerance on yield strength. The minimum allowable tolerance constraint could be replaced in the problem formulation by a constraint linking the two input variables as follows:

$$w_{11} \cdot \lambda_{i,1} = w_{22} \lambda_{i,2} = \dots = w_{nn} \lambda_{i,n}$$

In the case of the stretch-forming system, these weightings would be arbitrary, so we use a minimum allowable input tolerance instead. According to (Parris 1996) the standard material acquisition tolerance for sheet metal in the aerospace industry allows for a variation of up to  $\pm 5\%$  of the mean value. He states further that a variation of  $\pm 2\%$  of the mean value is common in practice. Both of these cases will be considered in this example.

We also need output target values and to determine process limits. As discussed previously, actual specifications were not available for this part. Based on measurements of acceptable production parts, we prescribe an end-of-line nominal target strain value of 0.1, with a tolerance of  $\pm 0.02$ . We also dictate the minimum allowable output thickness tolerance to be  $\pm 10\%$  of the mean value of stock material thickness.

We used the commercial software package *LINDO*, to evaluate the LP problem formulated above. The results show that the tolerance on input thickness was the active constraint. Process limits for the two cases evaluated are shown in Table 5.11.

**Table 5.11: Process Limit Values for the Stretch-Forming Operation.**

Minimum Input Thickness Tolerance (%)	Maximum Allowable Input Yield Strength Variation ( $\sigma$ )
$\pm 2$	3.04 MPa
$\pm 5$	1.46 MPa

The second column of Table 5.11 lists process limits for the stretch forming operation. These values prescribe the maximum allowable variation on the yield strength of workpieces entering the stretch forming operation, in order to ensure that 99.7% of these parts are capable of meeting end-of-line specifications. We can compare these values to the Tolerance Threshold values of the heat treatment operation, calculated in the previous section. If we assume an input thickness tolerance of  $\pm 2\%$ , the Tolerance Threshold value is smaller than the process limit, indicating that the process needs no additional variation reduction. If, however, we assume an input thickness tolerance of  $\pm 5\%$ , the Tolerance Threshold value is larger than the process limit. The implications of this result will become apparent in the next section.

### 5.8.2 Heat Treatment Process Limits

Once process limits have been calculated for one operation in a system, they can be used to determine limits values for the preceding operation. Having determined the process limits for the stretch forming operation, we can now apply the same methods to the heat treatment operation, in order to determine the maximum acceptable input variations for the stretch-forming system. As shown in Figure 5.21, the heat treatment operation has two input parameters, initial yield strength and aging time, and one output parameter, final yield strength.

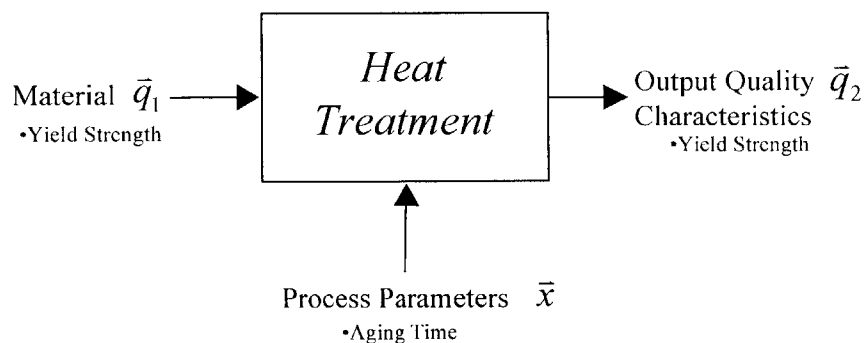


**Figure 5.21: Heat Treatment Inputs and Outputs.**



Since there is only one output parameter in this operation, we do not need to solve a linear programming problem. We can write the process limit constraint as:

$$\left| \frac{\partial Y_s}{\partial Y_{s_i}} \right| \cdot |\lambda_{y_s}| \leq |T_{y_s}| - 6 \cdot \left| \frac{\partial Y_s}{\partial t} \right| \cdot |\sigma_t| \quad (5.24)$$

This equation can be solved using the known value of the aging time variation,  $\sigma_t$ , and the maximum allowable tolerance on output yield strength,  $T_{y_s}$ . The latter quantity is also the allowable input tolerance for stretch forming, calculated in the previous section. For each of the two cases of allowable thickness variation, the maximum allowable input yield strength to the heat treatment operation is listed in Table 5.12.

**Table 5.12: Process Limits for the Heat Treatment Operation.**

Maximum Allowable Material Thickness Variation	Maximum Allowable Input Yield Strength Variation ( $\sigma$ )
0.002"	1.31 MPa
0.005"	Not Feasible

As shown by the results in Table 5.12, it is impossible to ensure that at least 99.7% of the final parts will meet end-of-line specifications when incoming material thickness varies by up to  $\pm 5\%$  of the specified nominal value. If, on the other hand, stock thickness variation is restricted to  $\pm 2\%$  of its nominal value *and* the standard deviation of stock yield strength is less than 1.31 Mpa, it is feasible for 99.7% of parts to meet end-of-line specifications. Note that meeting both of these conditions does not *guarantee* that 99.7% of parts will meet end-of-line specifications, because the inputs to successive processes could exceed their process limits. To ensure that 99.7% of final parts do meet end-of-line tolerances, input variation must fall within process limit values for every operation within the system.

In addition to prescribing the maximum acceptable input tolerances for an operation, process limit analysis is a means of determining where the use of process control is needed in a system. In the preceding example, process limit analysis for the case in which thickness varied by  $\pm 5\%$  of nominal showed that there is no feasible input yield strength value that enables 99.7% of parts to meet end-of-line specifications. This implies that the manufacturer should specify and purchase material with a tighter thickness tolerance, to reduce rework and scrap. In some situations, however, it may be infeasible to acquire different material due to cost or availability. In this situation, the process limit analysis shows that some form of process control is necessary on this operation, to guarantee end-of-line quality.

The back propagation of process limits through systems with multiple operations highlights those operations that require some form of process control. The effects of

control can be incorporated into the system model, allowing calculation of process limit values for the controlled system. In this way, we can determine whether the proposed change is sufficient to ensure end-of-line quality, or whether an alternate control strategy is more effective. The effects of process control on system variation are discussed in the following section.

### 5.9 Process Control Strategies

In this section, we discuss the use of process control to reduce end-of-line variation in manufacturing systems. We previously illustrated the use of process limit analysis in determining which operations in a system need control, to ensure that final products meet end-of-line specifications. Process control can also be used in systems where the final product is within specifications. As discussed in Chapter 2, Taguchi claims that even if every part produced meets target specifications, there is still the potential for quality loss in the system (Phadke 1989). Within this framework, any reduction in product variation also reduces quality loss. In accordance with the variation reduction methodology outlined at the beginning of this chapter, we now formulate and evaluate several variation reduction strategies for the sheet stretch-forming system.

The first step in developing a variation reduction strategy is to identify the major sources of variation in the system. In Section 5.5, we used the ISM to generate a table (5.9) listing the percentage contribution of each input to end-of-line strain and thickness variation. This table is reproduced below.

**Table 5.9: Major Sources of Variation in the Stretch-Forming System.**

Percent Contribution of Inputs to End-of-line Variation		Process Variables				
		Heat Treatment		Stretch Forming		
		Initial Yield Strength	Aging Time	Maximum Force	Wrap Angle	Initial Thickness
Output Quality Characteri	Strain (1)	16	23.3	49.7	.7	10.3
	Strain (2)	18.3	26.3	35.7	3.5	16.2
	Strain (3)	12.1	17.5	58.2	.9	11.3
	Thickness	6.2	8.8	18.7	.4	65.9

As discussed in Section 5.5, Table 5.9 clearly shows that process parameters are the major sources of strain variation. Forming force variation has the largest effect, followed by variation in aging time. The major source of end-of-line thickness variation, on the other hand, is the thickness variation of the incoming material. This is followed by variation in the forming force. For the purposes of example, we will only focus on reducing end-of-line strain variation in this chapter. If desired, we could also consider process control strategies that would reduce thickness variation.

We consider three broad categories of process control: source reduction, feedback control, and feed-forward control. Source reduction involves making a change to the process, in order to directly reduce the variation of a given input parameter. This is a passive form of control, involving no measurements or compensation. In feedback control, the value of an input parameter is measured in real-time, to ensure that a desired value is reached, and to limit variation around this value. Feed-forward control involves measuring an input to an operation, and using this value to determine the setting for a process parameter in that operation.

For the sheet stretch-forming system, we consider the following variants on these strategies:

- 1) Source Control: One option is to utilize a form of Source Control by standardizing aging time in heat treatment. Natural aging time is the second largest contributor to end-of-line variation in this system. The variation in aging time is unnecessary; it is a function of both shop-floor practice and a lack of knowledge about the effects of aging time. This variation could be virtually eliminated by specifying that each part be removed from the freezer and formed individually. This would eliminate the varying waiting time between parts that have been removed from the freezer prior to processing.
- 2) Feedback Control: Another possibility is to implement a form of feedback control on this system, by forming each part to a preset maximum force. As variation in forming force is such a large component of the end-of-line variation, it is likely that forming each part to a given force value will reduce the final variation. This does not account for the effects of material yield strength variations due to aging time, but should still improve the process. This mode of operation is known as Force Control.
- 3) Feed-forward Control: We can also consider a system-level control strategy, which involves feed-forward control across operations. This method involves measuring an input parameter in one operation (aging time in heat treatment) and using it to set another input parameter in a successive operation (force in stretch forming). Feed-forward control removes the need to control aging time variation; the operators are free to take as much time as they wish, provided the time is measured.

Although the numbers in Table 5.9 imply that force control will be the most effective strategy for the stretch-forming system, the feed-forward implementation is more likely to show significant results in practice. Although we have discussed the practice of removing three or four parts from the freezer and forming them sequentially, the production measurements and model predictions in this chapter are based on parts being removed and formed individually. As such, the effects of aging time variation reflected in Table 5.9 are limited. We can simulate standard practice by changing the nominal aging time and variation in the model to reflect a batch of four parts. As each part takes approximately 15 minutes to manufacture, we assume that the first part is out of the freezer for 15 minutes, the second for 30 minutes, the third for 45 minutes, and the fourth

for 60 minutes. Using the mean and standard deviation of these values, the new relative contributions of each input parameter are as shown in Table 5.13.

**Table 5.13: Major Sources of Variation During Standard Forming.**

Percent Contribution of Inputs to End-of-line Variation		Process Variables				
		Heat Treatment		Stretch Forming		
		Intitial Yield Strength	Aging Time	Maximum Force	Wrap Angle	Initial Thickness
Output Quality Characteri	Strain (1)	11.4	42.4	37.7	.5	8
	Strain (2)	12.7	47.4	25.7	2.5	11.7
	Strain (3)	8.9	33.2	47.8	.7	9.3
	Thickness	5.3	19.6	16.6	.4	58.3

Table 5.13 shows that variation in aging time is more significant than variation in force, in contributing to end-of-line strain variation under standard forming conditions. Feed-forward control of the aging time is thus likely to be more effective than force control for reducing strain variation. In this section, we use the ISM to compare both of these strategies. We first use the analytical expressions developed for feed-forward process control in Section 4.2.1, to predict end-of-line strain variation in a controlled system. We then verify these results with numerical simulation on the ISM. We also simulate the effect of several feedback control strategies on end-of-line variation for comparison.

### 5.9.1 Analytic Approach to Feed-Forward

In this section, we apply the analytical expressions derived for feed-forward process control in Section 4.2.1 to the sheet stretch-forming system model. The feed-forward loop in this example consists of a measurement of part aging time during heat treatment, which is then used to set the maximum force during stretch-forming. This approach is illustrated in schematic form in Figure 5.22.

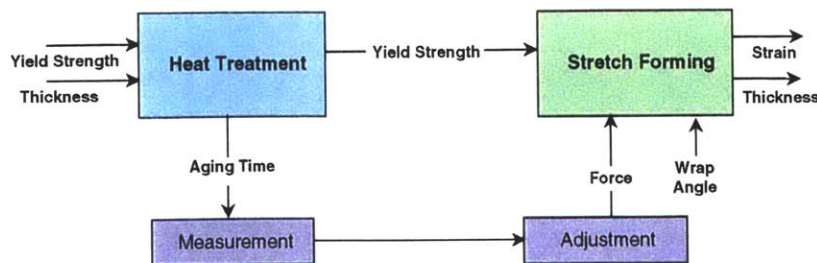


**Figure 5.22: Inter-operation Feed-forward Control.**

In Chapter 4, we presented a generalized schematic of a feed-forward process control implementation for a “controlled operation”, as shown in Figure 4.5. In this representation, the output of a previous operation and/or the fixed process parameters of the controlled operation are measured and used to change the setting of an adjustable process parameter in the controlled operation.

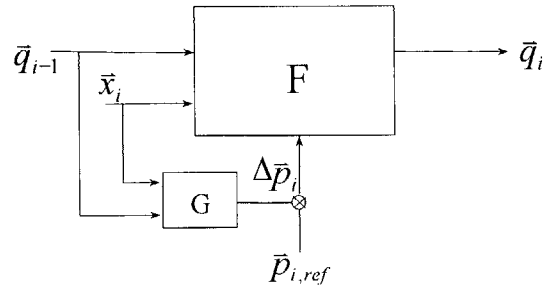


**Figure 4.5: Feed-Forward Control Loop.**

The example in this section is slightly different, in that we measure a process parameter from a previous operation and use the measurement to estimate the value of one of the outputs from that operation. The estimated value is then used to determine the value of an adjustable process parameter in the controlled operation. This inter-operation feed-forward implementation is shown in schematic form in Figure 5.23.

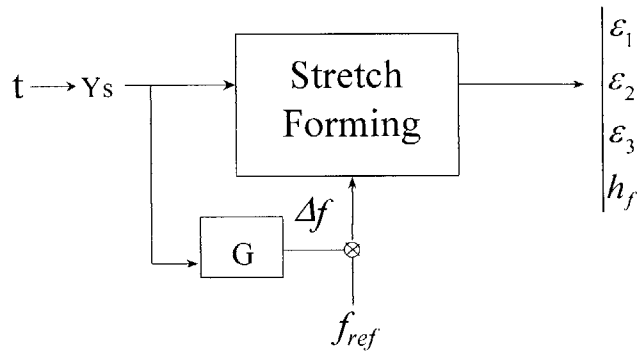


**Figure 5.23: Inter-Operation Feed-Forward Control.**

In Figure 5.23, the feed-forward implementation has a single input variable, aging time  $t$ , which is used as an estimator of the yield strength,  $Y_s$ . There is also a single control variable, force  $f$ .

We can write a simple model of system response based on these two variables as:

$$\begin{bmatrix} \varepsilon_1 \\ \varepsilon_2 \\ \varepsilon_3 \\ h_f \end{bmatrix} = \begin{bmatrix} \varepsilon_1^* \\ \varepsilon_2^* \\ \varepsilon_3^* \\ h_f^* \end{bmatrix} + \begin{bmatrix} \frac{\partial \varepsilon_1}{\partial f} \\ \frac{\partial \varepsilon_2}{\partial f} \\ \frac{\partial \varepsilon_3}{\partial f} \\ \frac{\partial h_f}{\partial f} \\ \frac{\partial f}{\partial f} \end{bmatrix} \cdot \Delta f + \begin{bmatrix} \frac{\partial \varepsilon_1}{\partial t} \\ \frac{\partial \varepsilon_2}{\partial t} \\ \frac{\partial \varepsilon_3}{\partial t} \\ \frac{\partial h_f}{\partial t} \\ \frac{\partial f}{\partial t} \end{bmatrix} \cdot \Delta t \quad (5.25)$$

Grouping terms and then dividing through will provide the required adjustable variable change  $\Delta f$ . If we assume that the operation is on target, this required adjustment is:

$$\Delta f = - \begin{bmatrix} \frac{\partial \varepsilon_1}{\partial f} \\ \frac{\partial \varepsilon_2}{\partial f} \\ \frac{\partial \varepsilon_3}{\partial f} \\ \frac{\partial h_f}{\partial f} \\ \frac{\partial f}{\partial f} \end{bmatrix}^{-1} \begin{bmatrix} \frac{\partial \varepsilon_1}{\partial t} \\ \frac{\partial \varepsilon_2}{\partial t} \\ \frac{\partial \varepsilon_3}{\partial t} \\ \frac{\partial h_f}{\partial t} \\ \frac{\partial f}{\partial t} \end{bmatrix} \cdot \Delta t \quad (5.26)$$

As discussed previously, the inverse matrix in (5.26) is actually a generalized inverse:

$$F^{-1*} = W^{-1} F^T (FW^{-1}F^T)^{-1} \quad (4.18)$$

Since there is only one process parameter in this example, the weighting matrix  $W$  has a single, unitary value. The second sensitivity matrix in (5.26), relating the output variables of the stretch forming operation to the input variable of the heat treatment operation, is obtained from the sensitivity matrices for each operation via the chain rule:

$$\begin{bmatrix} \frac{\partial \varepsilon_1}{\partial t} \\ \frac{\partial \varepsilon_2}{\partial t} \\ \frac{\partial \varepsilon_3}{\partial t} \\ \frac{\partial h_f}{\partial t} \\ \frac{\partial f}{\partial t} \end{bmatrix} = \begin{bmatrix} \frac{\partial \varepsilon_1}{\partial Y_s} \\ \frac{\partial \varepsilon_2}{\partial Y_s} \\ \frac{\partial \varepsilon_3}{\partial Y_s} \\ \frac{\partial h_f}{\partial Y_s} \\ \frac{\partial f}{\partial Y_s} \end{bmatrix} \cdot \begin{bmatrix} \frac{\partial Y_s}{\partial t} \\ \frac{\partial Y_s}{\partial t} \\ \frac{\partial Y_s}{\partial t} \\ \frac{\partial Y_s}{\partial t} \\ \frac{\partial Y_s}{\partial t} \end{bmatrix} \quad (5.27)$$

As per the discussion in Section 5.8.1, we use averaged process sensitivity values in order to simplify the example. A full listing of process sensitivity values is presented in Appendix B. Substituting the averaged values into equation (5.26) gives:

$$\Delta f = 570.75 \frac{N}{min} \cdot \Delta t \quad (5.28)$$

Equation (5.28) is the simple feed-forward rule for this system. This does not account for any errors in measurement or in actuation. If we include both errors and assume that they behave as random variables with normal distributions, equation (4.21) allows determination of the output variation of the controlled operation:

$$\bar{\sigma}_{\bar{q}_i}^2 = [F_x^2]_i^* \bar{\sigma}_{\bar{\varepsilon}_x}^2 + [F_q^2]_i^* \bar{\sigma}_{\bar{\varepsilon}_q}^2 + [F_p^2]_i^* \bar{\sigma}_{\bar{\varepsilon}_m}^2 + [F_r^2]_i^* \bar{\sigma}_{\bar{\varepsilon}_a}^2 \quad (4.21)$$

In this example, equation (4.21) can be written as:

$$\begin{pmatrix} \sigma_{\varepsilon_1}^2 \\ \sigma_{\varepsilon_2}^2 \\ \sigma_{\varepsilon_3}^2 \\ \sigma_{h_f}^2 \end{pmatrix} = \begin{pmatrix} \frac{\partial \varepsilon_1}{\partial f} \\ \frac{\partial \varepsilon_2}{\partial \varepsilon_2} \\ \frac{\partial f}{\partial \varepsilon_3} \\ \frac{\partial f}{\partial h_f} \end{pmatrix}^2 \cdot \sigma_a^2 + \begin{pmatrix} \frac{\partial \varepsilon_1}{\partial f} \\ \frac{\partial f}{\partial \varepsilon_3} \\ \frac{\partial f}{\partial h_f} \\ \frac{\partial f}{\partial f} \end{pmatrix}^2 \cdot \sigma_m^2 + \begin{pmatrix} \frac{\partial \varepsilon_1}{\partial t} \\ \frac{\partial t}{\partial \varepsilon_2} \\ \frac{\partial t}{\partial \varepsilon_3} \\ \frac{\partial t}{\partial t} \end{pmatrix}^2 \cdot \sigma_t^2 + \begin{pmatrix} \frac{\partial \varepsilon_1}{\partial Ys_i} \\ \frac{\partial Ys_i}{\partial \varepsilon_2} \\ \frac{\partial Ys_i}{\partial \varepsilon_3} \\ \frac{\partial Ys_i}{\partial t} \end{pmatrix}^2 \cdot \sigma_{Ys_i}^2 + \begin{pmatrix} \frac{\partial \varepsilon_1}{\partial h_i} & \frac{\partial \varepsilon_1}{\partial \theta} \\ \frac{\partial h_i}{\partial \varepsilon_2} & \frac{\partial \theta}{\partial \varepsilon_2} \\ \frac{\partial h_i}{\partial \varepsilon_3} & \frac{\partial \theta}{\partial \varepsilon_3} \\ \frac{\partial h_f}{\partial h_i} & \frac{\partial \theta}{\partial h_f} \end{pmatrix}^2 \cdot \begin{pmatrix} \sigma_{h_i}^2 \\ \sigma_{\theta}^2 \end{pmatrix} \quad (5.29)$$

The powers of 2 on each sensitivity matrix in equation (5.29) indicate that each value within the matrices should be squared. Note that  $\sigma_a$  is actuation error,  $\sigma_m$  is error in the control model, and  $\sigma_t$  is error in the aging time measurement. The variance terms  $\sigma_{h_i}^2$  and  $\sigma_{\theta}^2$  represent random variation of thickness and wrap angle, since these variables are not being controlled. For the purposes of this example, actuation error is estimated to be  $\pm 0.1$  tons, which is reasonable if the machine is being controlled manually. This translates to a standard deviation of the actuation error of  $\sigma_a = 1485$  N. Measurement error is estimated at  $\pm 30$  seconds, to account for the fact that the operators will be simultaneously moving the stock material, setting up the machine, and running the timer. This results in a standard deviation for the measurement error of  $\sigma_m = 10$ s.

Evaluating the effects of modeling error is complicated. For the purposes of this analysis, we assume that modeling error is a random variable with a normal distribution. The nominal value of this random variable is centered on the force correction value predicted by equation (5.28), and the standard deviation of the distribution is a percentage of this nominal value. This representation assumes no bias. The standard deviation of a model

with 10% error will be 3.33% of the nominal value; this model is assumed to predict values within  $\pm 10\%$  of the correct value, 99.7% of the time. A better estimator of modeling error might be a uniform distribution. In this case, we assume that the model prediction has an equal chance of being anywhere within  $\pm n\%$  of the correct value. In this chapter, we will use Monte Carlo simulation to compare use of the normal distribution with use of the uniform distribution.

We use equation (5.29) to predict the controlled end-of-line variation for the example system. From equation (5.28), the maximum force correction needed to account for aging time variation (which has a standard deviation of 5 minutes) is 8,561 N. We consider three cases of modeling error in the controlled system:

- Case 1: No modeling error
- Case 2: Modeling error of  $\pm 10\%$
- Case 3: Modeling error of  $\pm 50\%$

The input values for each of the three cases are listed in Table 5.14.

**Table 5.14: Input Values for Feed-Forward Control Analysis.**

Error Type	Range	1 $\sigma$ Value
Actuation Error	$\pm 0.1$ tons	296.5 N
Measurement Error	$\pm 30$ seconds	10 seconds
Modeling Error (case 1)	0	0
Modeling Error (case 2)	$\pm 10\%$	285.4 N
Modeling Error (case 3)	$\pm 50\%$	1426.9 N



Substituting the values from Table 5.14 back into equation (5.29) gives:

$$\begin{aligned}
 \begin{bmatrix} \sigma_{\varepsilon_1}^2 \\ \sigma_{\varepsilon_2}^2 \\ \sigma_{\varepsilon_3}^2 \\ \sigma_{h_f}^2 \end{bmatrix} &= \begin{bmatrix} 7.9152E^{-7} \\ 5.05E^{-7} \\ 9.23E^{-7} \\ -3.83E^{-10} \end{bmatrix} \cdot (296.5)^2 + \begin{bmatrix} 7.9152E^{-7} \\ 5.05E^{-7} \\ 9.23E^{-7} \\ -3.83E^{-10} \end{bmatrix} \cdot \sigma_m^2 + \begin{bmatrix} -.00142 \\ -.00142 \\ -.00107 \\ 7.05E^{-7} \end{bmatrix} \cdot (1.2)^2 \\
 &+ \begin{bmatrix} -.0005 \\ -.0005 \\ -.00037 \\ 2.45E^{-10} \end{bmatrix} \cdot (.167)^2 + \begin{bmatrix} -130.048 & 8.95E^{-5} \\ -177.155 & -4.23E^{-4} \\ -139.205 & 1.18E^{-4} \\ 1.04 & 6.7E^{-8} \end{bmatrix} \cdot \begin{bmatrix} (8.62E^{-6})^2 \\ (.78)^2 \end{bmatrix}
 \end{aligned} \tag{5.30}$$

Where the value of modeling error,  $\sigma_m$ , differs for each case. The predicted end-of-line variations are shown in Table 5.15.

**Table 5.15: Predicted Variation in a System with Feed-Forward Control.**

Standard Deviation	Case 1 ( $\sigma_m=0$ )	Case 2 ( $\sigma_m= \pm 10\%$ )	Case 3 ( $\sigma_m= \pm 50\%$ )
$\sigma_{\varepsilon_1}$ (Strain 1)	0.002056	0.002068	0.002346
$\sigma_{\varepsilon_2}$ (Strain 2)	0.002318	0.002322	0.002427
$\sigma_{\varepsilon_3}$ (Strain 3)	0.001782	0.001801	0.002216
$\sigma_t$ (Thickness)	$9.007 \cdot 10^{-6}$ m	$9.007 \cdot 10^{-5}$ m	$9.023 \cdot 10^{-5}$ m

The values in Table 5.15 are compared to the case of no control in Table 5.16.

**Table 5.16: Predicted Improvement With Feed-Forward Control.**

	No Control	Predicted Case 1 Improvement	Predicted Case 2 Improvement	Predicted Case 3 Improvement
Strain 1	0.006304	67%	67%	63%
Strain 2	0.004731	51%	51%	49%
Strain 3	0.006241	71%	71%	64%
Thickness	$9.38 \cdot 10^{-6}$	4%	4%	3.8%

This analysis shows that feed-forward control has a significant effect in reducing strain variation, even in the presence of modeling error. With a perfect model, the analysis predicts that end-of-line strain variation is reduced by 51% at the center of the sheet, and by 67%-71% towards the edges. With a modeling error of 50%, strain variation at the center of the sheet is still reduced by almost 50%, and variation at the edges drops by

64%. As we will show later in this chapter, use of the normal distribution to evaluate the effects of modeling error is less conservative than use of a uniform distribution.

This process control strategy has a small effect on thickness variation. This makes sense in light of the relatively small contribution of force variation to thickness variation in Table 5.9. We would have to formulate a different strategy in order to improve this quality characteristic as well.

Having demonstrated that feed-forward control is a viable strategy for reducing strain variation, we can calculate the maximum process variation that can be controlled with this method. In Chapter 4, this problem was formulated as:

$$\begin{aligned}
& \max \quad \left\| \bar{\sigma}_{\bar{q}_{i-1}} \right\| \\
& \text{s.t.} \quad [F_q]_i^* \bar{\sigma}_{\bar{q}_{i-1}} = \frac{1}{3} [F_p]_i^* \Delta \bar{p}_i - [F_x]_i^* \bar{\sigma}_x, \\
& \text{over} \quad \bar{p}_i \in \bar{P}_i \\
& \text{where} \quad \Delta \bar{p}_i = (\bar{p}_{i,\min} - \bar{p}_i) \text{ if } (\bar{p}_{i,\min} - \bar{p}_i) < \frac{\bar{p}_{i,\max} - \bar{p}_{i,\min}}{2} \\
& \quad \quad \Delta \bar{p}_i = (\bar{p}_{i,\max} - \bar{p}_i) \text{ otherwise} \\
& \quad \quad \bar{\sigma}_x \text{ is constant over } \bar{P}_i
\end{aligned} \tag{4.23}$$

For this example, the constraint in equation (4.23) can be re-written as:

$$\begin{aligned}
& \begin{vmatrix} \frac{\partial \varepsilon_1}{\partial Y_{s_i}} \\ \frac{\partial \varepsilon_2}{\partial \varepsilon_2} \\ \frac{\partial Y_{s_i}}{\partial \varepsilon_3} \\ \frac{\partial Y_{s_i}}{\partial t} \\ \frac{\partial Y_{s_i}}{\partial Y_{s_i}} \end{vmatrix} \bar{\sigma}_{Y_s} = \frac{1}{3} \cdot \begin{vmatrix} \frac{\partial f}{\partial \varepsilon_2} \\ \frac{\partial f}{\partial \varepsilon_3} \\ \frac{\partial f}{\partial h_f} \\ \frac{\partial f}{\partial f} \end{vmatrix} \cdot \Delta f + \begin{vmatrix} \frac{\partial \varepsilon_1}{\partial h_i} & \frac{\partial \varepsilon_1}{\partial \theta} \\ \frac{\partial \varepsilon_2}{\partial \varepsilon_3} & \frac{\partial \varepsilon_2}{\partial \varepsilon_3} \\ \frac{\partial h_i}{\partial \varepsilon_3} & \frac{\partial \theta}{\partial \varepsilon_3} \\ \frac{\partial h_i}{\partial h_f} & \frac{\partial \theta}{\partial h_f} \\ \frac{\partial h_i}{\partial h_i} & \frac{\partial \theta}{\partial \theta} \end{vmatrix} \cdot \begin{vmatrix} \sigma_{h_i} \\ \sigma_{\theta} \end{vmatrix}
\end{aligned} \tag{5.31}$$

Substituting the sensitivity values into this equation gives:

$$\begin{aligned}
& \begin{vmatrix} 0.00142 \\ 0.00142 \\ 0.00107 \\ 7.05 \cdot 10^{-7} \end{vmatrix} \bar{\sigma}_{Y_s} = \frac{1}{3} \cdot \begin{vmatrix} 7.92 \cdot 10^{-7} \\ 5.05 \cdot 10^{-7} \\ 9.23 \cdot 10^{-7} \\ -3.83 \cdot 10^{-10} \end{vmatrix} \cdot \Delta f - \begin{vmatrix} -130.05 & 8.95 \cdot 10^{-5} \\ -177.16 & -4.23 \cdot 10^{-4} \\ -139.21 & 1.18 \cdot 10^{-4} \\ 1.04 & 6.7 \cdot 10^{-8} \end{vmatrix} \cdot \begin{vmatrix} 8.62 \cdot 10^{-6} \\ 0.78 \end{vmatrix}
\end{aligned} \tag{5.32}$$

We now need to limit the range of acceptable values for the adjustable input parameter,  $f$ . This variable is loosely bounded in practice, since the forming force on the stretch press can be set to a very wide range of values. For this example, we limit the range of  $f$  to  $\pm 25000$  N (2.8 tons), a range of values known to produce acceptable parts in practice. Solving (4.23) using this range and the constraint (5.32) leads to a controllable input range of  $\pm 4.37$  MPa.

We can also determine both the probability density function of the controlled operation and the new, controlled, output variation, by using equation (4.24) developed by (Soyucayli and Otto 1998):

$$\sigma_{Ys\_new}^2 = \Delta_y^2 + \sigma_{Ys\_old}^2 - 2\sqrt{\frac{2}{\pi}}\sigma_{Ys\_old}\Delta_y \quad (4.24)$$

The output range,  $\Delta_y$ , in equation (4.24) can be written as:

$$\begin{pmatrix} \Delta \varepsilon_1 \\ \Delta \varepsilon_2 \\ \Delta \varepsilon_3 \\ \Delta h_f \end{pmatrix} = \begin{pmatrix} \frac{\partial \varepsilon_1}{\partial f} \\ \frac{\partial \varepsilon_2}{\partial f} \\ \frac{\partial \varepsilon_3}{\partial f} \\ \frac{\partial h_f}{\partial f} \end{pmatrix} \cdot \Delta f = \begin{pmatrix} 7.92E^{-7} \\ 5.05E^{-7} \\ 9.23E^{-7} \\ -3.83E^{-10} \end{pmatrix} \cdot (50000 \text{ N}) = \begin{pmatrix} 0.0396 \\ 0.0253 \\ 0.0462 \\ 1.92 \cdot 10^{-5} \end{pmatrix} \quad (5.33)$$

In equation (5.33), we again use the  $\pm 25000$  N range for the controllable variable  $f$ . The variation we wish to adjust out,  $\sigma_{Ys\_old}$ , is the result of fluctuations in aging time:

$$\begin{pmatrix} \sigma_{Ys\_old\_e_1}^2 \\ \sigma_{Ys\_old\_e_2}^2 \\ \sigma_{Ys\_old\_e_3}^2 \\ \sigma_{Ys\_old\_h_f}^2 \end{pmatrix} = \begin{pmatrix} \frac{\partial \varepsilon_1}{\partial t} \\ \frac{\partial \varepsilon_2}{\partial t} \\ \frac{\partial \varepsilon_3}{\partial t} \\ \frac{\partial h_f}{\partial t} \end{pmatrix}^2 \sigma_t^2 = \begin{pmatrix} 0.0005 \\ 0.0005 \\ 0.0004 \\ 2.44E^{-7} \end{pmatrix}^2 (5)^2 = \begin{pmatrix} 0.0025 \\ 0.0025 \\ 0.002 \\ 1.22E^{-6} \end{pmatrix} \quad (5.34)$$

We can substitute the values of  $\Delta_y$  and  $\sigma_{Ys\_old}$  into a multivariate form of equation (4.24), as follows:

$$\begin{bmatrix} \sigma_{Ys\_e1} \\ \sigma_{Ys\_e2} \\ \sigma_{Ys\_e3} \\ \sigma_{Ys\_ht} \end{bmatrix}^2 = \begin{bmatrix} 0.0396 \\ 0.0253 \\ 0.0462 \\ 1.92E^{-5} \end{bmatrix}^2 + \begin{bmatrix} 0.0025 \\ 0.0025 \\ 0.002 \\ 1.22E^{-6} \end{bmatrix}^2 - 2\sqrt{\frac{2}{\pi}} \cdot \begin{bmatrix} 0.0025 \\ 0.0025 \\ 0.002 \\ 1.22E^{-6} \end{bmatrix} \cdot \begin{bmatrix} 0.0396 \\ 0.0253 \\ 0.0462 \\ 1.92E^{-5} \end{bmatrix} = \begin{bmatrix} 0.00142 \\ 0.00055 \\ 0.002 \\ 3.33E^{-10} \end{bmatrix} \quad (5.35)$$

Equation (5.35) can be reduced to:

$$\begin{bmatrix} \sigma_{Ys\_e1} \\ \sigma_{Ys\_e2} \\ \sigma_{Ys\_e3} \\ \sigma_{Ys\_ht} \end{bmatrix} = \begin{bmatrix} 0.037 \\ 0.023 \\ 0.044 \\ 1.82E^{-5} \end{bmatrix} \quad (5.36)$$

Equation (5.36) lists the predicted values of yield strength variation in the heat treatment operation caused by variation in the aging time. These values can now be used in the system model along with a reduced value of force variation (since force is now being set to a predetermined value based on aging time), in order to determine the controlled end-of-line variation. If we assume that force variation will have a standard deviation of  $\sigma=1000$  N (based on non-repeatability inherent in manual control of the stretch press) and use the controlled yield strength variations from (5.36), the ISM predicts the end-of-line variations listed in Table 5.17.

**Table 5.17: Predicted Variation in a System with Feed-Forward Control.**

Output Quality Characteristic	Standard Deviation
Strain (Location 1)	0.002193
Strain (Location 2)	0.002345
Strain (Location 3)	0.001977
Thickness	$8.91E^{-6}$ m

The values of controlled end-of-line variation predicted using equation (4.24) are somewhat larger than those calculated from equation (5.30). This is due to the fact that the method using (4.24) incorporates limits on the force adjustment.

### 5.9.2 Numerical Simulation of Variation Propagation

In this section, we use Monte Carlo simulation on the ISM to numerically evaluate the effects of process control on end-of-line variation. Numerical simulation can be used to model situations that are too complex for analytical methods. We first predict end-of-line variation using feed-forward process control, assuming that modeling error follows either

a normal or a uniform distribution. We then compare several different types of feedback process control, including Force Control, Strain Control, and Part-to-Part Feedback.

*Feed-Forward Control*

The linearized spreadsheet-based system model discussed in section 5.3.3 can be used for numerical simulation. A technique such as Monte Carlo analysis can be used to simulate the production of hundreds of parts, and to predict quality characteristic nominal values and variation. Use of the linearized models reduces computational intensity, allowing for very rapid calculation of the outcome of each trial.

We used the Monte Carlo technique to both verify the analytical results derived in the previous section, and to investigate control strategies that cannot be expressed in simple analytic terms. Monte Carlo simulations of the system were conducted through the use of the commercial software package *Crystal Ball*, which works within the Microsoft *Excel* environment. Each input parameter to the system was assumed to be a random variable with a normal distribution. The nominal values and standard deviations of these variables were set to their measured values. We chose four output variables: strain at each measurement location, and average thickness across the sheet. All Monte Carlo simulations consisted of 1500 trials, except where specifically noted. Numerical simulation allowed for two refinements over the analytical approach of the previous sections: varying sensitivities, and non-normal distributions. The closed-form analytical expressions outlined in Chapters 3 and 4 require a constant value for each sensitivity term, and are only applicable to random variables with normal distributions. As discussed previously, the sensitivity values are dependent on the system operating point, and change with any changes in input parameter values. In addition, modeling error may be more accurately represented as a uniform, rather than normal distribution. In this section, we use Monte Carlo simulation to consider these various cases.

Table 5.18 lists the predicted end-of-line variations obtained through Monte Carlo analysis, using constant sensitivity terms and a normal distribution of modeling error. We present values for the uncontrolled system, as well as for the three cases of feed-forward process control evaluated in Section 5.9.1.

**Table 5.18: Output Standard Deviations With Constant Sensitivity Terms.**

Output Variable	Analytical	No Control	Feed-Forward (no modeling error)	Feed-Forward (10% modeling error)	Feed-Forward (50% modeling error)
Strain (Mark 1)	0.006304	0.006120	0.00199	0.002001	0.002238
Strain (Mark 2)	0.004731	0.004671	0.002443	0.002477	0.002544
Strain (Mark 3)	0.006614	0.006515	0.001929	0.001977	0.00228
Thickness	$9.38 \cdot 10^{-6} \text{m}$	$9.35 \cdot 10^{-6} \text{m}$	$8.67 \cdot 10^{-6} \text{m}$	$9.036 \cdot 10^{-6} \text{m}$	$9.04 \cdot 10^{-6} \text{m}$

As would be expected, the results of the Monte Carlo simulation are in close accord with the analytical results calculated previously. The values obtained through numerical simulation are 2-5% lower than the analytically derived values, but the effect of adding various levels of modeling error remains the same.

Table 5.19 lists the end-of-line variations calculated from the results of a Monte Carlo simulation using process sensitivity terms that vary with changes in the input parameter values. The values of these sensitivities are derived from quadratic polynomials, which have been fit to the output of the full finite-element model, with a least squares fitting coefficient  $R > 0.99$ .

**Table 5.19: Output Standard Deviations With Varying Sensitivities.**

Output Variable	Analytical	No Control	Feed-Forward (no modeling error)	Feed-Forward (10% modeling error)	Feed-Forward (50% modeling error)
Strain (Mark 1)	0.06304	0.006287	0.00205	0.002144	0.002453
Strain (Mark 2)	0.04731	0.004720	.00269	.002674	0.00276
Strain (Mark 3)	0.006614	0.006687	0.002012	.002078	0.002462
Thickness	$9.38 \cdot 10^{-6}$ m	$9.35 \cdot 10^{-6}$ m	$8.65 \cdot 10^{-6}$ m	$8.83 \cdot 10^{-6}$ m	$8.83 \cdot 10^{-6}$ m

The data in Table 5.19 shows that the effect of using varying sensitivities in the Monte Carlo simulation is a slight increase in the values of the end-of-line standard deviations. The relative effect of process control and modeling error remains the same. These results indicate that the assumption of constant values for the sensitivity terms in the analytical approach is reasonable, and does not introduce significant error into the analysis or change the predicted impact of process control.

Table 5.20 lists the outcome of Monte Carlo simulation using both varying sensitivities and a uniform distribution to represent modeling error. The upper and lower limits of this distribution are set to the  $\pm 3\sigma$  values of the normal distribution used in Section 5.9.1.

**Table 5.20: Output Standard Deviations with Error as a Uniform Distribution.**

Output Variable	$\sigma$ with No Control	10% Modeling Error	50% Modeling Error
Strain (Location 1)	0.006287	0.002183	0.002989
Strain (Location 2)	0.004720	0.002720	0.003018
Strain (Location 3)	0.006687	0.002161	0.003146
Thickness	$9.35E^{-6}$ m	$8.8E^{-6}$ m	$9.42E^{-6}$ m

As seen in Table 5.20, the difference in predicted end-of-line variation between use of the normal distribution and use of the uniform distribution is very small for a model with 10% modeling error. The discrepancy between the two methods increases with the level of modeling error, reaching 28% when the modeling error reaches 50%. The effects of feed-forward control are still quite significant; the model predicts a 35% reduction in end-of-line variation with a modeling error of 50%.

Both the closed-form analysis and numerical simulations indicate that use of feed-forward control will reduce the variation significantly, even the in the presence of

modeling error. It thus appears to be the best strategy for use in this system. In the next sections we will simulate several feedback control strategies for comparison.

### *Feedback Control*

There are two broad classes of feedback control in manufacturing systems: machine control, and part-to-part feedback. Machine control is a common feature on many manufacturing machines, and involves an internal control loop, which regulates the value of an input parameter. Some examples include the control of spindle speed on a lathe, barrel or cavity temperature regulation on an injection molding machine, and force control on a stretch forming press. Part-to-part feedback, on the other hand, involves the production of a part or batch of parts, measurement of their deviation from target specifications, and then a change in parameter settings before the manufacture of the next part. This form of control is rarely used explicitly in aerospace manufacturing, but often occurs in practice as a result of operator intervention. It is not uncommon in stretch-forming, for example, for an operator to produce a single part, examine its contour after springback, and to then change the carriage positions before producing the next part. While this form of control can correct for severe deviations from the target specifications, it often increases variation. Both machine control and part-to-part feedback will be explored through numerical simulation on the example system in this section.

### *Machine Feedback*

While many stretch-forming presses have some regulatory feedback control on forming force and/or table height, the machine in our example system had neither at the time the measurements were taken. Each part was formed under manual control, in which the operator raised the table until satisfied with the shape of the part. Machines that are instrumented for automatic control have several options for stopping-criteria. *Force control* is a method in which each part is formed to a certain target force, determined from past experience. This method does not account for variation in material properties, but does eliminate the effects of force variation. An internal feedback loop is used to reach and maintain the desired force. *Displacement control* is a similar approach, in which the die table is raised a given distance after snug for every part. Displacement control is more sophisticated than force control, since it effectively requires that each part be deformed the same amount. Force is allowed to vary from part to part as necessary, to compensate for variation in material properties. *Strain control* is the best operational strategy; this method involves using instrumentation on the part itself to measure the strain, and stop forming when a target strain is reached. This method directly accounts for all material and machine variations, ensuring that each part is pulled to the desired amount. In this section we use Monte Carlo simulation on the system model to compare the visual inspection stopping-criterion to both force control and strain control. Table 5.21 shows the results of a force control simulation, run with varying sensitivities. The simulation incorporated a feedback loop on the value of force, which raised the force up to, but not over, the target value. This target value was the mean value measured in simulation: 238412.8 N.

**Table 5.21: Predicted Outputs of a System Under Force Control.**

Output Variable	Predicted (no Control)	Predicted (Force Control)	% Change
Strain (mark 1)	11.14	11.13	0.1
Strain (mark 2)	8.82	8.82	0.0
Strain (mark 3)	11.15	11.13	0.1
Thickness	0.00125 m	0.00125 m	0.0
Variations			
Strain (mark 1)	0.006287	0.003036	51.7
Strain (mark 2)	0.004720	0.003434	27.2
Strain (mark 3)	0.006687	0.002459	63.0
Thickness	9.35E <sup>-6</sup> m	8.89E <sup>-6</sup> m	4.9

The simulation results show that by simply forming each part to the same force, the target part can be formed to the desired target values with a greater than 25% reduction in variation from the uncontrolled levels.

While force control shows a significant quality improvement over the use of visual inspection, a greater reduction in variation can be obtained through the use of strain control. This method is discussed in some detail by Parris (1996), who conducted experiments using strain control in the production environment. We implemented a Monte Carlo simulation of strain control by first generating a set of random variations for all input parameters, and then increasing the forming force until the target strain was predicted for the part. As in the case of force control, a feedback loop was used to increase the force until the target strain value was reached, without overshoot. Strain was controlled at one point (measurement location 1) for simplicity. The predicted value of strain with no control at measurement location 1 from Table 5.21 was used as the target strain value. Results of the strain control simulation are listed in Table 5.22.

**Table 5.22: Predicted Outputs of a System Under Strain Control.**

Output Variable	Predicted (no Control)	Predicted (Strain Control)	% Change
Strain (mark 1)	11.14	11.145	0.0
Strain (mark 2)	8.82	8.872	0.6
Strain (mark 3)	11.15	11.17	0.2
Thickness	0.00125 m	0.00125 m	0.0
Variations			
Strain (mark 1)	0.006287	0.000311	95
Strain (mark 2)	0.004720	0.002073	56
Strain (mark 3)	0.006687	0.000729	89
Thickness	9.35E <sup>-6</sup> m	8.32E <sup>-6</sup> m	11

Table 5.22 shows that the nominal strain values under Strain Control are within 1% of the target values, while the variations drop significantly from their uncontrolled values. The



improvement predicted for this system is of the same magnitude as that seen experimentally by Parris (1996), who showed a 92% reduction in the variation of stretch formed parts when using strain control as opposed to visual inspection.

*Part to Part Feedback Control*

As discussed previously, part-to-part feedback control usually increases variation, although it can decrease bias. This method involves producing a part, or batch of parts, and then measuring the deviation of some output quality characteristics from their target values. This data is then used to change parameter settings in the system, prior to producing additional parts. Some authors have explored these methods by using data collected from one batch of parts to update and improve running process models for use on additional parts (Boning, Moyne et al. 1996). This technique only works if accurate process models are available for the specific manufacturing system, and the system is allowed to equilibrate after changes.

Table 5.23 shows the results of part-to-part feedback control, in which the operator forms a part, measures the strain deviations from target values at three points on the part (the three strain measurement locations shown in Figure 5.16), and then changes the input force for the next part accordingly. All parameters other than force are allowed to vary as usual.

**Table 5.23: Predicted Outputs of a System Under Part-To-Part Feedback.**

Output Variable	Predicted (no Control)	Predicted (Part-to-part Feedback)	% Change
Strain (mark 1)	11.14	11.18	0.4
Strain (mark 2)	8.82	8.79	0.3
Strain (mark 3)	11.15	11.19	0.4
Thickness	0.00125 m	0.00125 m	0.0
Variations			
Strain (mark 1)	0.006287	0.004591	27.0
Strain (mark 2)	0.004720	0.004184	11.4
Strain (mark 3)	0.006687	0.004576	31.6
Thickness	9.35E <sup>-6</sup> m	9.11E <sup>-6</sup> m	2.6

The results in Table 5.23 show that part-to-part feedback reduces end-of-line variation over uncontrolled forming by more than 10%. These results are somewhat deceiving, as can be seen through a comparison with the output of force control (see Table 5.21). The end-of-line variation when using part-to-part feedback is roughly twice that when using force control. The reduction in variation over the uncontrolled condition seen in Table 5.23 is due to a decrease in the force variation, as force is now being set to predetermined values for each part. Although the force variation has decreased, the actual force settings are just as random as they were under visual inspection, since each setting is determined for a given set of material conditions *on a previous part*. The part being formed with the predetermined force values has a new set of properties, which are unrelated to the set for

the previous part. As such, both the force and material properties are again varying randomly. The only difference between part-to-part feedback and the uncontrolled state is that the force variation is restricted to a smaller range, based on the control algorithm. This form of process control is highly inefficient, however, since force control will provide greater variation reduction with less effort. Part-to-part feedback does have one advantage not apparent in this example; it can prevent process mean shifts, if an input parameter is subject to non-random variation.

The ability of part-to-part feedback to correct for mean shifts is an advantage over force control that cannot be disregarded. As such, we can explore variants of the part-to-part approach, which retain this ability while also providing a further reduction in variation. One such alternative involves producing and measuring a batch of  $n$  parts, averaging the deviations of their quality characteristic values from target values, and then determining a new set of parameter settings to use for the next  $n$  parts. We call this form of process control *batch-to-batch feedback*. Another related technique involves using the first  $n$  parts to determine a set of process parameter values that are then used for the remainder of the run. This method effectively calibrates the system for each batch of parts, while ignoring the variation between parts within that batch. This method is called *one-time batch feedback*. We simulated both of these approaches for part runs totaling 25 parts each. The simulations were conducted using spreadsheet macros in *Crystal Ball*. For each run, the model was used to generate some number ( $n$ ) of parts, and the deviation of their quality characteristic values from target values were used to make a feedback correction to the input force. Another  $n$  parts were then run through the model, and another force correction was calculated and applied. This procedure was repeated until a total of 25 parts were “manufactured.” The results of these simulations for batch-to-batch feedback and one-time batch feedback for batch sizes of 3 and 5 parts are listed in Table 5.24.

**Table 5.24: Predicted Strain Values with Batch Feedback.**

Strain (Mark 1)	Mean Value	Standard Deviation
No Control	11.14	0.006287
Batch-to-batch Feedback (n=3)	11.17	0.002937
Batch-to-batch Feedback (n=5)	11.15	0.002821
One-Time Batch Feedback (n=3)	11.18	0.002664
One-Time Batch Feedback (n=5)	11.16	0.002886

Comparing the results in Table 5.24 with those in Table 5.23 shows that batch-to-batch feedback is significantly better than part-to-part feedback in reducing variation. The batch-to-batch method can also correct for mean shifts after just a few parts. The use of one-time batch feedback, which is effectively force control with the parameters set at the beginning of each run, also reduces variation more than part-to-part feedback. While the one-time batch method can correct for changes in material properties or process parameters between runs, it is unable to correct for mean shifts during a run. For this reason, batch-to-batch feedback is likely to be a better method in practice than either one-time batch feedback or Force Control.

There is one more implementation of feedback that can be used to correct for bias errors: *running-average feedback*. In this method, each part is used to calculate a new mean value, which is then used to adjust a parameter setting before production of the next part. The mean value used for the correction is essentially a “running average” of all parts produced. This technique is similar to the work of (Boning, Moyne et al. 1996). Table 5.25 lists the results of a Monte Carlo simulation of running-average feedback. Simulations were run with varying numbers of trials, to simulate batches of significantly different sizes.

**Table 5.25: Output Strain Values with Running-Average Feedback Control.**

Strain (Mark 1)	Mean Value	Standard Deviation
No Control	11.14	0.006287
Running-average Feedback (10 pts)	11.23	0.004448
Running-average Feedback (100 pts)	11.14	0.003394
Running-average Feedback (500 pts)	11.14	0.003702
Running-average Feedback (1500 pts)	11.14	0.003862

The data in Table 5.25 shows that running-average feedback can both produce parts without bias error and reduce variation from its uncontrolled levels. Both mean correction and end-of-line variation reduction improve up to a run size of 100 parts, after which these quantities level out. Running-average feedback is not very effective for production processes with small part runs, since there are insufficient parts for a statistically significant mean value. For large batch sizes, however, this method can reduce variation by approximately 50%, while also correcting for mean shifts. Running-average feedback is not as effective as batch-to-batch feedback in reducing variation, but it compensates better for any mean shifts during a run.

We have now demonstrated a number of process control strategies through Monte Carlo simulation. Through the rest of this chapter, we will discuss the shop-floor implementation of one promising strategy: feed-forward control. Details and results of the process control experiment follow in the next section.

## 5.10 Feed-Forward Control Experiment

In the previous section, we presented simulation results for a number of process control strategies. We evaluated each of these methods based on its ability to reduce end-of-line variation. The simulations showed that strain control is the most effective strategy for both reducing strain variation and meeting quality characteristic target output values. This is because strain control is the only method that directly measures part strain *during forming*, allowing the operator or a control algorithm to directly account for the specific input variations experienced by each part. The efficacy of strain control has been demonstrated on the shop floor by Parris (1996).

The second most effective variation reduction strategy is an implementation of feed-forward control, in which the aging time during heat treatment is measured and used to set the force during stretch forming. This process control strategy, discussed in Section 5.5.4.1, is particularly interesting from a systems perspective, since it involves inter-operation control. Feed-forward is a desirable form of process control from a variation reduction standpoint because of the availability of closed-form equations that can be used to predict the controlled output variation.

In this section we describe an experimental implementation of feed-forward control in the production environment. We show that use of this strategy reduced strain variation by 30%, and thickness variation by 18%, on a batch of production parts.

### **5.10.1 Experiment Overview**

The feed-forward control strategy used in this experiment was discussed in detail in section 5.5.4.1. The approach involves measuring the aging time during heat treatment, estimating its effects on material yield strength, and then adjusting the forming force to compensate. When implementing this control strategy, we introduce two minor changes to the process; the operators must measure aging time for each part, and forming force is set to a prescribed value for each part.

The feed-forward analytical results and simulations in the previous sections show that strain variation can be reduced by 50-67% through the use of a perfect model. As would be expected, the addition of modeling error diminishes this value; a model with 50% error (assuming a uniform distribution as discussed previously) is predicted to reduce variation by 36-53%. In practice, the effects of modeling error are compounded by uncertainties in input parameter values, varying ambient conditions, and calibration errors in the forming press. For example, although the form of the function relating aging time to material yield strength is known, the actual curve must be calibrated to both the mean yield strength of the incoming material and ambient temperature. In addition, the relationship between forming force and strain at each measurement location is a function not only of the material properties, but of the press geometry and force transmission as well. This relationship can only be determined with any accuracy through experiment. In order to account for all of these factors, the ISM sensitivities were not used directly, but were estimated through the forming of some “calibration parts.” Details of the experiment procedure follow in the next section.

### **5.10.2 Experimental Procedure**

The feed-forward control experiment involved a batch of ten target parts. Prior to forming, we measured thickness at four points on each blank, and inscribed strain marks at three measurement locations on each blank. We used the same thickness and strain measurement locations as described in Section 5.4.1. Four parts were chosen for calibration. Each “calibration part” was formed according to standard operating practice, which at the time of this experiment was displacement control. We measured the total time each part was out of the freezer between quench and forming, and recorded the

maximum forming force from the press display. After the four calibration parts were formed, we measured the circumferential strain at measurement location 1 on each part. We designated the mean value of these measured strains as the “target strain” for the six remaining parts. We then used the measurement data from the calibration parts to generate the following three graphs:

### 1) Aging Time vs. Force

This chart, shown in Figure 5.24, shows the relationship between material yield strength just prior to forming and the maximum force required to form the part. As the required force increases with increasing material yield strength, the data on this chart should lie along a line with positive slope.

### 2) Force vs. Strain

This chart, depicted in Figure 5.25, reveals the actual relationship between measured force and strain on the sheet. This line incorporates any errors in force measurement, the effects of material slippage in the jaws, and the calibration state of the forming press. Basic physical principles suggest that strain should increase with increasing force, and thus the data on this chart should lie along a line with positive slope.

### 3) Strain Error vs. Aging Time

Strain error was defined as the difference between measured strain on a part and the target strain value. This chart, shown in Figure 5.26, reveals any bias effects in forming, relating strain error to material yield strength.

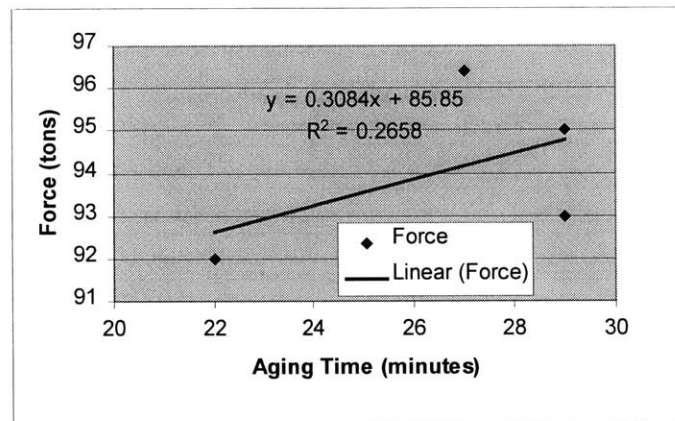


**Figure 5.24: Aging Time vs. Force for Calibration Parts.**

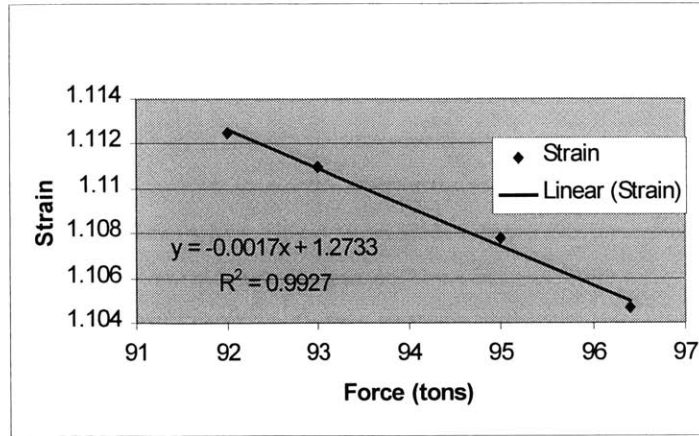


**Figure 5.25: Force vs. Strain for Calibration Parts.**

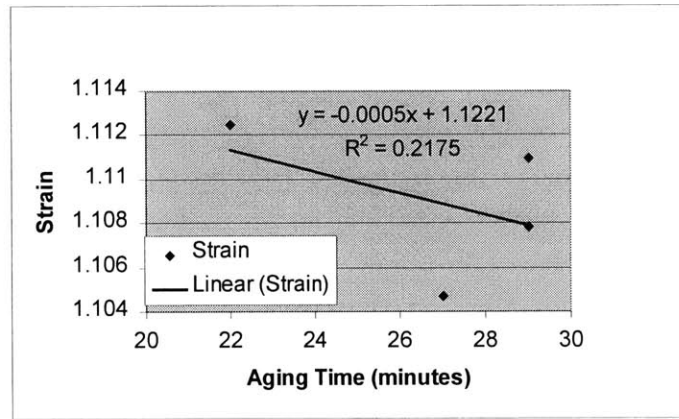


**Figure 5.26: Aging Time vs. Strain for Calibration Parts.**

A cursory examination of the charts in Figures 5.24 through 5.26 reveals several incongruities. In Figure 5.25, for example, the slope of the line that best fits the data is negative, rather than positive. This trend is counter-intuitive, and implies that part strain actually decreases as forming force increases. Also note that in Figures 5.24 and 5.25, the forming force recorded from the stretch press display is on the order of 90 tons. On our first trip, forming force for the target part was on the order of 50 tons (see Table 5.3). The latter value is in accordance with both the predicted value of force required to form this part, calculated based on material yield strength, and the results of the finite-element simulation. As such, we concluded that the force transducer on the stretch press was severely out of calibration at the time of this forming experiment. Although the force transducer errors were evident immediately after forming the calibration parts, we decided to proceed with the experiment, acting on the assumption that these errors were repeatable. We assumed that the calibration curves in Figures 5.24 through 5.26 would account for machine errors, and enable production of acceptable parts.

After plotting the three calibration curves above, we generated a table linking input force values to a series of different aging time values. This table was developed by applying the following steps to each given value of aging time:

- 1) Use graph 1 (Figure 5.24) to determine the force value that would be used to form a part with the measured aging time during normal operation
- 2) Use graph 3 (Figure 5.26) to determine the approximate strain error during normal operation, based on the measured aging time
- 3) Use graph 2 (Figure 5.25) to determine a force adjustment value that will offset the strain error from Step 2
- 4) Add the force adjustment value determined in Step 3 to the force value found in Step 1 in order to obtain the correct value of forming force for the given value of aging time.

The table of force input values calculated for various aging times during the experiment is shown in Table 5.26. The units of aging time in Table 5.26 are minutes, and the units of force are tons.

**Table 5.26: Force Correction Based on Aging Time.**

Aging Time	Original Force	Strain Error	Force Correction	New Force
17	91.09	0.0046	-2.71	88.39
18	91.40	0.0041	-2.41	88.99
19	91.71	0.0036	-2.12	89.59
20	92.02	0.0031	-1.82	90.19
21	92.33	0.0026	-1.53	90.80
22	92.63	0.0021	-1.24	91.40
23	92.94	0.0016	-0.94	92.00
24	93.25	0.0011	-0.65	92.60
25	93.56	0.0006	-0.35	93.21
26	93.87	1E-04	-0.06	93.81
27	94.18	-0.0004	0.24	94.41
28	94.49	-0.0009	0.53	95.01
29	94.79	-0.0014	0.82	95.62
30	95.10	-0.0019	1.12	96.22
31	95.41	-0.0024	1.41	96.82
32	95.72	-0.0029	1.71	97.42

After generating Table 5.26, the remaining six parts were formed using feed-forward control. Each part was removed from the freezer, and allowed to naturally age between 8 and 28 minutes. This aging time, when combined with the 6 minutes required to move parts from the quench batch to the freezer and the 6 minutes required to straighten the coils, gave each part a total natural aging time of 20-30 minutes. The aging times were staggered in order to improve experimental validity. After aging, each part was formed to a force value determined from Table 5.26. The results of this experiment are presented in the following section.

### 5.10.3 Experimental Results

The nominal values and variations of strain and thickness after forming are listed in Table 5.27 for both the calibration parts and the controlled parts. Note that the standard deviations of the calibration parts are much lower than the standard deviations of the uncontrolled parts measured previously (see Table 5.8). This is because standard practice in the plant changed from visual inspection to displacement control between our visits, based on the recommendations of Parris (1996). The data in Table 5.27 is based on 4 calibration parts and 5 controlled parts. Initially there were 6 controlled parts, but the operators suspected a problem during forming of one of these parts, and stopped the press. The blank was removed from the jaws, and then re-loaded and re-formed to the target force value after the press had been inspected. Data for this part differed significantly different from that for the other 9 parts, most likely due to a different deformation path and some inconsistency during re-loading. Data for this part has thus been omitted from the results.

**Table 5.27: Results of Feed-Forward Control**

	Calibration Parts		Controlled Parts	
	Mean	Standard Dev.	Mean	Standard Dev.
Strain (location 1)	0.1094	0.00346	0.1091	0.00230
Strain (location 2)	0.1082	0.00346	0.0997	0.00313
Strain (location 3)	0.1105	0.00346	0.01073	0.00235
Thickness	0.001213 m	0.001210 m	1.10E <sup>-5</sup> m	9.01E <sup>-6</sup> m

The data in Table 5.27 shows that use of feed-forward control resulted in a 30% reduction of variation at locations 1 and 3, and a 9% reduction of variation at location 2. Thickness variation was reduced by an average of 18% across the sheet. Although the amount of variation reduction is lower than the improvement predicted in the previous sections, these results are still quite impressive. The nominal value of strain at the controlled location was within 3% of the target value. Nominal values at the other two measurement locations show greater bias, which could be reduced by simultaneously measuring and controlling strain at all three locations.

### 5.10.4 Discussion

There are several reasons why the variation reduction seen in the feed-forward experiment is lower than that predicted through simulation. As discussed previously, the force measurement system on the stretch press was severely out of calibration during this experiment. The press display indicated that the force required to form the target part was between 90 and 95 tons, whereas this value had historically been between 50 and 55 tons. The 90 ton value is also clearly infeasible based on the stress/strain curve of the material. We did not ascertain whether this measurement error was merely an offset, or whether the bias was non-linear. In addition, the algorithm used to calibrate the feed-



forward adjustment was based on some amount of operator consistency during uncontrolled forming. As was mentioned previously, at the time of these experiments, the operators were forming parts using a form of displacement control, rather than by visual inspection. The displacement control used to form these parts involved raising the die table to the same pre-determined height for every part. This procedure differs from proper displacement control as described by Parris (1996), in which the die table is raised by the same amount after snug for each part. The procedure described by Parris accounts for variations in material yield strength and thickness; the method used currently in the plant does not. This means that “standard” forming press operation was not as consistent as it should have been. Our feed-forward algorithm was thus forced to account for two significant sources of error, as well as an undetermined amount of modeling error. Despite this, the control strategy was successful in reducing variation by a sizeable amount. Greater gains could be expected on a system with more reliable force measurement.

In addition to its robustness, this feed-forward strategy requires no specialized equipment and is easily implemented by the operators. Unlike strain control, which requires that the both the sheet and stretch press be instrumented, feed-forward only requires measurement of the time out of freezer, and the development of a force adjustment table. Once this chart has been developed, the operators can determine the required forming force directly, with no additional effort.

## **5.11 Chapter Summary**

In this chapter, we presented an example of the variation reduction method outlined in the introduction. We first developed an Integrated System Model for a sheet stretch-forming system used to manufacture aircraft skin components. We derived predictive and variational models for the heat treatment and stretch-forming operations, and then linked linearized versions of these models in a spreadsheet environment. Next we validated the ISM against production data, and used it to identify the major sources of variation in the stretch-forming system. We then used system-level parameter design to reduce end-of-line variation by 24% in simulation, with only minor process changes. We calculated process limits for each operation in the system, and formulated several variation reduction strategies. We explored the effects of various feedback and feed-forward process control implementations analytically and numerically, and then selected feed-forward control as the most promising strategy for this system. Finally, we presented the results of a feed-forward experiment, evaluated on production parts, in which strain variation was reduced by 30%, and thickness variation was reduced by 18% over uncontrolled levels.

## Chapter 6: Summary and Conclusions

In this thesis, we presented a new method for reducing variation in manufacturing systems, through the use of physics-based mathematical process models. This approach involves the development of an Integrated System Model, which can predict end-of-line quality characteristic nominal values and variation. In Chapters 3 and 4, we developed a number of variation reduction techniques for use in conjunction with the ISM. With these methods, we can identify the major sources of variation in a system, make the system more robust to input variation, and evaluate the need for process control. We also used the ISM to explore the effects of feedback and feed-forward process control, and developed analytical expressions to predict output variation in a system with feed-forward control. Finally, we demonstrated all of these techniques on a sheet stretch-forming system used to manufacture aircraft skin components.

### 6.1 Major Contributions

The overarching contribution of this thesis is a model-based method to variation reduction in manufacturing systems. This approach utilizes a number of mathematical tools developed in this work. In this section, we summarize the major contributions of our research.

#### 6.1.1 Variation Reduction Method

The variation reduction techniques developed in this thesis are all components of an integrated variation reduction method for manufacturing systems. This method consists of the following steps:

- 2) Develop an Integrated System Model of the manufacturing system
  - Build predictive models of each operation
  - Derive variational models of each operation
  - Link the models into an ISM
  - Validate system predictions against measured data
- 1) Identify major sources of variation in the system
- 2) Conduct system-level parameter design
- 3) Evaluate the need for measurement or control in a system
- 4) Formulate several variation reduction strategies
  - Source reduction
  - Feed-forward control
  - Feedback control
- 5) Evaluate strategies in simulation using the ISM
- 6) Implement the most promising strategy

In this thesis, we developed mathematical tools enabling each of these steps, and demonstrated the entire method on an industrial example. Chapter 5 is a step by step implementation of this approach on a sheet stretch-forming manufacturing system. Use

of this method resulted in a process control implementation that reduced strain variation by 30%, and thickness variation by 18% in production parts.

### **6.1.2 Integrated System Model**

The Integrated System Model is a framework for analyzing variation propagation in manufacturing systems. As such, it is the foundation for all the variation reduction strategy described above. The ISM is based on analytical expressions for variation propagation in systems, and on process sensitivities derived from mathematical process models. Methods for developing an ISM were presented in Chapter 3, and demonstrated on the sheet stretch-forming system in Chapter 5.

### **6.1.3 Tolerance Threshold**

The Tolerance Threshold, presented in Chapter 3, is the predicted output variation of a manufacturing operation or system. The Tolerance Threshold value can be used to guide in tolerance design, or to evaluate existing tolerances. Unlike traditional measures of process capability, determination of the Tolerance Threshold does not pre-suppose the existence of either a physical manufacturing system or product tolerances.

### **6.1.4 System-Level Parameter Design**

In Chapter 3, we developed a formulation for system-level parameter design. This technique uses the ISM to identify the combination of process operating points that produces parts meeting output specifications with minimum variation. System-level parameter design differs from traditional parameter design methods, in that we simultaneously select input parameter settings across the entire system. As demonstrated in Chapter 5, this can result in lower end-of-line variation than applying traditional parameter design methods to each operation individually. The system level approach was shown to reduce end-of-line strain variation by 24% in simulation on the stretch-forming system.

### **6.1.5 Process Limits**

In Chapter 4, we developed a method for back-propagating end-of-line tolerances through a system, in order to determine process limits for each operation. A process limit is the maximum allowable output variation for an operation, which ensures that 99.7% of produced parts can meet end-of-line tolerances. Process limit analysis also provides a means for determining whether control is needed in a system. The use of process limits was demonstrated on the example ISM, showing that the existing input specifications on material thickness are insufficient to ensure that stretch-formed parts will meet end-of-line tolerances.

### **6.1.6 Analytical Treatment of Feed-Forward Control**

Also in Chapter 4, we discussed the use of feedback and feed-forward process control. We developed analytical expressions to predict end-of-line variation in a feed-forward

controlled system. These expressions incorporated the effects of modeling error, actuation error, and measurement error. We also developed methods for determining the maximum controllable input variation to an operation, and the maximum allowable modeling error in the controller.

### **6.1.7 Stretch-Forming ISM**

In addition to the contributions listed above, which apply to any manufacturing system, this thesis presents several developments specific to stretch-forming. Foremost among these is the sheet stretch-forming ISM, developed in Chapter 5. In order to generate the ISM, we developed a robust finite-element simulation of drape forming and an analytical model of natural aging, neither of which existed previously. We used the ISM to identify the major sources of variation in the stretch-forming system; this information is also unique to this thesis.

### **6.1.8 Feed-Forward Control Validation**

Another contribution specific to stretch-forming is the feed-forward control experiment, presented in Chapter 5. The experiment is an implementation of inter-operation control, in which a process parameter measurement in one operation is used to determine a process parameter setting for a successive operation. This process control strategy was suggested by the results of the ISM analysis. Data presented in Chapter 5 showed that this method reduced strain variation by 30%, and thickness variation by 18%, on a batch of production parts. This form of process control has several advantages over other methods; it requires little change to standard operating procedure, and adds no cost to the operation. Based on the results of our experiment, Northrop-Grumman Corporation is now considering implementing this process control technique during standard production.

## **6.2 Generalizing These Methods**

Although the variation modeling and reduction methods outlined in this thesis are only demonstrated on one manufacturing process, they can be applied to other systems as well. For this reason, the mathematical techniques in Chapters 3 and 4 have been developed in a generalized form. The only requirement of a candidate system is that it exhibit linear behavior in a small region about a given operating point. As discussed in chapter 3, this criterion encompasses a wide range of manufacturing systems, from machining to injection molding. Mathematical modeling approaches similar to those outlined in this work have been successfully demonstrated on the production of Multi-Chip Modules (Frey and Otto 1996), low-temperature ceramic components for electronic assemblies (Soyucayli and Otto 1998), welded aluminum automotive frames (Suri and Otto 1998), and injection-molded parts (Kazmer, Barkan et al. 1996). Research is currently underway to extend these methods to continuous processes, such as steel rolling.

## **6.3 Opportunities for Further Research**

The research presented in this thesis introduces a number of areas deserving of further exploration. As discussed in Chapter 3, we used designed experiments to derive variational models from complex numerical simulations. While these variational models

are accurate in the vicinity of a given operating point, any changes to input parameter values require re-derivation of the process sensitivities. We are currently exploring the use of neural nets to capture the information contained within complex predictive models. While the neural nets are also complex non-linear models, once they have been trained with data from the predictive model, they can be used to very quickly recalculate sensitivities at varying operating points.

Another area for additional work is feedback control. While we presented a series of analytical derivations in Chapter 4 that predict the effects of feed-forward control on variation, we limited our involvement with feedback control to numerical simulation. The effects on variation of part-to-part, batch-to-batch, and running-average feedback could also be expressed analytically, in terms of the frequency of the input variation, and the time constant of the feedback loop. Closed-form expressions predicting controlled variation in the presence of feedback would be useful for both modeling and process design.

## **6.4 Conclusions**

In conclusion, this thesis presented a model-based method for variation reduction in manufacturing systems. We developed a model of sheet stretch-forming, which was used to reduce variation on production parts. Although the techniques outlined in this work have only been demonstrated on one manufacturing system, related work and the underlying theory indicate that they can be generalized to other systems as well. It is our hope that model-based quality improvement will one day be standard practice in industry.

## References

- Azushima, A. (1995). "Direct Observation of Contact Behavior to Interpret the Pressure Dependence of the Coefficient of Friction in Sheet Metal Forming." Annals of the CIRP **44**(1): 209-212.
- Boning, D., W. Moyne, et al. (1996). "Run by Run Control of Chemical-Mechanical Polishing." IEEE Trans. CPMT (C) **19**(4): 307-314.
- Bonvik, A., M. (1996). Performance Analysis of Manufacturing Systems Under Hybrid Control Policies. Operations Research. Cambridge, MA, Massachusetts Institute of Technology: 179.
- Box, G. E. and N. R. Draper (1969). Evolutionary Operation: A Statistical Method for Process Improvement. New York, John Wiley and Sons.
- Chang, T.-S., A. C. Ward, et al. (1994). Distributed Design With Conceptual Robustness: A Procedure Based on Taguchi's Parameter Design. Concurrent Product Design, Chicago, ASME.
- Chen, W., J. Allen, et al. (1996). "A Procedure for Robust Design: Minimizing Variations Caused by Noise Factors and Control Factors." Journal of Mechanical Design **118**(4): 478-493.
- Chen, W., J. K. Allen, et al. (1997). "A Robust Concept Exploration Method for Enhancing Productivity in Concurrent Systems Design." Concurrent Engineering: Research and Applications **5**(3): 203-218.
- Chinnam, R. B. and W. J. Kolarik (1997). "Neural network-based quality controllers for manufacturing systems." International Journal of Production Research **35**(9): 2601-2620.
- Clausing, D. P. (1988). Taguchi Methods Integrated into the Improved Total Development. Proceedings IEEE International Conference on Communications, Philadelphia, IEEE.
- Davis, J. R., Ed. (1993). Aluminum and Aluminum Alloys. Materials Park, Ohio, American Society for Metals.
- DeVor, R., T.-h. Chang, et al. (1992). Statistical Quality Design and Control. New York, Macmillan Publishing Company.
- Drake, A. (1967). Fundamentals of Applied Probability Theory. New York, McGraw-Hill.

- Fletcher, A. J. (1989). Thermal Stress and Strain Generation in Heat Treatment. New York, Elsevier Science.
- Ford, R. B. and P. Barkan (1995). Beyond Parameter Design-- A Methodology Addressing Product Robustness at the Concept Formation Stage. Design for Manufacturability, Chicago, ASME.
- Frey, D. (1997). Using Product Tolerances to Drive Manufacturing System Design. Mechanical Engineering. Cambridge, MA, Massachusetts Institute of Technology: 365.
- Frey, D. and K. Otto (1996). The Process Capability Matrix: A Tool for Manufacturing Variation Analysis at the Systems Level. ASME Design Theory and Methodology Conference, 1997, Sacramento, CA.
- Frey, D., K. Otto, et al. (1997). "Manufacturing Block Diagrams and Optimal Adjustment Procedures." Submitted to ASME Journal of Manufacturing Science and Engineering.
- Frey, D., K. Otto, et al. (1998). "Evaluating Process Capability Given Multiple Acceptance Criteria." To appear in ASME Journal of Manufacturing Science and Engineering.
- Garcia, F. and R. D. Sriram (1997). "Developing Knowledge Sources to Identify and Evaluate Tradeoffs Among Alternate Designs in a Cooperative Engineering Framework." Concurrent Engineering: Research and Applications 5(3): 279-292.
- Gershwin, S. B., R. R. Hildebrandt, et al. (1984). A Control Theorist's Perspective on Recent Trends in Manufacturing Systems. 23rd IEEE Conference on Decision and Control, Las Vegas, NV, IEEE.
- Guo, R.-S. and E. Sachs (1993). "Modeling, Optimization, and Control of Spatial Uniformity in Manufacturing Processes." IEEE Transactions on Semiconductor Manufacturing 6(1): 41-57.
- Hardt, D. (1998). 2.810 Control of Manufacturing Processes Class Notes.
- Harry, M. J. and J. R. Lawson (1992). Six Sigma Producibility Analysis and Process Characterization. Reading, MA, Addison Wesley.
- Hu, S. J. (1997). "Stream-of-Variation Theory for Automotive Body Assembly." CIRP Annals 1997 46(1): 1-6.
- Jaikumar, R. (1996). . 10th Ralph E. Cross Sr. Distinguished Lecture, Cambridge, MA, Massachusetts Institute of Technology.
- Kacker, R. (1985). "Off-line Quality Control, Parameter Design, and the Taguchi Method." Journal of Quality Technology 17(4): 176-188.

- Kalpakjian, S. (1995). Manufacturing Engineering and Technology. Reading, MA, Addison-Wesley.
- Kane, V. E. (1986). "Process Capability Indices." Journal of Quality Technology **18**(1): 41-52.
- Kazmer, D., P. Barkan, et al. (1996). Quantifying Design and Manufacturing Robustness Through Stochastic Optimization Techniques. ASME Design Automation Conference, Irvine, CA, ASME.
- Kinnear, K. (1998). Model of Yield Strength Based on Quench, Personal Communication. ALCOA.
- Mantipragada, R. (1997). Assembly Oriented Design: Concepts Algorithms and Computational Tools. Mechanical Engineering. Cambridge, MA, Massachusetts Institute of Technology: 182.
- Mantripragada, R. and D. E. Whitney (1997). "Modeling and Controlling Variation Propagation in Mechanical Assemblies Using State Transition Models." Submitted to IEEE Transactions on Robotics and Automation.
- Mantripragada, R. and D. E. Whitney (1997). "State Transition Models of Mechanical Assembly Processes." Submitted to IEEE Transactions on Robotics and Automation.
- Montgomery, D. C. (1984). Design and Analysis of Experiments. New York, John Wiley and Sons.
- Ogata, K. (1990). Modern Control Engineering. Englewood Cliffs, New Jersey, Prentice-Hall Inc.
- Otto, K. (1994). Robust Product Design Using Manufacturing Adjustments. ASME Design Theory and Methodology 1994.
- Parris, A. (1996). Precision Stretch Forming of Metal for Precision Assembly. Mechanical Engineering. Cambridge, Massachusetts, MIT: 404.
- Peplinski, J., J. Allen, et al. (1996). Integrating Product Design With Manufacturing Process Design Using the Robust Concept Exploration Method. ASME Design Theory and Methodology, Irvine, CA, ASME.
- Phadke, M. (1989). Quality Engineering Using Robust Design. Englewood Cliffs, NJ, Prentice Hall.
- Rohsenow, W. and H. Choi (1961). Heat, Mass, and Momentum Transfer. Englewood Cliffs, New Jersey, Prentice-Hall Inc.



Sachs, E., G. Prueger, et al. (1992). "An Equipment Model for Polysilicon LPCVD." IEEE Transactions on Semiconductor Manufacturing 5(1): 3-13.

Socrates, S. and M. Boyce (1996). Reconfigurable Tooling For Flexible Forming 2nd Annual Review. Dallas, Northrop Grumman Commercial Aircraft Division.

Soons, H. (1993). Accuracy Analysis of Multi-Axis Machines. The Netherlands, Eindhoven University of Technology: 211.

Soyucayli, S. and K. Otto (1998). "Simultaneous Engineering of Quality Through Integrated Modeling." To Appear in the Journal of Mechanical Design.

Suri, R. and K. Otto (1998). Concurrent Part and Process Design for Quality Improvement. ASME Design for Manufacturing, Atlanta, ASME.

Suri, R. and K. Otto (1998). Process Capability to Guide Tolerancing in Manufacturing Systems. NAMRC XXVII, Berkeley, CA, NAMRI/SME.

Suri, R. and K. Otto (1999). "Variation Modeling for a Sheet Stretch Forming Manufacturing System." Annals of the CIRP.

Tiryakioglu, M. and M. P. Menguc (1996). The Effect of Quenching Process Parameters on the Predictability of Residual Stresses in Aluminum Castings. 16th Heat Treating Conference and Exposition, Cincinnati, Ohio, ASM.

Van Horn, K., Ed. (1967). Aluminum. Metals Park, Ohio, American Society for Metals.

## Appendix A: Abaqus Input Deck for Drape Forming

```
*HEADING, UNSYMM
**
**Smooth Die MARK geometry, drape forming SR4 Element
**This is the input deck for the nacelle doubler
**
**This section determines sheet meshing in the X direction
*NODE
2010, 0., 0, .0014351
2030, 0.762, 0, .0014351
2039, 1.2192, 0, .0014351
2049, 1.67005, 0, .0014351
2054, 1.7272, 0, .0014351
*NGEN, NSET=Y0
2010, 2030, 1
2030, 2039, 1
2039, 2049, 1
2049, 2054, 1
**
**This section meshes the sheet in the Y direction
**A finer mesh is used around the point of initial contact (3510)
**
*NCOPY, CHANGE NUMBER=1100, OLDSET=Y0, NEWSET=YINT, SHIFT
0., .2794, 0.
0., 0., 0., 0., 0., 1., 0.
*NFILL, NSET=NSHEET1
YINT, Y0, 11, -100
*NCOPY, CHANGE NUMBER=800, OLDSET=YINT, NEWSET=YINT2, SHIFT
0., .1016, 0.
0., 0., 0., 0., 0., 1., 0.
*NFILL, NSET=NSHEET2
YINT2, YINT, 8, -100
*NCOPY, CHANGE NUMBER=2100, OLDSET=YINT2, NEWSET=Y1, SHIFT
0., .5334, 0.
0., 0., 0., 0., 0., 1., 0.
*NFILL, NSET=NSHEET
Y1, YINT2, 21, -100
*NSET, NSET=NALL
NSHEET1, NSHEET2, NSHEET,
*NSET, NSET=X0, GEN
2010, 6010, 100
**
**Here we define a nodeset along the edge of the sheet
*NSET, NSET=CLAMP, GEN
2054, 6054, 100
*ELEMENT, TYPE=S4R, ELSET=SHEET
2010, 2010, 2011, 2111, 2110
*ELGEN, ELSET=SHEET
2010, 44, 1, 1, 40, 100, 100, 1
*NSET, NSET=NOUT
2049
**
```

```

**Here we define the PULL nodeset which is used to constrain
**edge nodes as if they were clamped in a jaw
*NSET, NSET=PULL
2049
*NSET, NSET=XOY0
2010
**
**The nodeset PTFIXE is the initial contact point with the die
*NSET, NSET=PTFIXE
3510
*NSET, NSET=MID, GEN
3510,3549
*NODE, NSET=DREF
99999, 0, .4572, -.721106
*NODE, NSET=DUMMY
99998, 0, .4572, -.721106
*ELEMENT, ELSET=SPRING, TYPE=SPRING1
99998, 99998
*SPRING, ELSET=SPRING
1,
100.
**
**This section introduces the dashpots which will be
**used to aid in relaxation
*ELEMENT, ELSET=DASHPOT, TYPE=DASHPOT1
8001,2054
8002,2154
8003,2254
8004,2354
8005,2454
8006,2554
8007,2654
8008,2754
8009,2854
8010,2954
8011,3054
8012,3154
8013,3254
8014,3354
8015,3454
8016,3554
8017,3654
8018,3754
8019,3854
8020,3954
8021,4054
8022,4154
8023,4254
8024,4354
8025,4454
8026,4554
8027,4654
8028,4754
8029,4854
8030,4954
8031,5054
8032,5154

```

```
8033,5254
8034,5354
8035,5454
8036,5554
8037,5654
8038,5754
8039,5854
8040,5954
8041,6054
8101,2049
8102,2149
8103,2249
8104,2349
8105,2449
8106,2549
8107,2649
8108,2749
8109,2849
8110,2949
8111,3049
8112,3149
8113,3249
8114,3349
8115,3449
8116,3549
8117,3649
8118,3749
8119,3849
8120,3949
8121,4049
8122,4149
8123,4249
8124,4349
8125,4449
8126,4549
8127,4649
8128,4749
8129,4849
8130,4949
8131,5049
8132,5149
8133,5249
8134,5349
8135,5449
8136,5549
8137,5649
8138,5749
8139,5849
8140,5949
8141,6049
*DASHPOT, ELSET=DASHPOT
3
196000
**
**This user MPC will constrain all edge nodes to the PULL nodeset
**to simulate the sheet being clamped in the jaws
*MPC,USER
```

1, 2149, 2049  
1, 2249, 2049  
1, 2349, 2049  
1, 2480, 2049  
1, 2549, 2049  
1, 2649, 2049  
1, 2749, 2049  
1, 2849, 2049  
1, 2949, 2049  
1, 3049, 2049  
1, 3149, 2049  
1, 3249, 2049  
1, 3349, 2049  
1, 3449, 2049  
1, 3549, 2049  
1, 3649, 2049  
1, 3749, 2049  
1, 3849, 2049  
1, 3949, 2049  
1, 4049, 2049  
1, 4149, 2049  
1, 4249, 2049  
1, 4349, 2049  
1, 4449, 2049  
1, 4549, 2049  
1, 4649, 2049  
1, 4749, 2049  
1, 4849, 2049  
1, 4949, 2049  
1, 5049, 2049  
1, 5149, 2049  
1, 5249, 2049  
1, 5349, 2049  
1, 5449, 2049  
1, 5549, 2049  
1, 5649, 2049  
1, 5749, 2049  
1, 5849, 2049  
1, 5949, 2049  
1, 6049, 2049  
2, 2149, 2049  
2, 2249, 2049  
2, 2349, 2049  
2, 2449, 2049  
2, 2549, 2049  
2, 2649, 2049  
2, 2749, 2049  
2, 2849, 2049  
2, 2949, 2049  
2, 3049, 2049  
2, 3149, 2049  
2, 3249, 2049  
2, 3349, 2049  
2, 3449, 2049  
2, 3549, 2049  
2, 3649, 2049  
2, 3749, 2049

2,3849,2049  
2,3949,2049  
2,4049,2049  
2,4149,2049  
2,4249,2049  
2,4349,2049  
2,4449,2049  
2,4549,2049  
2,4649,2049  
2,4749,2049  
2,4849,2049  
2,4949,2049  
2,5049,2049  
2,5149,2049  
2,5249,2049  
2,5349,2049  
2,5449,2049  
2,5549,2049  
2,5649,2049  
2,5749,2049  
2,5849,2049  
2,5949,2049  
2,6049,2049  
3,2149,2049  
3,2249,2049  
3,2349,2049  
3,2449,2049  
3,2549,2049  
3,2649,2049  
3,2749,2049  
3,2849,2049  
3,2949,2049  
3,3049,2049  
3,3149,2049  
3,3249,2049  
3,3349,2049  
3,3449,2049  
3,3549,2049  
3,3649,2049  
3,3749,2049  
3,3849,2049  
3,3949,2049  
3,4049,2049  
3,4149,2049  
3,4249,2049  
3,4349,2049  
3,4449,2049  
3,4549,2049  
3,4649,2049  
3,4749,2049  
3,4849,2049  
3,4949,2049  
3,5049,2049  
3,5149,2049  
3,5249,2049  
3,5349,2049  
3,5449,2049

```

3,5549,2049
3,5649,2049
3,5749,2049
3,5849,2049
3,5949,2049
3,6049,2049
** DUMMY MPC TO SIMULATE DRAPE
4,99998,2049
*****
**
**This first user subroutine constrains the clamped region through
**the first 10 steps of the simulation
**The second was used to calculate Z displacement of the sheet edge
**based on a given wrap angle. This did not work for large wrap angles
**and has been replaced by a hand-calculation detailed in Section
5.3.2.2
**
*USER SUBROUTINES
  subroutine mpc (ue,a,jdof,mdof,n,jtype,x,u,unit,maxdof,
&      lmpc,kstep,kinc,time,nt,nf,temp,field)
    include 'ABA_PARAM.INC'
    common / keep / uxold,uyold,uxnew,uynew,kincold
    common /kshare/ aa,bb,cc,dd,x0n,y0n,z0n,del0
    dimension a(n),jdof(n),x(6,n),u(maxdof,n),unit(maxdof,n),
&      time(2),temp(nt,n),field(nf,nt,n)
c
c
    if (kstep.ge.10.or.(kstep.ge.7.and.
&      (JTYPE.EQ.1.OR.JTYPE.EQ.2.OR.JTYPE.EQ.4))) then
      lmpc=0
      return
    endif
c
    if(jtype.ne.1.and.jtype.ne.2.and.jtype.ne.3.and.
&      jtype.ne.4) then
      write(*,*) 'mpc type = ',itype
      stop
    endif
    if(jtype.eq.1) then
      jdof(1)=1
      jdof(2)=1
    elseif(jtype.eq.2) then
      jdof(1)=3
      jdof(2)=3
    elseif(jtype.eq.3) then
      jdof(1)=5
      jdof(2)=5
    elseif(jtype.eq.4) then
      if(kinc.ne.kincold.and.kstep.gt.1) then
        uxold=uxnew
        uyold=uynew
        kincold=kinc
      endif
      uxnew= unit(1,2)
      uynew= unit(2,2)
c
    R=0.79

```

```

pi=4*atan(1.)
aa=sin(pi/4)
bb=0.0
cc=cos(pi/4)
dd=R*(1-cos(pi/4))
x0n=x(1,2)
y0n=x(2,2)
z0n=x(3,2)
del0=aa*x0n+bb*y0n+cc*z0n-dd
  if (kstep.ne.3) then
    lmpc=0
    return
  endif
  jdof(1)=1
  jdof(2)=3
endif
c
  a(1) =1.D0
  a(2) =-1.0D0

  return
end
c*****
c***** disp subroutine for draping step *****
subroutine disp (U,kstep,kincl,time,node,jdof)
  include 'ABA_PARAM.INC'
  common / keep / uxold,uyold,uxnew,uynew,kinclold
  common /kshare/ aa,bb,cc,dd,x0n,y0n,z0n,del0
  dimension u(3),time(2)
c
  if (node.eq.2049.and.jdof.eq.3) then
del=del0*(1-time(1))**2
if(kincl.eq.kinclold) then
xn=x0n+uxold
yn=y0n+uyold
else
xn=x0n+uxnew
yn=y0n+uynew
endif
uzn=(del+dd-aa*xn-bb*yn)/cc -z0n
u(1) = uzn
else
write(*,*) 'error in disp',node,jdof
stop
endif

  return
end
c
*****
*****
**
** Die Geometry: this profile was determined from an IGES file of the
** actual die
**
**RIGID SURFACE,NAME=DIE, TYPE=REVOLUTION,REF NODE=99999, SMOOTH=0.45

```



```

0.,0,-.85234,0,-1.E-03,-.85234
START,0,0
LINE,0.79353392,0
LINE,0.80139776,-0.037338
LINE,0.80926922,-0.0745744
LINE,0.817161,-0.1117092
LINE,0.82506294,-0.1486916
LINE,0.83296488,-0.1855216
LINE,0.84086682,-0.2222246
LINE,0.84775784,-0.2587498
LINE,0.85186756,-0.2950972
LINE,0.8531401,-0.3302
LINE,0.85157292,-0.3672078
LINE,0.84717364,-0.4031488
LINE,0.83996258,-0.439801
LINE,0.82998292,-0.4771136
LINE,0.81759026,-0.514858
LINE,0.80527634,-0.552831
LINE,0.79357456,-0.590804
LINE,0.78247984,-0.6285738
LINE,0.7719871,-0.6659372
LINE,0.76208618,-0.7030974
LINE,0.75276946,-0.740283
LINE,0.74402932,-0.7774686
LINE,0.7358556,-0.8146288
LINE,0.72823814,-0.8518144
LINE,0.72116932,-0.889
LINE,0,-0.889
*ELSET,ELSET=CDIE
SHEET,
*SURFACE DEFINITION, NAME=SDIE
CDIE, SNEG
*CONTACT PAIR, INTERACTION=FRIC
SDIE, DIE
*SURFACE INTERACTION, NAME=FRIC
*SURFACE BEHAVIOR, SOFTENED
6.3755E-4, 10.E+6
*FRICTION
0.1
*****
**
** The following material is Al 2024
**
*SHELL SECTION, ELSET=SHEET, MATERIAL=ALUMI
1.2751E-03, 5
*MATERIAL, NAME=ALUMI
*ELASTIC
68.9475E+9, 0.3
*PLASTIC
118372469,0
122926469,0.000230211
127353831.2,0.00142422
131815543,0.00258756
136183913.5,0.00373271
140934609.8,0.00529044
146266262,0.00712688
151037866.7,0.0087842

```

```

159833599.4,0.0131134
167145579.6,0.0179713
175803055.6,0.0228538
183138152.9,0.0277528
189546542,0.0326637
195258839.3,0.0375837
200426810.3,0.0425108
206506695.6,0.0474437
210831644.5,0.0524009
214851353.7,0.0573605
218611424.3,0.0623228
222147190,0.0672874
225487022.6,0.072254
228654089.3,0.0772224
231667525.2,0.0821924
234543330.8,0.0871638
237295086.3,0.0921365
239934381,0.0971104
242470990.6,0.102085
244913975.4,0.107061
247270732.2,0.112038
249547494.6,0.117015
251751084.5,0.121994
253885864.2,0.126973
255956558.7,0.131952
257968200.9,0.136933
259923765.7,0.141914
261826704.7,0.146895
263680516.2,0.151877
265487663.5,0.156859
267251098.9,0.161842
268973180,0.166826
270655404.8,0.171809
272300463.1,0.176793
273910191.9,0.181778
275485664.6,0.186762
277029106.9,0.191747
278541979.8,0.196733
292236795,0.246601
303926944.9,0.296489
314178411.4,0.346392
323341178,0.396306
331648002.8,0.446228
339262328,0.496157
346303348.1,0.546091
352861331.1,0.596031
359005676.6,0.645974
364791747.9,0.695921
370263833,0.74587
375458590.8,0.795823
380406044.6,0.845778
385131587.3,0.895735
389656758.7,0.945694
394000000,0.995655
*****
*AMPLITUDE, NAME=AM1, DEFINITION=SMOOTH STEP
0.,0.,1.,1.

```

```
*****
**
** In this step, dashpots are removed prior to forming
** STEP 1
**
*STEP, NLGEOM
*STATIC
*MODEL CHANGE, REMOVE
8001
8002
8003
8004
8005
8006
8007
8008
8009
8010
8011
8012
8013
8014
8015
8016
8017
8018
8019
8020
8021
8022
8023
8024
8025
8026
8027
8028
8029
8030
8031
8032
8033
8034
8035
8036
8036
8037
8038
8039
8040
8041
8101
8102
8103
8104
8105
8106
8107
```

```

8108
8109
8110
8111
8112
8113
8114
8115
8116
8117
8118
8119
8120
8121
8122
8123
8124
8125
8126
8127
8128
8129
8130
8131
8132
8133
8134
8135
8136
8136
8137
8138
8139
8140
8141
*END STEP
*****
**
** Here the sheet is pre-stretched to about .5% of yield stress
** STEP 2
**
*STEP, INC=1000, NLGEOM
*STATIC
1.0, 1.0
*RESTART, WRITE, FREQ = 10
*BOUNDARY, OP=NEW
Y0, YSYMM
Y1, YSYMM
X0, XSYMM
X0, 3, 3
DREF, 1, 6
DUMMY, 1, 6
*CLOAD, OP=NEW, FOLLOWER
PULL, 1, 1025
*EL PRINT, FREQ=0
S
*END STEP

```

```

*****
**
** The sheet is lowered to touch the die: the ends are lowered
** by an amount equal to the sheet thickness= .05",
**
** STEP 3
**
*STEP, INC=1000,NLGEOM
*STATIC
0.5,1.0,1.E-7,0.5
*RESTART, WRITE,FREQ=20
*BOUNDARY, OP=NEW
Y0,YSYMM
Y1,YSYMM
X0,XYMM
DREF,1,6
DUMMY,1,6
*BOUNDARY, OP=NEW
PULL,3,3,-1.2751E-03
*CLOAD, FOLLOWER, OP=NEW
PULL, 1,1025
*EL PRINT,FREQ=0
S
*END STEP
*****
**
** The sheet is draped around the die by the Z displacement
** calculated in section 5.3.2.2 for a wrap angle of 86 degrees
** Force is increased to the measured snug force
**
** STEP 4
**
*STEP,INC=1000, NLGEOM
*STATIC
0.001,1.0,1.E-6,0.1
*RESTART,WRITE, FREQ=50
*CONTROLS, ANALYSIS=DISCONTINUOUS
*CONTROLS, PARAMETER=FIELD
0.01, 0.01
*BOUNDARY, OP=NEW
X0,XYMM
DREF,1,6
DUMMY,2,6
*BOUNDARY, OP=NEW
PULL,3,3,-1.218
*BOUNDARY, FIXED, OP=NEW
PTFIXE,2,2
*CLOAD, FOLLOWER, OP=NEW
PULL, 1, 100249.024
*EL PRINT,FREQ=0
S
*END STEP
*****
**
** Grips are rotated by 86 degrees
** STEP 5
**

```

```

*STEP,INC=1000, NLGEOM
*STATIC
0.1,1.0,1.E-6,0.1
*RESTART,WRITE, FREQ=50
*CONTROLS, ANALYSIS=DISCONTINUOUS
*CONTROLS, PARAMETER=FIELD
0.01, 0.01
*BOUNDARY, OP=NEW
X0, XSYMM
DREF,1,6
DUMMY,2,6
*BOUNDARY, FIXED, OP=NEW
PULL,1,3
DUMMY,1,1
PTFIXE,2,2
*BOUNDARY, OP=NEW
PULL, 5, 5, 1.5
*CLOAD, FOLLOWER, OP=NEW
PULL, 1, 100249.024
*EL PRINT,FREQ=0
S
*END STEP
*****
**
** This is the forming step; force is increased to
** 238412.8 N which is the measured forming force
** for half the sheet
**
** STEP 6
**
*STEP,INC=1000, NLGEOM
*STATIC
0.01,1.0,1.E-6,0.04
*RESTART,WRITE, FREQ=60
*CONTROLS, ANALYSIS=DISCONTINUOUS
*CONTROLS, PARAMETER=FIELD
0.01, 0.01
*BOUNDARY, OP=NEW
X0, XSYMM
DREF,1,6
DUMMY,1,6
*BOUNDARY, FIXED, OP=NEW
PULL,5,5
PTFIXE,2,2
*CLOAD, FOLLOWER, OP=NEW
PULL, 1, 238412.8
*EL PRINT,FREQ=0
S
*END STEP
*****
**
** In this step the die is removed from the model
**
** STEP 7
**
*STEP, INC=100,NLGEOM,AMPLITUDE=STEP
*STATIC

```



```
8036
8037
8038
8039
8040
8041
8101
8102
8103
8104
8105
8106
8107
8108
8109
8110
8111
8112
8113
8114
8115
8116
8117
8118
8119
8120
8121
8122
8123
8124
8125
8126
8127
8128
8129
8130
8131
8132
8133
8134
8135
8136
8136
8137
8138
8139
8140
8141
*END STEP
*****
**
** Membrane stress is released while grip angle is held fixed
**
** STEP 9
**
*STEP,INC=1000, NLGEOM
*STATIC
```



```

0.1,1.0
*RESTART, WRITE,FREQ = 20
*CONTROLS, ANALYSIS=DISCONTINUOUS
*CONTROLS, PARAMETER=FIELD
0.001,0.01,
*BOUNDARY, OP=NEW
X0, XSYMM
DREF, 1, 6
DUMMY, 1, 6
*BOUNDARY, FIXED, OP=NEW
PULL, 5, 5
PTFIXE, 2, 3
*CLOAD, OP=NEW
*EL PRINT, FREQ=0
S
*END STEP
*****
**
** Membrane stress is released while grip angle is held fixed
** The constraints on the clamped region are released
** by the user subroutine
**
** STEP 10
**
*STEP, INC=1000, NLGEOM
*STATIC
0.1, 2220.0
*RESTART, WRITE, FREQ = 20
*CONTROLS, ANALYSIS=DISCONTINUOUS
*CONTROLS, PARAMETER=FIELD
0.001, 0.01,
*BOUNDARY, OP=NEW
X0, XSYMM
DREF, 1, 6
DUMMY, 1, 6
*BOUNDARY, FIXED, OP=NEW
PULL, 5, 5
PTFIXE, 2, 3
*CLOAD, OP=NEW
*END STEP
*****
**
** Here the dashpots are removed for the last time
**
** STEP 11
**
*STEP, INC=100, NLGEOM, AMPLITUDE=STEP
*STATIC
1., 1., 1., 1.,
*CLOAD, OP=NEW
*CONTROLS, ANALYSIS=DISCONTINUOUS
*CONTROLS, PARAMETER=FIELD
0.001, 0.01,
*BOUNDARY, FIXED, OP=NEW
NALL, 1, 6
DREF, 1, 6
DUMMY, 1, 6

```

\*MODEL CHANGE, REMOVE

8001  
8002  
8003  
8004  
8005  
8006  
8007  
8008  
8009  
8010  
8011  
8012  
8013  
8014  
8015  
8016  
8017  
8018  
8019  
8020  
8021  
8022  
8023  
8024  
8025  
8026  
8027  
8028  
8029  
8030  
8031  
8032  
8033  
8034  
8035  
8036  
8036  
8037  
8038  
8039  
8040  
8041  
8101  
8102  
8103  
8104  
8105  
8106  
8107  
8108  
8109  
8110  
8111  
8112  
8113  
8114

```

8115
8116
8117
8118
8119
8120
8121
8122
8123
8124
8125
8126
8127
8128
8129
8130
8131
8132
8133
8134
8135
8136
8136
8137
8138
8139
8140
8141
*END STEP
*****
**
** Membrane stress is released while grip angle is held fixed
** The dashpots are no longer present
**
** STEP 12
**
*STEP, INC=1000, NLGEOM
*STATIC
0.1, 1.0
*RESTART, WRITE, FREQ = 20
*CONTROLS, ANALYSIS=DISCONTINUOUS
*CONTROLS, PARAMETER=FIELD
0.001, 0.01,
*BOUNDARY, OP=NEW, AMPLITUDE=AM1
X0, XSYMM
DREF, 1, 6
DUMMY, 1, 6
*BOUNDARY, FIXED, OP=NEW
PULL, 5, 5
PTFIXE, 2, 4
*CLOAD, OP=NEW, AMPLITUDE=AM1
*EL PRINT, FREQ=0
S
*END STEP
*****

```

```
*****
**
**The grip angle is released, and the sheet is
**allowed to spring back
**
** STEP 13
**
*STEP,INC=1000, NLGEOM
*STATIC
0.1,1.0
*RESTART, WRITE, FREQ = 20
*BOUNDARY, OP=NEW, AMPLITUDE=AM1
X0, XSYMM
DREF, 1, 6
*BOUNDARY, FIXED, OP=NEW
PTFIXE, 2, 4
*CLOAD, OP=NEW, AMPLITUDE=AM1
*EL PRINT, FREQ=0
S
*END STEP
```

## Appendix B: Stretch Forming Sensitivity Matrices

### Sensitivity of Thicknesses to Stretch Forming Inputs

THICKNESS SENSITIVITIES		FORCE	YIELD STRENGTH	THICKNESS	ANGLE
Location	Element Number				
2	3310	-4.82698E-10	1.1391E-06	1.1192400	3.544E-07
	3410	-2.89523E-10	6.7669E-07	1.0560200	2.188E-07
5	4210	-2.03174E-10	4.0682E-07	1.0206300	9.68E-08
8	5110	-3.67079E-10	7.2434E-07	1.0664400	0
	5210	-3.62798E-10	6.9686E-07	1.0689400	0
3	3327	-3.98256E-10	7.1017E-07	0.9955100	0
	3427	-4.38256E-10	6.9913E-07	0.9930600	0
6	4227	-4.54605E-10	6.53E-07	1.0007700	0
9	5127	-4.13524E-10	6.6291E-07	1.0461700	0
	5227	-4.24381E-10	6.8201E-07	1.0526500	0
Average		-3.83429E-10	7.0511E-07	1.041943	6.7E-08

# Sensitivity of Strains to Stretch Forming Inputs

Location 1

Part	Element Number	Yield Strength	Angle	Force	Thickness
1	3532	-0.0010143	0.00010044	1.12651E-06	-156.1279155
	3632	-0.0007943	0.0001026	7.39686E-07	-151.362661
2	3629	-0.0014362	0.00007	6.96035E-07	-115.6835844
	3729	-0.0010762	0.00008	8.56035E-07	-107.9149588
3	3932	-0.0006543	0.00014348	1.09969E-06	-149.786121
4	3631	-0.0024362	9.884E-05	6.42861E-07	-134.7054382
	3731	-0.0020962	0.0001084	6.92861E-07	-127.4260796
5	3428	-0.0009862	6.26E-05	6.5921E-07	-109.4958684
	3528	-0.0007862	8.348E-05	7.5921E-07	-104.884755
6	3428	-0.0009862	6.26E-05	6.5921E-07	-109.4958684
	3630	-0.0021562	0.0000700	6.92861E-07	-129.6302622
7	3730	-0.0017862	0.0000900	8.52861E-07	-121.9378786
	3631	-0.0024362	9.884E-05	6.42861E-07	-134.7054382
8	3731	-0.0020962	0.0001084	6.92861E-07	-127.4260796
	3530	-0.0023762	7.26E-05	1.06969E-06	-135.3122418
9	3630	-0.0021562	0.0000700	6.92861E-07	-129.6302622
	3632	-0.0007943	0.0000900	7.39686E-07	-151.362661
10	3732	-0.0004543	0.00010348	9.09686E-07	-144.1924154
	3732	-0.0004543	0.00010348	9.09686E-07	-144.1924154
11	3629	-0.0014362	0.00007	6.96035E-07	-115.6835844
Averages		-0.001420602	0.000089462	7.9152E-07	-130.0478244

Location 2

1	4310	-0.0008740	-0.00084	4.27206E-07	-124.463258
2	3910	-0.0012981	-0.00058	5.1038E-07	-184.2235434
	4010	-0.0010960	-0.00038	4.83428E-07	-168.9446674
3	4310	-0.0008740	-0.00084	4.27206E-07	-124.463258
4	3910	-0.0012981	-0.00058	5.1038E-07	-184.2235434
5	3410	-0.0024481	-0.00014	5.9965E-07	-227.0017964
	3510	-0.0021081	-0.00024	5.38063E-07	-204.9846978
6	4210	-0.0009255	-0.00065	4.01841E-07	-136.2473462
	4310	-0.0008740	-0.00084	4.27206E-07	-124.463258
7	3810	-0.0013881	-0.00032	5.42698E-07	-190.2339788
	3910	-0.0012981	-0.00058	5.1038E-07	-184.2235434
8	3610	-0.0015681	-0.00016	4.93428E-07	-187.6758326
	3710	-0.0013881	-0.00037	6.0038E-07	-189.8140874
9	3710	-0.0013881	-0.00037	6.0038E-07	-189.8140874
	3510	-0.0021081	-0.00024	5.38063E-07	-204.9846978
10	3610	-0.0015681	-0.00016	4.93428E-07	-187.6758326
	3610	-0.0015681	-0.00016	4.93428E-07	-187.6758326
11	3610	-0.0015681	-0.00016	4.93428E-07	-187.6758326
12	3610	-0.0015681	-0.00016	4.93428E-07	-187.6758326
Average		-0.001424371	-0.000422778	5.05054E-07	-177.1549497

Location 3

1	4332	-0.0002162	0.00017012	7.8921E-07	-85.7643664
2	3833	-0.0016762	0.00009956	8.82861E-07	-119.3604484
	3933	-0.0020362	0.00013	7.12861E-07	-122.0382544
3	4336	-0.0009462	0.00018072	9.66035E-07	-103.8955882
4	3636	-0.0007943	0.0001026	7.39686E-07	-151.362661
5	3534	-0.0003743	1E-05	7.49686E-07	-146.8535684
	3634	-0.0001543	0.0001035	8.49686E-07	-141.3575996
6	3938	-0.0012943	0.00014392	9.39686E-07	-163.0318384
7	3538	-0.0021543	0.00012348	1.08651E-06	-172.5197262
	3638	-0.0006543	0.00011324	1.16969E-06	-145.0517652
8	3836	-0.0007743	0.00012	9.73338E-07	-150.6484493
9	3539	-0.0026943	0.00016044	1.09334E-06	-179.234433
	3639	-0.0012243	0.00013368	1.14651E-06	-153.6085248
10	3635	-0.0010743	0.0000985	1.17651E-06	-155.2193202
	3735	-0.0006943	0.0001104	9.09686E-07	-148.3255504
11	3636	-0.0007943	0.0001026	7.39686E-07	-151.362661
	3736	-0.0006943	0.00011044	9.09686E-07	-148.3255504
12	4230	-0.0009344	0.00011824	7.78733E-07	-67.7296242
Averages		-0.00106581	0.000118413	9.22967E-07	-139.2049961

